

# Optimizing Turfgrass Management Strategies Using Aerial Imagery and Wireless Capacitive Soil Sensors of Bermudagrass

Travis Leon Roberson

Dissertation submitted to the faculty of the Virginia Polytechnic Institute and State  
University in partial fulfillment of the requirements for the degree of

Doctor of Philosophy  
In  
Plant Pathology, Physiology and Weed Science

David S. McCall, Chair  
Daniel S. Sandor  
Shafian Sanaz  
Chase M. Straw

February 24, 2025  
Blacksburg, Virginia

Keywords: (CBG; creeping bentgrass, CCV; catch can volume, ET; evapotranspiration, FC; field capacity, light reflectance, HBG; Hybrid bermudagrass, NIR; near-infrared region, NDVI; normalized difference vegetation index, PAW; plant available water, TDR; time-domain reflectometry, ST; soil temperature, SSMU; site-specific management units, sUAV; small unmanned aerial vehicle, VIR; visible light region, VWC; volumetric water content)

Copyright © 2025 Travis L. Roberson

# Optimizing Water Management Strategies Using Aerial Imagery and Wireless Capacitive Soil Sensors of Bermudagrass

Travis Leon Roberson

## Academic Abstract

Hybrid bermudagrass (HBG) (*Cynodon dactylon* (L.) Pers. x *transvaalensis* Burt Davy) is one of the most commonly used turfgrasses in the transition zone due to its drought and wear tolerance. Over the years, a combination of history, experience and research has provided best management practices for abiotic stress management of HBG through chemical and cultural field trials. As new tools and technologies to apply to HBG management emerge, research is necessary in order to better understand how these can be implemented in the decision making process for optimal HBG management. As technology rapidly evolves, understanding how to properly implement innovation is vital for outputs to be greater than the inputs for sustainable management. Three studies were conducted between 2021 and 2024 in Virginia to enhance understanding of how small unmanned aerial vehicles and wireless capacitive soil sensors can aid in expediting data collection for actionable decision making related to irrigation practices and winterkill stress mitigation. The first study assessed the impact of morning leaf wetness from dew and subsequent removal on remotely sensed visible imagery for creeping bentgrass and HBG. The data suggests that leaf wetness minimally influences drone-derived green to red ratio index data while maintaining a moderate correlation with soil water content ( $r^2 = 0.48$ ). The second study evaluates the effectiveness of aerial thermal imagery in assessing the distribution uniformity of golf course irrigation systems. A modest correlation existed between irrigation applied as measured by catch can volume and thermal mean canopy temperature ( $T_c$ ) values ( $r = 0.40$ ). Furthermore, the coefficient of determination between  $T_c$  and catch can volume, varied between tee ( $r^2 = 0.19-0.41$ ) and green ( $r^2 = 0.54-0.68$ ) locations, influenced by turfgrass canopy density and soil physical properties. The use of drone-captured thermal imagery shows potential irrigation distribution uniformity through drone thermal imagery to make these evaluation metrics seamless, though techniques need refinement for widescale industry adoption to be applied for potential irrigation management decision making. The final study focuses on utilizing capacitive soil sensors to monitor soil temperature and moisture during winter covering events for ultradwarf bermudagrass (UDB), indicating that wireless sensors can accurately document soil moisture and temperature trends prior, during, and post-covering events. Within the study, the lowest recorded soil temperatures at 33.0°F for Green 9 and 31.0°F for Green 1 under the no cover treatment, and no winter injury was observed, suggesting that UDB may be able to tolerate these soil temperatures for brief periods under fully dormant conditions. Lastly, for the coldest covering event on Green 1, soil moisture fluctuated the most within the uncovered treatment compared to single and double covers, likely due to freeze and thaw cycles of the soil water, suggesting that soil moisture levels are a likely contributor to winterkill potential. Collectively, these studies highlight the potential of advanced technologies in enhancing turfgrass management and water conservation efforts in golf course maintenance of hybrid bermudagrass areas.

# Optimizing Water Management Strategies Using Aerial Imagery and Wireless Capacitive Soil Sensors of Bermudagrass

Travis Leon Roberson

## General Audience Abstract

Hybrid bermudagrass is extensively used in the transition zone due to its excellent drought and wear tolerance. Recent research has aimed to refine hybrid bermudagrass management through incorporating technologies to help make management more efficient and practical. From 2021 to 2024, studies explored the use of drone vehicles and wireless soil sensors to enhance irrigation practices and mitigate winter stress. The first study examined the influence of surface moisture on leaves of creeping bentgrass and hybrid bermudagrass species under green and fairway mowing heights, in conjunction, with two different flight times of 9:00 and 14:00 to induce differing sun incidence angles to explore how all these factors may impact visual drone pixel data. The research found a positive correlation between green and red pixel data when compared to soil water content for all factors but was not similar for pixel data involving blue light. Furthermore, little influence was observed with natural dew deposits or light irrigation on the turfgrass surface when evaluated by green and red pixel data for all locations and flight times. This suggests that drone flights are not impacted by these factors under consistent environmental conditions and field drone flight times can be expanded beyond solar noon timeframes. The second study evaluated the use of aerial thermal imagery to assess irrigation uniformity on golf courses. Thermal imagery to be used as a metric for thermal canopy temperature data and was collected for pre and post irrigation applications compared to catch can volume data. Our data indicates a stronger correlation with ultradwarf bermudagrass greens than fairway height management zones. Key findings indicate thermal imagery can be used to identify moisture stress areas caused by limitations in irrigation system design or delivery for ultradwarf bermudagrass greens more confidently than fairway height of cut areas. The data is likely more related to the influence of physical soil properties within these tested locations and how water infiltration occurs in relation to irrigation applications. Identifying these irrigation limitations with drone data potentially allows for identifying irrigation system operational weaknesses and overall improvement in water use efficiency. The final study focused on using wireless soil sensors to monitor soil conditions during winter, aiding in the prevention of winterkill. Wireless soil sensors provided efficient soil temperature and moisture data delivery during extreme weather events as recorded during covering and uncovering for winter covering treatments of no cover, single cover or double covers for extreme weather events leading to putting green cover protection. Collectively, these studies underscore the potential of advanced technologies to improve turfgrass management, the health and playability of intensively managed turf, and to and promote water conservation on golf courses.

## Dedication

I dedicate this dissertation to Jesus who is my Lord and Savior and has been with me throughout my entire graduate school journey and completely changed my life in this process such as **2 Corinthians 5:17** states *the man of God has a new nature of righteousness that was exchanged for his sinful nature at the cross*. I have spent time reflecting on past decisions that I must take full ownership towards that led me to my personal dark abyss, but I am honored to fall under God's provision and have my sins exchanged for a new righteousness. One verse that was poured over me during these moments - **Jeremiah 29:11** - *For I know the plans I have for you,* "declares the Lord, *plans to prosper you and not to harm you, plans to give you hope and a future*. In life, we never know the plans God has for us, but they are never intended to harm us but strengthen us for a future that assembles us to become ambassadors for God if we so chose to embrace it. In my story, I was a selfish, arrogant, and prideful husband and regret my actions every day, but I refuse to let that control my future decisions. Men's Alliance has taught me to never let my past define me so no matter what choices have transpired, the next day is a new beginning - **2 Corinthians 5:20** states *Therefore, we are ambassadors for Christ, God making his appeal through us*. So as God uses me to make his appeal, I take these moments to etch into history my deep regret for not living up to God's standards that he called upon me, but in those times I was not searching for the truth and God's unfailing love. Nonetheless, the divorce between my ex-wife and myself has been a critical moment in my story because I know I pushed against Gods plan for so long not wanting to lose my wife and the life we had but what I could not begin to fathom is the perfect elegance of gaining the true bride in my heart. I use this dedication to dig deep into my soul and attempt to make an amends for the pain I caused, for my spirit to resolve, and spread peace and love. I was as lost as they come and all I want to do is use these failures to save souls through my story. So, if anyone reading this questions if God can redeem you for His glory, I hope this dedication depicts a broken man fallen so far from grace that only the true creator himself could save a man such as myself.

## Acknowledgments

First, I'd like to acknowledge the blessings in life to have such supportive parents throughout this journey. Larry and Karen Roberson have been the true gift from God to listen, be patient, and provide every facet of support possible to pave an avenue for me to strive for my hearts desires. I'd also like to extend my deepest gratitude towards Dr. David McCall. No one could ask for a more patient and compassionate advisor. He provided advice and wisdom with just enough space to allow me to grow independently and pioneer myself through some hardships and struggles. At the time, I did not appreciate how invaluable that skill would become for future endeavors. We have been alongside each other for almost 10 years to this point, and David has seen me at mountain tops, but equally in the valleys, and never once did he think to give up on me and for that I am eternally grateful. I'd also like to extend thanks towards Maddie and Lee Coppock. These two individuals may have the biggest hearts I know, and they may never know the true impact they have had on the trajectory of my life. It is not an understatement to say in the most crucial tipping point of my life, they only acted out of love and kindness. I admire their grace, stability, and willingness to put everyone above themselves, this world doesn't deserve them but absolutely needs them. Furthermore, I extend my deepest appreciation for key individuals at Independence Golf Club, Giff Breed, Megan Kidd and Dan Taylor for always having my best interest at heart. Whether it was advice during hard moments, listening to my life story, or simply providing a positive culture and environment to cultivate a willingness to succeed, they have stamped their kindness and unselfishness onto my heart. Independence has become a home and a place where it seems the world aligns properly for people's lives to grow in prosperity, and I will always appreciate the toughest period of my life being surrounded by the best people I have had the pleasure of getting to know. Dr. Mike Goatley has also been a truly impactful individual in my life. Whether it is our banter between Duke and Kentucky basketball, or deep and meaningful life conversations, he always had an open life of honest communication, and I learned so much from him as one of the most grounded individuals I have ever met. I want to thank Dr. Wendell Hutchens for not only providing guidance and using his leadership abilities to always push the limits in research, but he is also a close friend. Growing up together and watching our paths be so similar, yet so different, has been a true honor from my perspective and can't wait to see how our paths continue to cross over. I'd also like to thank Dr. Jordan Booth for his guidance and establishment of the research site at Independence Golf Club. Without his gumption to go against the grain, I would not have the ability to follow my dreams of doing research in such an unorthodox manner. Furthermore, I'd like to extend my appreciation towards the lab mates at Virginia Tech, Kevin Hensler, Caleb Henderson, Aaron Tucker, Elizabeth Kitchen, and Ava Veith for all their support. Each person has a unique identity that I hope to carry a portion with me on future chapters of life, but Kevin Hensler has truly given me wisdom from a perspective of a true individual of culture. He never withheld any advice or comment regardless of the circumstance, he only provided the facts, and I will always admire his character and honesty. I would also like to thank the many collaborators at Virginia Tech and outside of the institution that have provided support to make these research dreams become a reality. Lastly, I acknowledge the lifelong impression Men's Alliance has left on my life and training me how to be a strong spiritual and physical leader. The men I surrounded myself with each and every Monday were men of God who guided me in difficult moments of personal life and education. I do not deserve these men yet; they welcomed me with open arms and kept me grounded in

challenging times through physical and spiritual sharpening just as Proverbs 27:17 says ‘As iron sharpens iron, so one man sharpens another’ so I WILL FINISH STRONG!

## Table of Contents

Academic Abstract.....	ii
General Audience Abstract.....	iii
Dedication.....	iv
Acknowledgments.....	v
List of Tables .....	ix
List of Figures.....	xi
Chapter 1: Literature Review.....	1
Water and the Importance of Conservation .....	1
Turfgrass, Water, and Soil Relationship.....	1
Soil Moisture Measurements and Management.....	4
Light and Thermal Reflectance Through Remote Sensing.....	7
Ultradwarf Bermudagrass Winterkill Management.....	13
Research Objectives.....	16
References.....	17
Chapter 2: Assessing the Influence of Leaf Wetness on Remote Sensing Data for Creeping Bentgrass and Hybrid Bermudagrass.....	31
Abstract .....	31
Introduction.....	33
Materials and Methods.....	35
Results and Discussion .....	39
Conclusions.....	45
References.....	46
Chapter 3: An Evaluation of Aerial Thermal Imagery for Assessing the Distribution Uniformity of Golf Course Irrigation Systems .....	60
Abstract .....	60

Introduction.....	62
Materials and Methods.....	65
Results and Discussion .....	71
Conclusions.....	77
References.....	79
Chapter 4: Enhancing Winter Cover Decisions for Ultradwarf Bermudagrass Putting Greens Using Capacitive Soil Sensors in the Transition Zone .....	
Abstract .....	92
Introduction.....	94
Materials and Methods.....	98
Results and Discussion .....	101
Conclusions.....	107
References.....	108

## List of Tables

Chapter 1: Literature Review.....	1
Chapter 2: Assessing the Influence of Leaf Wetness on Remote Sensing Data for Creeping Bentgrass and Hybrid Bermudagrass.....	31
<b>Table 1.</b> Multivariate analysis showing the significant probabilities for leaf wetness, soil water content, ground derived hyper-spectral data (blue = 475 nm, green = 550 nm and red = 670 nm bands along with green to blue (GBI = Green/Blue) and red (GRI = Green/Red) ratios) and aerial drone pixel derived data (blue green and red pixel values along with GBI and GRI ratios for all data sampled at the Pete Dye River Course in Radford, Virginia and The Country Club of Virginia in Richmond, Virginia for 2022.....	56
<b>Table 2.</b> Mixed model effects test results for the response variables of leaf wetness collected by way of a custom PVC roller sampling a 387.35 cm <sup>2</sup> area, soil water content derived as percent volumetric water content from a time-domain reflectometer and the green to red ratio (GRI = Green/Red) index derived from drone pixel data from field data collected at the Pete Dye River Course in Radford, Virginia and The Country Club of Virginia in Richmond, Virginia in the Fall of 2022.....	58
<b>Table 3.</b> One way analysis of variance test results for creeping bentgrass ( <i>Agrostis stolonifera</i> ) and bermudagrass ( <i>Cynodon dactylon</i> x <i>C. transvaalensis</i> ) response variables of leaf wetness collected by way of a custom PVC roller sampling a 387.35 cm <sup>2</sup> area, soil water content derived as percent volumetric water content from a time-domain reflectometer, and the green to red ratio (GRI = Green/Red) index derived from drone pixel data from field data. Treatment effects are separated by the interactions of time of data collection × grass species with mean separation across rows from field data collected at the Pete Dye River Course in Radford, Virginia and The Country Club of Virginia in Richmond, Virginia in the Fall of 2022.....	59
Chapter 3: An Evaluation of Aerial Thermal Imagery for Assessing the Distribution Uniformity of Golf Course Irrigation Systems.....	60
<b>Table 1.</b> Historical weather data for all ultradwarf bermudagrass ( <i>Cynodon dactylon</i> x <i>C. transvaalensis</i> ) greens and hybrid bermudagrass tees locations at Independence Golf Club in Richmond, Virginia in 2023. Weather data is logged based on DJI Mavic 3T small unmanned aerial vehicles (sUAV) flights before and after irrigation, date and time of one hour prior, current, and one hour after all testing periods, ambient temperature, wind speed and direction, humidity, and cloud conditions.....	83
<b>Table 2.</b> Irrigation head and model for each ultradwarf bermudagrass ( <i>Cynodon dactylon</i> × <i>Cynodon transvaalensis</i> ) green and hybrid bermudagrass tee locations at Independence Golf	

Club in Richmond, Virginia in 2023 along with minimum, maximum, and average operating pressures in kilopascals for an average of four irrigation heads at each location..... 86

**Table 3.** Multivariate analysis of all continuous data pooled across ultradwarf bermudagrass (*Cynodon dactylon* × *Cynodon transvaalensis*) green and hybrid bermudagrass tee locations at Independence Golf Club in Richmond, Virginia in 2023 were Catch Can Volume in milliliters of irrigation, Soil Moisture, Red Mean, Green Mean, Blue Mean, and Thermal Mean pixel values derived from a DJI Mavic 3T small unmanned aerial vehicle (sUAV) image acquisition. .... 87

**Table 4.** Displaying summarized statistical data (sample #, minimum and maximum (Min and Max) values, Mean, standard deviation (Std Dev), standard error mean (Std Err Mean), and lower and upper 95%) related to canopy temperature (°C) and soil moisture (%) values along with the delta (Δ) change of before and after sampling events separated by each ultradwarf bermudagrass (*Cynodon dactylon* × *Cynodon transvaalensis*) greens and B). all hybrid bermudagrass tee locations at Independence Golf Club in Richmond, Virginia in 2023..... 89

Chapter 4: Enhancing Winter Cover Decisions for Ultradwarf Bermudagrass Putting Greens Using Capacitive Soil Sensors in the Transition Zone ..... 92

**Table 1.** Mix model effect effects test for sources location, treatment, and their interaction analyzing both daily average soil temperature (°F) and moisture (%) response variables for covering events of Green 9 in 2022-2023 and Green 1 in 2023-2024 at Independence Golf Club in Richmond, Virginia..... 114

**Table 2.** Least square means for covering treatments with location data pooled for soil temperature (°F) and soil moisture (%) separated by locations for covering events on a ‘TifEagle’ ultradwarf bermudagrass (*Cynodon dactylon* x *C. transvaalensis*) Green 9 in 2022–2023 and experimental variety from the University of Florida (FAES 1302 from University of Florida) Green 1 in 2023-2024 at Independence Golf Club in Richmond, Virginia. .... 115

**Table 3.** Covering event dates for a ‘TifEagle’ ultradwarf bermudagrass (*Cynodon dactylon* x *C. transvaalensis*) Green 9 in 2022-2023 and an experimental variety from the University of Florida (FAES 1302 from University of Florida) Green 1 in 2023-2024, total covering dates, dates of precipitation before covering (B) and during covering (D) at Independence Golf Club in Richmond, Virginia. .... 118

## List of Figures

Chapter 1: Literature Review.....	1
Chapter 2: Assessing the Influence of Leaf Wetness on Remote Sensing Data for Creeping Bentgrass and Hybrid Bermudagrass.....	31
<p><b>Figure 1.</b> Visual example of the experimental treatments of light irrigation (LI), rolling (R), and leaf wetness (UTC) on a ‘TifEagle’ ultradwarf bermudagrass (<i>Cynodon dactylon</i> x <i>C. transvaalensis</i>) . The small square with an absence of surface moisture (black box) within the UTC plot is an example of the reference area where surface moisture data were collected using the custom PVC roller with a spatial sampling size of 387.35 cm<sup>2</sup> post treatment initiation... 51</p> <p>..... 51</p>	51
<p><b>Figure 2.</b> Visual example of the Custom PVC roller measuring 3.18 cm in diameter x 12.7 cm in length that has a smaller PVC handle inserted through the center and traversed across a length of 30.48 cm sampling a total area of 387.35 cm<sup>2</sup> on ‘Northbridge’ hybrid bermudagrass (<i>Cynodon dactylon</i> x <i>C. transvaalensis</i>) at the Country Club of Virginia in Richmond, Virginia. ....</p>	52
<p><b>Figure 3.</b> Representation of the custom-made PVC stand with a retrofitted arm that extends out 91.44 cm in length and holds the radiometer 5° field of view lens in order at a height of 127 cm to standardize the ground spectral data collection process at a spot sampling size of 10 cm<sup>2</sup>. This sampling standard was done for each location at the Pete Dye River Course in Radford, Virginia and The Country Club of Virginia in Richmond, Virginia. ....</p>	53
<p><b>Figure 4.</b> Visual for standardized process flow using QGIS (version 3.28) spatial analysis software to A) Generate individual plot polygons from stitched orthomosaic at the time of study B) determining the centroid of the polygons comprised of the entire plot areas and C). using the processing tool ‘Rectangles, Ovals, and Diamonds’, to generate 1.5 m × 1.5 m polygons to eliminate potential edge effects of plots for a ‘L-93’ creeping bentgrass (<i>Agrostis stolonifera</i>) fairway at the Pete Dye River Course in Radford, Virginia.....</p>	54
<p><b>Figure 5.</b> Relationship between Green to Blue Ratio Index (GBI) and Green to Red Ratio Index (GRI) pixel data derived from Mavic 2 drone aerial imagery and soil water content estimated as volumetric water content derived from a time-domain reflectometer for all locations between The Pete Dye River Course and Country Club of Virginia in Radford and Richmond, Virginia in 2022 .....</p>	55
<p><b>Figure 6.</b> Relationship between Green to Red Ratio Index (GRI) pixel data derived from Mavic 2 drone aerial imagery and ground-based GRI data extracted from spectral data samples using a Spectral Evolution hyper-spectral radiometer for all locations separated by the time of</p>	

data collection (morning or afternoon) at The Pete Dye River Course and Country Club of Virginia in Radford and Richmond, Virginia in 2022. .... 57

Chapter 3: An Evaluation of Aerial Thermal Imagery for Assessing the Distribution Uniformity of Golf Course Irrigation Systems ..... 60

**Figure 1 A).** Thermal orthomosaic derived from a DJI Mavic 3T small unmanned aerial vehicle (sUAV) image acquisition displaying the catch can locations on a ‘TifEagle’ ultradwarf bermudagrass (*Cynodon dactylon* x *C. transvaalensis*) green 4 (G4) at Independence Golf Club in Richmond, Virginia in 2023 after irrigation application occurred and B). thermal orthomosaic showing the multipoint that are used to identify the catch cans within the thermal orthomosaic to be used for further pixel processing and data extraction. .. 84

**Figure 2.** Thermal orthomosaic derived from a DJI Mavic 3T small unmanned aerial vehicle (sUAV) image acquisition of a ‘Tif-eagle’ ultradwarf bermudagrass (*Cynodon dactylon* x *C. transvaalensis*) green 4 at Independence Golf Club in Richmond, Virginia in 2023 displaying polygon buffers centered around points corresponding to catch can locations within the image on a 1.5 m radius with approximately 360 pixels per polygon and designated based on the spacing of the catch cans to compensate for any pixel resampling. .... 85

**Figure 4.** Distribution uniformity for the soil moisture before irrigation ( $SMDU_{BI}$ ), after irrigation ( $SMDU_{AI}$ ), and for irrigation water physically applied by measuring water volumes caught in evenly distributed catch cans (DU) separated by all ultradwarf bermudagrass (*Cynodon dactylon* × *Cynodon transvaalensis*) greens and hybrid bermudagrass tee locations at Independence Golf Club in Richmond, Virginia in 2023. .... 91

Chapter 4: Enhancing Winter Cover Decisions for Ultradwarf Bermudagrass Putting Greens Using Capacitive Soil Sensors in the Transition Zone ..... 92

**Figure 1.** Visual representation of the experimental design for two winter covering events on Green 9 in January and March 2023 on a ‘Tif-Eagle’ ultradwarf bermudagrass (*Cynodon dactylon* x *C. transvaalensis*) green at Independence Golf Club showing no cover (NC), single cover (SC), and double cover (DC) treatments..... 111

**Figure 2.** Visual representation of the experimental design for two winter covering events on Green 1 in November 2023 and January 2024 on an experimental ultradwarf bermudagrass (*Cynodon dactylon* x *C. transvaalensis*) green variety (FAES 1302 from University of Florida) at Independence Golf Club in Richmond, Virginia showing no cover (NC), single cover (SC), and double cover (DC) treatments. .... 112

**Figure 3.** Illustrations showing the installation of the capacitive soil sensor using the Miltons square plugger on Green 9 in December 2022 at Independence Golf Club in Richmond, Virginia for (Figure 3A), a close-up of the capacitive soil sensor positioned horizontally before replacing the plug (Figure 3B), and the sensor in the hole rotated to ensure the moisture plate was perpendicular to the soil walls (Figure 3C). .... 113

**Figure 4.** The minimum observed daily ambient temperature during the winter season of 2022-2023 in Richmond, Virginia. Red boxes indicate the two covering events that occurred

on Green 9. The black horizontal line represents the ambient temperature threshold used to trigger a covering event. .... 116

**Figure 5.** The minimum observed daily ambient temperature during the winter of 2023-2024 in Richmond, Virginia. Red boxes indicate the two covering events that occurred on Green 1. The black horizontal line represents the ambient temperature threshold used to trigger a covering event. .... 117

**Figure 6.** Box and whisker plots of soil temperature (°F) and moisture (%) for each covering treatment No Cover, Single Cover, and Double Cover by covering events (CE 1– 4) at each location with CE1 and CE2 in Winter 2022-2023 on a ‘TifEagle’ ultradwarf bermudagrass (*Cynodon dactylon* x *C. transvaalensis*) Green 9 and CE3 and CE4 in Winter 2023-2024 on an experimental variety from the University of Florida (FAES 1302 from University of Florida) Green 1 at Independence Golf Club in Richmond, Virginia. .... 119

**Figure 7.** Soil temperature data pooled by treatments of no cover, single cover, and double cover during covering event 4 in the winter 2023-2024 season on an ultradwarf bermudagrass (*Cynodon dactylon* x *C. transvaalensis*) Green 1 on an experimental variety from the University of Florida (FAES 1302 from University of Florida). The red dashed line indicates when the covering treatments were applied, and the black dashed line indicates when they were removed. The black horizontal line represents the 25°F ambient temperature threshold used to justify covering events. .... 120

**Figure 8.** Soil temperature and moisture pooled by covering treatments of no cover, single cover and double covering during covering event 4 in winter 2023-2024 season on an experimental ultradwarf bermudagrass (*Cynodon dactylon* x *C. transvaalensis*) green variety (FAES 1302 from University of Florida). Red dashed line indicates when the covering treatments were applied, and the black dashed line indicates when the covers were removed. .... 121

## **Chapter 1: Literature Review**

### **Water and the Importance of Conservation**

In 1995, people used approximately 3,900 km<sup>3</sup> of water globally for domestic, industrial, and agricultural purposes, and this amount is projected to increase by 50% by 2025. As the global population grows, freshwater demand will rise, with more emphasis on domestic and industrial uses than agriculture. Developing countries will account for 93% of this demand due to rapid population growth, while developed countries will see minimal changes in water scarcity, except for luxury uses like irrigation for lawns and golf courses (Rosegrant & Cai, 2002; Rosegrant et al., 2002). Globally, people irrigate 250 million hectares for various uses, with the U.S. having 165,000 km<sup>2</sup> of turfgrass, and by land surface coverage, is one of the largest irrigated crops (Milesi et al., 2005). Golf courses alone cover 1.2 million acres, using 1.9 million acre-feet of water in 2014, a 22% decrease from 2005 (Norman & Throssell, 2009; Throssell & Norman, 2007, 2014; Throssell et al., 2009). Furthermore, Shaddox et al. (2022) showed a 29% decline in total golf course water usage from 2.38 to 1.69 million acre feet due to a 12% decline in total facilities and 25% water reductions all since 2005. Properly managing turfgrass areas is crucial to mitigate water scarcity as freshwater becomes more limited (Jury & Vaux Jr, 2005).

#### **Turfgrass, Water, and Soil Relationship**

Turfgrasses offer significant recreational and environmental benefits, but limited soil moisture can cause desiccation, browning, and total stand loss, compromising their functionality and necessitating irrigation (Huang, 2008; White et al., 1992). However, these permanent losses of turfgrass quality are under periods of long-term duration at soil moisture levels near permanent wilting conditions. Under short periods, turfgrasses can sustain adequate turfgrass quality and functionality under soil moisture levels of half their total consumptive water content

with no induced traffic (Mahdavi et al., 2017). To maintain turfgrass quality during dry periods, we need to understand their water requirements, determined by reference evapotranspiration (ET) rates, which include water lost through transpiration (via stomates) and soil surface evaporation (K. Peterson et al., 2017; K. W. Peterson et al., 2017).

The ET equation is expressed as:

$$ET = I + P - RO - DP + CR \pm \Delta SF \pm \Delta SW$$

where irrigation (I), precipitation (P), surface runoff (RO), percolation depth (DP), capillary rise (CR), subsurface flow change ( $\Delta SF$ ), and soil water content change ( $\Delta SW$ ) are considered (Allen et al., 1998). Reference ET rates depend on soil moisture, grass type, climatic conditions, and soil properties (Feldhake et al., 1983). By understanding ET rates, turfgrass genotypes are selected based on drought resistance, rooting depth, shoot density, growth habit, and metabolic pathways ((Hopkins, 2009).

Turfgrasses are classified into cool-season (C3) and warm-season (C4) types. C4 grasses, like zoysiagrass (*Zoysia japonica*) and bermudagrass (*Cynodon dactylon*), are more water-efficient and thrive in warmer climates due to their photosynthetic pathway, which reduces water loss and photorespiration (Edwards & Smith, 2010). C3 grasses, such as tall fescue and Kentucky bluegrass, generally consume more water (3-8 mm/day) compared to C4 grasses (2-5 mm/day) (Dean et al., 1996). Water consumption varies within species. High water users among C3 grasses include tall fescue, creeping bentgrass (*Agrostis stolonifera*), Kentucky bluegrass (*Poa pratensis*), and perennial ryegrass (*Lolium perenne*), consuming 8-10 mm/day. Low water users among C3 grasses include Chewing's fescue and creeping red fescue, consuming 7-8.5 mm/day (Huang & Gao, 1999; Kjelgren & Rupp, 1997; O'neil & Carrow, 1983). Among C4 grasses, high water users like Bahiagrass, St. Augustinegrass, and seashore paspalum consume 7-

8.5 mm/day, while low water users like hybrid bermudagrass, zoysiagrass, and centipedegrass consume 6 mm/day or less (Kim & Beard, 1988). Genetic differences affecting ET rates cause these variations (Romero & Dukes, 2008).

Turfgrasses with a prostrate growth habit use less water than those with an upright growth habit. Those with rhizomes can survive longer without sufficient soil moisture (Jensen et al., 2016; Lee, 2011), and they experience less damage under water-deficit conditions if other stressors are minimized (Braun et al., 2022). Bunch-type grasses, with their upright growth, use more water due to greater leaf surface area and higher stomatal density (Kim & Beard, 1988). Kentucky bluegrass cultivars with more upright growth habits show higher water use, unlike warm-season prostrate grasses like bermudagrass and zoysiagrass (Beard et al., 1992; Shearman, 1986).

Dense grass canopies reduce water loss by acting as a barrier to solar radiation and wind, which helps maintain the atmospheric vapor barrier above the grass and soil surface (Biran et al., 1981). Genetic mechanisms also play a role in drought tolerance. Turfgrasses enter dormancy during water-deficit conditions to minimize water loss, adjusting solute concentrations and cell structures to cope with stress (Bray, 1993, 1997; Serraj & Sinclair, 2002). Stomatal conductance and water use efficiency depend on stomatal density and leaf area, with hormonal responses like adjustments in abscisic acid levels helping to regulate water loss (Anjum et al., 2011; Bray, 1993; Close, 1996; Lu et al., 2009; McCann & Huang, 2008).

Rooting characteristics also affect water uptake. Deep-rooted turfgrasses like tall fescue can access more water, but water use is determined by physiological needs rather than root system size alone (Culpepper et al., 2019). Soil moisture management influences root development, with well-drained soils promoting deeper root growth for turfgrasses such as tall

fescue that possess deep and extensive rooting systems when exposed to soil conditions that do not limit root growth due to limitations from physical and chemical soil properties. (Huang, 2008; Huang et al., 1997a, 1997b). Root systems adapt to water availability by increasing root hair production and adjusting osmotic balance (Huang & Fry, 1998; Moreno-Espíndola et al., 2007), but can they can become compromised and lose root biomass under prolonged drought conditions.

Furthermore, environmental factors such as wind, temperature, solar radiation, and humidity impact turfgrass water use. Wind increases transpiration by reducing the boundary layer resistance, while higher temperatures and solar radiation increase ET rates (Brown, 2014; Brown & Kopec, 2014). Relative humidity inversely affects ET rates, with lower humidity leading to higher water loss (Carrow, 1995).

Soil physical properties, particularly texture, determine soil water availability. Coarser textured soils have higher infiltration rates but lower water retention, while finer soils retain more water but have lower infiltration rates (Saxton et al., 1986; Tuller et al., 2004). The balance between field capacity and permanent wilting point defines the plant available water (PAW) (Zotarelli et al., 2010). Understanding these interactions helps manage soil water efficiently in turfgrass systems.

### **Soil Moisture Measurements and Management**

Effective irrigation management on golf courses requires a crucial understanding of how soil water movement impacts soil water content or volumetric water content (VWC). Hand-watering greens to maintain surface firmness while limiting water use is a common practice (Linde et al., 2011; Stowell et al., 2009). Monitoring soil moisture in small areas requires precision and accuracy, which time-domain reflectometry (TDR) provides, and for this reason it

is a very popular tool used by many golf superintendents in specific areas such as golf putting greens (Moeller, 2012; Noborio, 2001). Other VWC estimation methods include gravimetric, neutron probes, tensiometers, gypsum block probes, and dual-probe heat-pulse techniques, though these can be destructive or require power sources (Bristow et al., 1993; Campbell et al., 1991; Evett et al., 2002; Evett & Steiner, 1995; O'neil & Carrow, 1983; Sharma, 2018). TDR technology relies on the dielectric constant difference between soils and water, reported as the weight of water to the total soil volume (Selig & Mansukhani, 1975). Despite some underestimation issues, TDR is reliable for documenting historical VWC, especially in large, undulated areas like fairways (Topp et al., 1982; Young et al., 1997). Capacitive and frequency domain sensors, similar to TDR, use electrodes and soil to form a capacitor and measure charge time and capacitance (Gardner et al., 1998). However, using devices like the Field Scout TDR 350 with GNSS technology is labor-intensive for larger turfed areas beyond putting greens, requiring 80–300 sampling points per fairway for accurate VWC distribution (Hejl et al., 2022; Straw et al., 2022).

Research has explored the time and labor needed to gather VWC data for categorizing sight-specific management units (SSMUs) on golf courses and sports fields (Straw et al., 2017; Straw, Carrow, et al., 2018; Straw, Grubbs, et al., 2020; Straw & Henry, 2018; Straw, Samson, et al., 2018, 2020). The Toro Mobile MultiUnit prototype measured VWC, NDVI, and penetration resistance, covering substantial areas but inefficiently due to the distribution of sampled points required to build an accurate representation of a given area (Carrow et al., 2010; Medina et al., 2012). Developing SSMUs is vital for optimizing irrigation scheduling, especially in regions with water usage limits but a need exists in being able to develop these SSMUs more efficiently and cost effectively (Straw et al., 2022). Despite the complexity of creating SSMUs, similar

results can be achieved through the historical knowledge of turfgrass managers (Straw & Henry, 2018; Straw, Wardrop, et al., 2020).

Prescription water applications can be derived from ET-based models and applied to SSMUs for optimized irrigation (Davis & Dukes, 2010). Subsurface electromagnetic soil moisture sensors, which communicate wirelessly with irrigation control stations, can significantly reduce water usage compared to traditional schedules ((Blonquist et al., 2009; Blonquist Jr et al., 2006; McLaughlin, 2021). Studies show that rain and soil moisture sensors can guide irrigation applications, resulting in substantial water savings (Cardenas-Lailhacar & Dukes, 2012; Cardenas-Lailhacar & Dukes, 2007; Cardenas-Lailhacar et al., 2005, 2008; Sandor et al., 2022).

Continuous soil sensors provide real-time feedback for watering decisions, though many wireless sensors remain too expensive for widespread adoption (Cardenas-Lailhacar & Dukes, 2007; Ham et al., 2021). Researchers have found that irrigation system distribution uniformity influences soil VWC but is not the sole contributing factor due to other influential factors (Miller et al., 2014; Whitlark et al., 2023). In fact, Straw, Carrow, et al. (2018) found that when considering the  $DU_{Iq}$  for soil moisture, that there was a higher estimation within native soils compared to  $DU_{Iq}$  derived from catch can volumes but more similar within sand-capped athletic fields. Furthermore, they also determined spatial variability of soil water content was not reflected within maps derived from catch can volume data. Those findings align with other research that states influential factors such as the slope aspect of an area that affects water movement plays a large role in soil VWC along with physical soil properties (Ruth Kerry et al., 2023; R Kerry et al., 2023). Combining ET-based decision-making, soil property knowledge,

irrigation system efficiency, and real-time soil moisture sensors can improve irrigation programming.

Rapid and accurate spatial surveys are the next step in turfgrass water conservation. Precision turfgrass management (PTM) involves adopting new technologies to improve input efficiency while maintaining turfgrass quality (Carlson et al., 2022). Light reflectance data, converted to the most widely used vegetation index, the Normalized Difference Vegetation Index values ( $NDVI = \frac{R_{NIR} - R_{RED}}{R_{NIR} + R_{RED}}$ ), can assess large, irrigated areas influenced by irrigation systems and management practices (Fenstermaker-Shaulis et al., 1997). However, small unmanned aerial vehicles (sUAV) for large-scale soil moisture assessments face limitations like software accuracy, data processing, and lighting conditions (Parra et al., 2024). While they face limitations, the technology is still important to understand for other implications.

### **Light and Thermal Reflectance Through Remote Sensing**

The electromagnetic spectrum spans a wide range of photon energy states, but in plant science, measurements from 400-2500 nm are crucial. Within this range, key regions for spectral reflectance data analysis include the visible light region (VIR = 400-700 nm), red edge (RE = 700-750 nm), near-infrared region (NIR = 800–1000 nm), and shortwave infrared region (SIR = 1000-2500 nm) (Cimtay et al., 2021; Horler et al., 1983). Light reflectance is used to predict biomass, yield, and crop stress, determine health status, estimate crop growth, assess nitrogen status, isolate soil and water regions, and identify many other factors through objective data (Blackmer et al., 1994; Fitz-Rodríguez & Choi, 2002; Thenkabail et al., 2000). Various aspects of turfgrasses have been correlated with these light regions, bandwidths of spectral data, and combinations involving multiple light regions. One significant relationship is the varying reflectance in the VIR and NIR regions concerning turfgrass quality (shoot density, color,

canopy uniformity) (Trenholm et al., 1999). These relationships have been demonstrated between stressed and non-stressed bermudagrass and seashore paspalum plots through simulated wear tolerance and comparisons of bentgrass and bermudagrass species (Trenholm et al., 2000).

Due to the low, compact, and dense canopies of mature turfgrasses, transmittance is negligible, and reflectance is generally low within the VIR. This low reflectance occurs when turfgrass is under minimal-to-no stress and operates in a normal physiological state where chlorophyll a and b are absorbed, and solar radiation energy is converted into food through photosynthesis (Gitelson & Merzlyak, 1994). When abiotic or biotic stressors are introduced, VIR reflectance shifts due to changes in chlorophyll concentrations that affect the amount of photosynthetically active radiation (PAR) absorbed for plant use. These trends have been observed in turfgrass, forest canopies, and shrubs under various stresses, where more VIR light is reflected toward a sensor or lens of a multispectral unit depending on the degree of stress (Carter, 1993, 1998; Carter et al., 1996; Carter & Miller, 1994). As turfgrasses become stressed, the VIR region shifts through other pigment concentrations, such as carotenoids and xanthophylls. These secondary pigments increase because compromised chlorophyll components require them to capture free oxygen radicals and quench excited chlorophyll states to prevent detrimental buildup (Horton et al., 1996; Maslova et al., 2021). While VIR shifts due to stress, overall reflectance remains minimal compared to the NIR region. During optimal growth, the NIR can result in 80 to 90% total reflectance due to light scattering from the available tissue water content within the plant (Peñuelas et al., 1993; Peñuelas et al., 1994; Peñuelas et al., 1997). When turfgrass is subject to drought stress, correlations at wavelengths of 750 nm, 775 nm, and 850 nm are significant among seashore paspalums in terms of leaf firing, a symptom of drought stress (Jiang & Carrow, 2005, 2007; Jiang et al., 2003). Jiang reported that 700–800 nm is significant for

modeling most grasses under drought stress. Changes in NIR reflectance indicate leaf water potential due to available soil moisture. Limitations of total tissue water content lead to more NIR light being transmitted through plant leaves (Bowman, 1989). Understanding these relationships is crucial for developing mathematical indicators involving these regions to identify stressors, mainly soil water limitations, within turfgrass systems through vegetation indices (VIs).

One popular VI is the NDVI, which has been correlated with various aspects influencing turfgrass quality. However, in terms of soil water content, low-to-moderate correlations exist in the literature (Badzmierowski et al., 2019; Bremer et al., 2011a, 2011b; Lee et al., 2011; Leinauer et al., 2014; McCall et al., 2017; Roberson et al., 2021). NDVI variability increases as the turfgrass canopy thins from moisture stress, leading to a loss of stand density and exposure of bare soil (Park et al., 2007). Moisture stress assessments using hyperspectral or multispectral radiometers are more accurate for soil moisture assessment when VIs dedicated to VIR or NIR areas alone are used. The water band index ( $WBI = R_{900}/R_{970}$ ) is of interest because water absorption occurs between these wavelengths (Blank et al., 2021; Claudio et al., 2006; Peñuelas et al., 1994). The WBI is accurate and reliable for evaluating plant tissue water status at a localized level but scaling it up for drone use in larger assessments is costly and infeasible for consumers. Roberson et al. (2021) demonstrated an alternative VI using the green-to-red ratio ( $GRI = R_{GREEN} / R_{RED}$ ) as a reliable indicator of soil moisture stress and a predictor of creeping bentgrass and hybrid bermudagrass visual symptoms up to 9 hours prior during a dry-down event. However, these events were conducted under controlled greenhouse conditions.

Field studies have shown the potential of using handheld meters or spectrometers to calculate NDVI or other VIs along with VWC, turf quality, and other parameters during field

dry-down events. Results indicate the potential of spectral reflectance to detect drought stress up to 48 hours before visual symptoms appear (Dettman-Kruse et al., 2008; Johnsen et al., 2009). Drones equipped with sensors specializing in narrowband reflectance or thermal imagery have documented the relationship between spectral or canopy temperature data and prescription irrigation amounts under drought conditions (Hong & Bremer, 2021; Hong et al., 2019a, 2019b). Hong's findings revealed that drones or sUAV could detect drought symptoms five days before stress onset via the normalized green-to-blue index ( $NGBI = R_{GREEN} - R_{BLUE} / R_{GREEN} + R_{BLUE}$ ) and thermal imagery, strongly correlated with turf quality and percent green cover ( $r = 0.60 - 0.78$ ). These findings are significant for the industry because sUAV can expedite large-scale moisture stress assessments and irrigation applications through data-driven decisions. However, Friell and Straw (2021) highlighted the complexities of scaling remote sensing-based principles from small-plot research to industry adoption. They compared NDVI from a ground-driven unit equipped with a spectral sensor and a drone sensor, finding significance only after an irrigation event ( $r = 0.26$ ). As water infiltrated the soil, this relationship became nonexistent, possibly due to soil properties leading to nonuniform water distribution or other factors like traffic stress from golfers not observed in small-plot research. The need for continual expansion of soil moisture stress research and its relation to sUAV in real-world conditions remains. As sUAV adoption increases, relevant information is needed sooner, making VIR data more pertinent. Drones have become less expensive and user-friendly, with some equipped with high-resolution visual and thermal cameras, such as the Mavic 3T Enterprise (DJI, Nanshan, China). Developing protocols for using these drones under stable, non-changing environmental conditions during sUAV flights is crucial for providing meaningful image pixel data. These protocols could include camera angle, lighting conditions (incoming solar radiation and cloud conditions), known grass variety,

mowing height, moisture on the plant surface, current soil type, and flight area elevation. In addition to light reflectance, thermal and temperature data are used for soil moisture response evaluation.

Thermal infrared data have proven valuable for identifying presymptomatic diseases caused by plant pathogens like downy mildew in cucumbers (Ishimwe et al., 2014; Oerke et al., 2006). Turfgrass managers can use thermal remote sensing for irrigation scheduling to conserve water by detecting physiological and biological changes in plants not yet perceptible to the human eye (Johnsen et al., 2009). The thermal radiation emitted by the canopy surface relates to canopy temperature ( $T_c$ ), an important by-product of turfgrass physiological response to the environment and stressors (Blonquist et al., 2009; K. W. Peterson et al., 2017). Canopy temperature can be directly related to transpiration rates, influenced by plant stomatal closure in response to stress. Combining canopy temperature and ambient temperature difference ( $T_c - T_a$ ), known as the crop water stress index, normalized by vapor pressure deficit, can be a reliable metric for identifying stomatal regulation (Ballester et al., 2018; Jackson et al., 1981). UAVs equipped with thermal sensors detect infrared changes related to crops like vineyards and cotton (Alchanatis et al., 2010; Cohen et al., 2005; Zarco-Tejada et al., 2012; Zarco-Tejada et al., 2013). Thermal infrared data converted to the crop water stress index have been directly related to ET of turfgrasses under irrigation regimens and show a nonlinear relationship with watering depth (Taghvaeian et al., 2013). Hong et al. (2019a) investigated the relationships of  $T_c$  with soil VWC, TQ, percent green color, and soil temperature (ST) of creeping bentgrass subjected to ET-based deficit irrigation ranging from 15–100%. Results revealed that  $T_c$  data were more strongly associated with TQ (-0.60 to -0.77) and PGC (-0.58 to -0.78) than with VWC ( $r = -0.43$  to  $-0.63$ ) and ST ( $r = 0.27$  to  $0.41$ ).

While these results show that Tc has a greater influence on visual response data, most thermal infrared data are related to inducing stress to understand the Tc response for research purposes. Zúñiga Espinoza et al. (2017) found significant correlations between Tc data and stomatal conductance ( $r = -0.63$  to  $-0.68$ ) and yield ( $r = -0.80$  to  $-0.83$ ) for subsurface irrigated vineyards 80 and 44 days before harvest when looking at Tc data related to 15, 30, and 60% subsurface irrigation from a standard replenishment level. Limited research has focused on irrigation scheduling for turfgrass based on Tc data, but it has proven useful when correlating thermal data to irrigation scheduling treatments from soil water potential changes for Kentucky bluegrass (Throssell et al., 1987). The strong correlation between the crop water stress index and leaf water potential ( $r^2 = 0.82$ ) for cotton, tomato, and peanut plants subjected to limited soil moisture and the development of site-specific irrigation prescriptions derived from these responses are positive results (Meron et al., 2010). Research related to thermal Tc data for crops continues to expand, but a method for scanning the effectiveness of irrigation distribution using similar principles has not been developed. This limitation exists because Tc data focus on documenting a stress response; however, considering similar data for a turfgrass canopy immediately after an irrigation application could provide valuable information about where water is physically applied across an area.

These factors have led to the development of mower-mounted devices that passively use dual-polarization brightness temperature values within the microwave radiation region to estimate soil moisture (Houtz et al., 2023; Houtz et al., 2020). Passive L-band radiometry occurs in the frequency band of approximately 1400 MHz and uses an empirical model known as the microwave emission model (Schwank et al., 2018). These devices can collect dense datasets related to soil moisture while performing traditional maintenance practices such as mowing.

Passively estimating soil moisture allows for a simple, non-destructive method for collecting data related to soil moisture for irrigation adjustments on a frequent historical basis without the time-consuming use of consistent drone thermal imagery that impedes day-to-day operations. Light and thermal reflectance applications are of great interest for soil moisture assessments on golf courses to make practical management decisions or determine areas that historically express drought symptoms first compared to other areas. However, these management decisions focus on turfgrass water management during the peak growing season. Moisture management for warm-season turfgrasses such as ultradwarf bermudagrass is equally crucial during non-growing seasons using available technologies for practical decision-making and assessments.

### **Ultradwarf Bermudagrass Winterkill Management**

Ultradwarf bermudagrass (UBG) (*Cynodon dactylon* [L.] Pers. × *C. transvaalensis* Burt-Davy) greens have increased in popularity in the transition zone climate because of their improved traffic tolerance and fewer inputs, such as fungicides, during the summer growing season as compared to creeping bentgrass greens. However, the transition zone climate can experience drastic fluctuations in low ambient temperature exposure, increasing the risk for winter damage. Winterkill is a common term for lethal exposure to extremely-low temperatures that UBG experiences in the transition zone and leads to visual confirmation of UBG damage or death as it emerges from winter dormancy (Gopinath et al., 2021a; Hutchens et al., 2024). The probability of winter injury occurring has been shown to increase when the UBG is predisposed to ambient temperatures of  $-6.67^{\circ}\text{C}$  and a critical threshold exists for triggering the need for golf course superintendents to protect these sensitive areas with covering materials (Trenholm, 2000). However, not all UBGs exhibit the same trend of lethal temperature exposure ( $LT_{50}$ ) of  $\geq 50\%$  damage, with damage often observed as being more cultivar specific. For example, Gopinath et

al. (2021b) reported that the  $LT_{50}$  for ‘Champion Dwarf’ ranged from  $-5.2$  to  $-5.9^{\circ}\text{C}$ , while the  $LT_{50}$  of ‘Tahoma 31’ ranged from  $-7.8$  to  $-9.0^{\circ}\text{C}$  when they were predisposed to control conditions in the ambient temperature range of  $-4$  to  $-14^{\circ}\text{C}$ . However, these  $LT_{50}$  differences are related to their genetic variety variations since their mowing heights were both 1.3 cm prior to freeze chamber work. Furthermore, covering applications at  $-9.44$  to  $-3.88^{\circ}\text{C}$  demonstrated that ‘Champion’ UBG had unacceptable injury for the noncovered treatments during these temperature thresholds compared with ‘Tifway’ and ‘MiniVerde’ (DeBoer et al., 2020). The use of specialized covers increases mean surface temperatures by way of heat retention following cover applications. Additionally, reports of covering when predicted night temperatures of  $\leq 4.44^{\circ}\text{C}$  occurred provided a four to-six-week earlier green-up period than not covering at any period during winter conditions (Goatley et al., 2005). The cold hardiness of UBG varieties influences the critical thresholds necessary for covering events based on ambient temperatures, but the covers themselves also possess inherent benefits and drawbacks. Goatley et al. (2017) reported that translucent covering materials have the highest transmission of photosynthetically active radiation and that geotextile covering materials have the greatest wet weight post-irrigation and the smallest percent change in soil moisture. Both research data and practical reporting by golf superintendents find that covering events help to the revenue of the golf course. Owing to the sporadic climatic conditions exhibited in the transition zone, golf courses are expected to remain open when playing conditions are optimal for members and other customers. This poses challenges between the goal of optimizing winter protection by using covers, the labor and time required to cover and uncover UBG greens, and the overall loss of revenue (or golfing availability) by the course. The cost of labor alone for covering UBG can range from \$2,500 to \$24,000 in labor, depending on the frequency of covering events required for winter

protection (DeBoer et al., 2019). For these reasons, researchers and golf turf managers alike continue to search for other methods and strategies to help minimize the frequency of covering events to reduce golf courses' revenue losses.

In addition to covering events to regulate temperature extremes, other turf maintenance strategies are also employed for winterkill management of UBG. One such example involves increasing the mowing height prior or during the cold acclimation period that leads to eventual winter dormancy. The higher turf canopy improves traffic tolerance and provides additional insulation of greater canopy biomass (Strunk et al., 2022). Furthermore, the UBG in the transition zone can occasionally face cold de-acclimation periods in late winter, leaving the plant in a susceptible state for potential late-season cold extremes. Plant growth regulators have been shown to help reduce this risk and allow for earlier spring green up of UBG when late fall and spring applications are made with trinexapac-ethyl (Booth et al., 2024). Another factor that influences potential winterkill events is shading effects on bermudagrass (Frank, 2016).

Understanding the scope of extended shaded areas across a property is critical to assess areas that will likely experience winter injury. Additionally, preserving the health of UBG during winter dormancy allows the plant to have a greater chance of surviving winter stress during a dormant state. Applications of  $\leq 97.68 \text{ kg N ha}^{-1}$  in late summer and early fall can retain green color longer into the season and promote earlier spring greening without increasing winterkill risk (Park et al., 2017). The application of potassium can also alleviate winterkill risks, but only when it is deficient in the soil prior to application; if potassium is at optimum levels, no additional benefits are observed from applications beyond these soil loads (Miller & Dickens, 1996).

Ultradwarf bermudagrass on a sand-based rootzone can exhibit localized dry spot from water repellency, leading to irregularly-shaped areas of damage (Beard & Beard, 2005). The soil

moisture challenges can be further exaggerated by periods of limited precipitation or irrigation, or by soil hydrophobicity where sand particles are coated with organic compounds (Miller & Wilkinson, 1977). This is why moisture management for the prevention of winter desiccation is crucial during dry periods, especially for putting green areas with higher elevations (Kreuser, 2014). Wetting agents can improve soil moisture retention at the soil: thatch interface to help diminish the probability of winter injury due to moisture limitations. Winter desiccation occurs when internal plant structures degrade during winter drought periods due to permanent dehydration and eventual loss of physiological function (Pessarakli, 2007). Conversely, the same is true for poorly drained soils and excessive moisture occurring during low-temperature extremes (Henry, 1985). Wetting agents can help both retain soil moisture or move water throughout the soil profile to mitigate both low and high moisture extremes observed in the transition zone when UBGs have hardened into a dormancy period with limited ET rates. Overall, DeBoer et al. (2020) reported that over three years, wetting agents helped minimize winter injury and enhance early spring green-up, but the results were inconsistent from year to year.

### **Research Objectives**

The inconsistencies in utilizing remote sensing and soil sensor data for large-scale moisture stress assessments in intensively managed golf turf is critical for future improvements in water conservation and management. There are four main research objectives that will help bridge the gap from small plot research to large-scale remote sensing data of bermudagrass fairways and ultradwarf bermudagrass winter management for this dissertation.

1. Determine the effects that surface moisture has on remotely sensed visual pixel data that has been used for estimating soil moisture.

2. Assess the feasibility of utilizing thermal pixel data derived from small unmanned aerial vehicles to evaluate the distribution uniformity and efficiency of a golf course irrigation system for hybrid bermudagrass greens and tees.
3. Evaluate the feasibility of using wireless capacitive soil sensors to understand how winter covering applications impact soil temperature and moisture data for ultradwarf bermudagrass putting greens.

## References

- Alchanatis, V., Cohen, Y., Cohen, S., Moller, M., Sprinstin, M., Meron, M., Tsipris, J., Saranga, Y., & Sela, E. (2010). Evaluation of different approaches for estimating and mapping crop water status in cotton with thermal imaging. *Precision Agriculture*, 11(1), 27-41. doi:10.1007/s11119-009-9111-7
- Allen, R. G., Pereira, L. S., Raes, D., & Smith, M. (1998). Crop evapotranspiration-Guidelines for computing crop water requirements-FAO Irrigation and drainage paper 56. *Fao, Rome*, 300(9), 1-50. [https://www.avwatermaster.org/filingdocs/195/70653/172618e\\_5xAGWAx8.pdf](https://www.avwatermaster.org/filingdocs/195/70653/172618e_5xAGWAx8.pdf)
- Anjum, S. A., Xie, X., Wang, L. C., Saleem, M. F., Man, C., & Lei, W. (2011). Morphological, physiological and biochemical responses of plants to drought stress. *African journal of agricultural research*, 6(9), 2026-2032. doi:10.5897/AJAR10.027
- Badzmierowski, M. J., McCall, D. S., & Evanylo, G. (2019). Using hyperspectral and multispectral indices to detect water stress for an urban turfgrass system. *Agronomy*, 9(8), 1-15. <https://doi.org/10.3390/agronomy9080439>
- Ballester, C., Zarco-Tejada, P. J., Nicolás, E., Alarcón, J. J., Fereres, E., Intrigliolo, D. S., & Gonzalez-Dugo, V. (2018). Evaluating the performance of xanthophyll, chlorophyll and structure-sensitive spectral indices to detect water stress in five fruit tree species. *Precision Agriculture*, 19(1), 178-193. <https://doi.org/10.1007/s11119-017-9512-y>
- Beard, J., Green, R., & Sifers, S. (1992). Evapotranspiration and leaf extension rates of 24 well-watered, turf-type *Cynodon* genotypes. *HortScience*, 27(9), 986-988.
- Beard, J. B., & Beard, H. J. (2005). Beard's turfgrass encyclopedia for golf courses, grounds, lawns, sports fields.
- Biran, I., Bravdo, B., Bushkin-Harav, I., & Rawitz, E. (1981). Water Consumption and Growth Rate of 11 Turfgrasses as Affected by Mowing Height, Irrigation Frequency, and Soil Moisture 1. *Agronomy Journal*, 73(1), 85-90. <https://doi.org/10.2134/agronj1981.00021962007300010020x>

- Blackmer, T. M., Schepers, J. S., & Varvel, G. E. (1994). Light reflectance compared with other nitrogen stress measurements in corn leaves. *Agronomy Journal*, 86(6), 934-938. <https://doi.org/10.2134/agronj1994.00021962008600060002x>
- Blank, V., Skidanov, R., Doskolovich, L., & Kazanskiy, N. (2021). Spectral diffractive lenses for measuring a modified red edge simple ratio index and a water band index. *Sensors*, 21(22), 1-13. <https://doi.org/10.3390/s21227694>
- Blonquist, J. M., Norman, J. M., & Bugbee, B. (2009). Automated measurement of canopy stomatal conductance based on infrared temperature. *Agricultural and Forest Meteorology*, 149(12), 2183-2197. <https://doi.org/10.1016/j.agrformet.2009.10.003>
- Blonquist Jr, J., Jones, S. B., & Robinson, D. (2006). Precise irrigation scheduling for turfgrass using a subsurface electromagnetic soil moisture sensor. *Agricultural water management*, 84(1-2), 153-165. doi:10.1016/j.agwat.2006.01.014
- Booth, J., Hutchens, W., Askew, S., Goatley, J., Zhang, X., & McCall, D. (2024). Evaluation of Fall and Winter Trinexapac-ethyl Applications on Ultradwarf Bermudagrass Putting Green Color, Quality, and Green Cover. *HortScience*, 59(3), 355-361. <https://doi.org/10.21273/HORTSCI17519-23>
- Bowman, W. D. (1989). The relationship between leaf water status, gas exchange, and spectral reflectance in cotton leaves. *Remote Sensing of Environment*, 30(3), 249-255. [https://doi.org/10.1016/0034-4257\(89\)90066-7](https://doi.org/10.1016/0034-4257(89)90066-7)
- Braun, R. C., Bremer, D. J., & Hoyle, J. A. (2022). Simulated traffic on turfgrasses during drought stress: II. Soil moisture, soil compaction, and rooting. *International Turfgrass Society Research Journal*, 14(1), 516-527. <https://doi.org/10.1002/its2.62>
- Bray, E. A. (1993). Molecular responses to water deficit. *Plant Physiology*, 103(4), 1035-1040. doi: 10.1104/pp.103.4.1035
- Bray, E. A. (1997). Plant responses to water deficit. *Trends in plant science*, 2(2), 48-54. doi: 10.1016/S1360-1385(97)82562-9
- Bremer, D. J., Lee, H., Su, K., & Keeley, S. J. (2011a). Relationships between normalized difference vegetation index and visual quality in cool-season turfgrass: I. Variation among species and cultivars. *Crop Science*, 51(5), 2212-2218. <https://doi.org/10.2135/cropsci2010.12.0728>
- Bremer, D. J., Lee, H., Su, K., & Keeley, S. J. (2011b). Relationships between normalized difference vegetation index and visual quality in cool-season turfgrass: II. Factors affecting NDVI and its component reflectances. *Crop Science*, 51(5), 2219-2227. <https://doi.org/10.2135/cropsci2010.12.0729>
- Bristow, K. L., Campbell, G. S., & Calissendorff, K. (1993). Test of a heat-pulse probe for measuring changes in soil water content. *Soil Science Society of America Journal*, 57(4), 930-934. <https://doi.org/10.2136/sssaj1993.03615995005700040008x>

- Brown, P. (2014). Basics of evaporation and evapotranspiration. <http://hdl.handle.net/10150/311700>
- Brown, P., & Kopec, D. (2014). Converting reference evapotranspiration into turf water use. <http://hdl.handle.net/10150/312654>
- Campbell, G., Calissendorff, C., & Williams, J. (1991). Probe for measuring soil specific heat using a heat-pulse method. *Soil Science Society of America Journal*, 55(1), 291-293. <https://doi.org/10.2136/sssaj1991.03615995005500010052x>
- Cardenas-Lailhacar, B., & Dukes, M. (2012). Soil moisture sensor landscape irrigation controllers: A review of multi-study results and future implications. *Transactions of the ASABE*, 55(2), 581-590. doi: 10.13031/2013.41392
- Cardenas-Lailhacar, B., & Dukes, M. D. (2007). Turfgrass irrigation controlled by soil moisture sensor systems. *Proc., 28th Int. Irrigation Show*.
- Cardenas-Lailhacar, B., Dukes, M. D., & Miller, G. L. (2005). Sensor-based control of irrigation in bermudagrass. 2005 ASAE Annual Meeting,
- Cardenas-Lailhacar, B., Dukes, M. D., & Miller, G. L. (2008). Sensor-based automation of irrigation on bermudagrass, during wet weather conditions. *Journal of irrigation and drainage engineering*, 134(2), 120-128. [https://doi.org/10.1061/\(ASCE\)0733-9437\(2008\)134:2\(120\)](https://doi.org/10.1061/(ASCE)0733-9437(2008)134:2(120))
- Carlson, M. G., Gaussoin, R. E., & Puntel, L. A. (2022). A review of precision management for golf course turfgrass. *Crop, Forage & Turfgrass Management*, 8(2), 1-11. doi: 10.1002/cft2.20183
- Carrow, R. N. (1995). Drought resistance aspects of turfgrasses in the southeast: Evapotranspiration and crop coefficients. *Crop Science*, 35(6), 1685-1690. <https://doi.org/10.2135/cropsci1995.0011183X003500060029x>
- Carrow, R. N., Krum, J. M., Flitcroft, I., & Cline, V. (2010). Precision turfgrass management: Challenges and field applications for mapping turfgrass soil and stress. *Precision Agriculture*, 11(2), 115-134. <https://doi.org/10.1007/s11119-009-9136-y>
- Carter, G. A. (1993). Responses of leaf spectral reflectance to plant stress. *American journal of botany*, 80(3), 239-243. <https://doi.org/10.1002/j.1537-2197.1993.tb13796.x>
- Carter, G. A. (1998). Reflectance wavebands and indices for remote estimation of photosynthesis and stomatal conductance in pine canopies. *Remote Sensing of Environment*, 63(1), 61-72. doi: 10.1016/S0034-4257(97)00110-7
- Carter, G. A., Cibula, W. G., & Miller, R. L. (1996). Narrow-band reflectance imagery compared with thermalimagery for early detection of plant stress. *Journal of plant physiology*, 148(5), 515-522. [https://doi.org/10.1016/S0176-1617\(96\)80070-8](https://doi.org/10.1016/S0176-1617(96)80070-8)

- Carter, G. A., & Miller, R. L. (1994). Early detection of plant stress by digital imaging within narrow stress-sensitive wavebands. *Remote Sensing of Environment*, 50(3), 295-302. [https://doi.org/10.1016/0034-4257\(94\)90079-5](https://doi.org/10.1016/0034-4257(94)90079-5)
- Cimtay, Y., Özbay, B., Yilmaz, G., & Bozdemir, E. (2021). A new vegetation index in short-wave infrared region of electromagnetic spectrum. *IEEE Access*, 9, 148535-148545. doi: 10.1109/ACCESS.2021.3124453
- Claudio, H. C., Cheng, Y., Fuentes, D. A., Gamon, J. A., Luo, H., Oechel, W., Qiu, H.-L., Rahman, A. F., & Sims, D. A. (2006). Monitoring drought effects on vegetation water content and fluxes in chaparral with the 970 nm water band index. *Remote Sensing of Environment*, 103(3), 304-311. <https://doi.org/10.1016/j.rse.2005.07.015>
- Close, T. J. (1996). Dehydrins: emergence of a biochemical role of a family of plant dehydration proteins. *Physiologia plantarum*, 97(4), 795-803. <https://doi.org/10.1111/j.1399-3054.1996.tb00546.x>
- Cohen, Y., Alchanatis, V., Meron, M., Saranga, Y., & Tsipris, J. (2005). Estimation of leaf water potential by thermal imagery and spatial analysis. *Journal of Experimental Botany*, 56(417), 1843-1852. <https://doi.org/10.1093/jxb/eri174>
- Culpepper, T., Young, J., Montague, D. T., Sullivan, D., & Wherley, B. (2019). Physiological responses in C3 and C4 turfgrasses under soil water deficit. *HortScience*, 54(12), 2249-2256. <https://doi.org/10.21273/HORTSCI14357-19>
- Davis, S., & Dukes, M. (2010). Irrigation scheduling performance by evapotranspiration-based controllers. *Agricultural water management*, 98(1), 19-28. <https://doi.org/10.1016/j.agwat.2010.07.006>
- Dean, D. E., Devitt, D. A., Verchick, L. S., & Morris, R. L. (1996). Turfgrass quality, growth, and water use influenced by salinity and water stress. *Agronomy Journal*, 88(5), 844-849. <https://doi.org/10.2134/agronj1996.00021962008800050026x>
- DeBoer, E. J., Karcher, D. E., McCalla, J. H., & Richardson, M. D. (2020). Effect of late-fall wetting agent application on winter survival of ultradwarf bermudagrass putting greens. *Crop, Forage & Turfgrass Management*, 6(1), 1-7. <https://doi.org/10.1002/cft2.20035>
- DeBoer, E. J., Richardson, M. D., McCalla, J. H., & Karcher, D. E. (2019). Reducing ultradwarf bermudagrass putting green winter injury with covers and wetting agents. *Crop, Forage & Turfgrass Management*, 5(1), 1-9. doi:10.2134/cftm2019.03.0019
- Dettman-Kruse, J. K., Christians, N. E., & Chaplin, M. H. (2008). Predicting soil water content through remote sensing of vegetative characteristics in a turfgrass system. *Crop Science*, 48(2), 763-770. doi: 10.2135/cropsci2006.01.0040
- Edwards, E. J., & Smith, S. A. (2010). Phylogenetic analyses reveal the shady history of C4 grasses. *Proceedings of the National Academy of Sciences*, 107(6), 2532-2537. <https://doi.org/10.1073/pnas.0909672107>

- Evett, S., Laurent, J.-P., Cepuder, P., & Hignett, C. (2002). Neutron scattering, capacitance, and TDR soil water content measurements compared on four continents. 17th World Congress of Soil Science,
- Evett, S., & Steiner, J. (1995). Precision of neutron scattering and capacitance type soil water content gauges from field calibration. *Soil Science Society of America Journal*, 59(4), 961-968. <https://doi.org/10.2136/sssaj1995.03615995005900040001x>
- Feldhake, C., Danielson, R., & Butler, J. (1983). Turfgrass evapotranspiration. I. factors influencing rate in urban environments 1. *Agronomy Journal*, 75(5), 824-830. <https://doi.org/10.2134/agronj1983.00021962007500050022x>
- Fenstermaker-Shaulis, L., Leskys, A., & Devitt, D. (1997). Utilization of remotely sensed data to map and evaluate turfgrass stress associated with drought. *Journal of Turfgrass Management*, 2(1), 65-81. [https://doi.org/10.1300/J099v02n01\\_06](https://doi.org/10.1300/J099v02n01_06)
- Fitz-Rodríguez, E., & Choi, C. (2002). Monitoring turfgrass quality using multispectral radiometry. *Transactions of the ASAE*, 45(3), 865. doi: 10.13031/2013.8839
- Frank, K. (2016). The war on winter: Preparing your turfgrass for the snowy, icy, frigid months. *GreenMaster*, 51, 22-23.
- Friell, J., & Straw, C. (2021). Comparing ground-based and aerial data at field scale during dry down on golf course fairways. *International Turfgrass Society Research Journal*, 377-384. doi: 10.1002/its2.46
- Gardner, C., Dean, T., & Cooper, J. (1998). Soil water content measurement with a high-frequency capacitance sensor. *Journal of Agricultural Engineering Research*, 71(4), 395-403. <https://doi.org/10.1006/jaer.1998.0338>
- Gitelson, A., & Merzlyak, M. N. (1994). Spectral reflectance changes associated with autumn senescence of *Aesculus hippocastanum* L. and *Acer platanoides* L. leaves. Spectral features and relation to chlorophyll estimation. *Journal of plant physiology*, 143(3), 286-292. [https://doi.org/10.1016/S0176-1617\(11\)81633-0](https://doi.org/10.1016/S0176-1617(11)81633-0)
- Goatley, J., Maddox, V., Lang, D., Elmore, R., & Stewart, B. (2005). Temporary covers maintain fall bermudagrass quality, enhance spring greenup, and increase stem carbohydrate levels. *HortScience*, 40(1), 227-231.
- Goatley, M., Askew, W., Askew, S., Dickerson, J., & McCall, D. (2017). Turfgrass Cover Sources Vary in Temperature, Light and Moisture Penetration, and Weight. *International Turfgrass Society Research Journal*, 13(1), 297-304. doi: 10.2134/itsrj2016.06.0484
- Gopinath, L., Moss, J. Q., & Wu, Y. (2021a). Evaluating the freeze tolerance of bermudagrass genotypes. *Agrosystems, Geosciences & Environment*, 4(2), 1-4. doi: 10.1002/agg2.20170

- Gopinath, L., Moss, J. Q., & Wu, Y. (2021b). Quantifying freeze tolerance of hybrid bermudagrasses adapted for golf course putting greens. *HortScience*, 56(4), 478-480. <https://doi.org/10.21273/HORTSCI15606-20>
- Ham, J., Aksland, I., Casey, D., Koski, T., Qian, Y., & McClelland, C. (2021). Wireless Soil Moisture Measurement in Turfgrass with Internet-of-Things (IoT) Technology and Low-Cost Sensors. 6th Decennial National Irrigation Symposium, 6-8, December 2021, San Diego, California,
- Hejl, R., Straw, C., Wherley, B., Bowling, R., & McInnes, K. (2022). Factors leading to spatiotemporal variability of soil moisture and turfgrass quality within sand-capped golf course fairways. *Precision Agriculture*, 23(5), 1908-1917. <https://doi.org/10.1007/s11119-022-09912-4>
- Henry, M. L. (1985). *Winter survival of bermudagrass (Cynodon sp.) as influenced by traffic, mineral nutrition, plastic covers, cultural treatments, overseeding and freezing in late-winter dormancy* Virginia Polytechnic Institute and State University].
- Hong, M., & Bremer, D. J. (2021). Minimum water requirements of Japanese lawngrass for survival during prolonged drought. *Crop Science*, 61(5), 2978-2988. doi: 10.1002/csc2.20404
- Hong, M., Bremer, D. J., & van der Merwe, D. (2019a). Thermal imaging detects early drought stress in turfgrass utilizing small unmanned aircraft systems. *Agrosystems, Geosciences & Environment*, 2(1), 1-9. doi:10.2134/age2019.04.0028
- Hong, M., Bremer, D. J., & van der Merwe, D. (2019b). Using small unmanned aircraft systems for early detection of drought stress in turfgrass. *Crop Science*, 59(6), 2829-2844. doi: 10.2135/cropsci2019.04.0212
- Hopkins, G. W. (2009). *Introduction to plant physiology*. John Wiley & Sons, Inc.
- Horler, D., Dockray, M., & Barber, J. (1983). The red edge of plant leaf reflectance. *International Journal of Remote Sensing*, 4(2), 273-288. <https://doi.org/10.1080/01431168308948546>
- Horton, P., Ruban, A., & Walters, R. (1996). Regulation of light harvesting in green plants. *Annual review of plant biology*, 47(1), 655-684. <https://doi.org/10.1146/annurev.arplant.47.1.655>
- Houtz, D., Horvath, L., & Schwank, M. (2023). Vehicle mounted l-band radiometer for remote sensing of turfgrass soil moisture. IGARSS 2023-2023 IEEE International Geoscience and Remote Sensing Symposium,
- Houtz, D., Naderpour, R., & Schwank, M. (2020). Portable l-band radiometer (polra): Design and characterization. *Remote Sensing*, 12(17), 1-15. doi:10.3390/rs12172780

- Huang, B. (2008). Turfgrass water requirements and factors affecting water usage. *Water quality and quantity issues for turfgrass in urban landscapes. Council Agr. Sci. Technol. Spec. Publ*, 27, 193-205.
- Huang, B., Duncan, R., & Carrow, R. (1997a). Drought-resistance mechanisms of seven warm-season turfgrasses under surface soil drying: I. Shoot response. *Crop Science*, 37(6), 1858-1863. <https://doi.org/10.2135/cropsci1997.0011183X003700060032x>
- Huang, B., Duncan, R., & Carrow, R. (1997b). Root spatial distribution and activity of four turfgrass species in response to localized drought stress. *Int. Turfgrass Soc. Res. J*, 8, 681-690. <https://www.researchgate.net/publication/265204790>
- Huang, B., & Fry, J. D. (1998). Root anatomical, physiological, and morphological responses to drought stress for tall fescue cultivars. *Crop Science*, 38(4), 1017-1022. <https://doi.org/10.2135/cropsci1998.0011183X003800040022x>
- Huang, B., & Gao, H. (1999). Physiological responses of diverse tall fescue cultivars to drought stress. *HortScience*, 34(5), 897-901.
- Hutchens, W., Carr, T., Patton, A., Bigelow, C., DeBoer, E., Goatley, J., Martin, D., McCall, D., Miller, G., & Powlen, J. (2024). Management strategies for preventing and recovering from bermudagrass winterkill. *Crop, Forage & Turfgrass Management*, 10(2), 1-23. doi: 10.1002/cft2.20302
- Ishimwe, R., Abutaleb, K., & Ahmed, F. (2014). Applications of thermal imaging in agriculture—A review. *Advances in remote Sensing*, 3(03), 128-140. <http://dx.doi.org/10.4236/ars.2014.33011>
- Jackson, R. D., Idso, S., Reginato, R., & Pinter Jr, P. (1981). Canopy temperature as a crop water stress indicator. *Water resources research*, 17(4), 1133-1138. <https://doi.org/10.1029/WR017i004p01133>
- Jensen, M. E., Allen, R. G., American Society of Civil Engineers. Task Committee on Revision of, M., Environmental, Water Resources Institute . Committee on Evapotranspiration in, I., & Hydrology. (2016). *Evaporation, evapotranspiration, and irrigation water requirements* (Second edition. ed.). American Society of Civil Engineers.
- Jiang, Y., & Carrow, R. N. (2005). Assessment of narrow-band canopy spectral reflectance and turfgrass performance under drought stress. *HortScience*, 40(1), 242-245. doi: 10.21273/HORTSCI.40.1.242
- Jiang, Y., & Carrow, R. N. (2007). Broadband spectral reflectance models of turfgrass species and cultivars to drought stress. *Crop Science*, 47(4), 1611-1618. <https://doi.org/10.2135/cropsci2006.09.0617>
- Jiang, Y., Carrow, R. N., & Duncan, R. R. (2003). Correlation analysis procedures for canopy spectral reflectance data of seashore paspalum under traffic stress. *Journal of the American Society for Horticultural Science*, 128(3), 343-348.

- Johnsen, A. R., Horgan, B. P., Hulke, B. S., & Cline, V. (2009). Evaluation of remote sensing to measure plant stress in creeping bentgrass (*Agrostis stolonifera* L.) fairways. *Crop Science*, 49(6), 2261-2274. <https://doi.org/10.2135/cropsci2008.09.0544>
- Jury, W. A., & Vaux Jr, H. (2005). The role of science in solving the world's emerging water problems. *Proceedings of the National Academy of Sciences*, 102(44), 15715-15720. <https://doi.org/10.1073/pnas.0506467102>
- Kerry, R., Ingram, B., Hammond, K., Shumate, S. R., Gunther, D., Jensen, R. R., Schill, S., Hansen, N. C., & Hopkins, B. G. (2023). Spatial Analysis of Soil Moisture and Turfgrass Health to Determine Zones for Spatially Variable Irrigation Management. *Agronomy*, 13(5), 1267. <https://doi.org/10.3390/agronomy13051267>
- Kerry, R., Ingram, B., Henrie, A., Sanders, K., Hammond, K., Hansen, N., Jensen, R., & Hopkins, B. (2023). Assessing the ability of ECa and drone data to capture spatial patterns in soil moisture for more precise turfgrass irrigation. In *Precision agriculture'23* (pp. 277-284). Wageningen Academic. [https://doi.org/10.3920/978-90-8686-947-3\\_33](https://doi.org/10.3920/978-90-8686-947-3_33)
- Kim, K., & Beard, J. (1988). Comparative turfgrass evapotranspiration rates and associated plant morphological characteristics. *Crop Science*, 28(2), 328-331. <https://doi.org/10.2135/cropsci1988.0011183X002800020031x>
- Kjelgren, R., & Rupp, L. (1997). Water Conservation in the Urban Landscape. *HortScience*, 32(3), 549E-549. <https://doi.org/10.21273/HORTSCI.32.3.549E>
- Kreuser, W. C. (2014). Turfgrass winterkill observations from the upper great plains: desiccation and cold temperature. *Applied Turfgrass Science*, 1-3. doi:10.2134/ATS-2014-0053-BR
- Lee, H., Bremer, D. J., Su, K., & Keeley, S. J. (2011). Relationships between NDVI and visual quality in turfgrasses: Effects of mowing height. *Crop Science*, 51(1), 323-332. doi:10.2135/cropsci2010.05.0296
- Lee, J.-H. (2011). Turfgrass Responses to Water Deficit: A Review. *Asian Journal of Turfgrass Science*, 25(2), 125-132.
- Leinauer, B., VanLeeuwen, D. M., Serena, M., Schiavon, M., & Sevostianova, E. (2014). Digital image analysis and spectral reflectance to determine turfgrass quality. *Agronomy Journal*, 106(5), 1787-1794. doi:10.2134/agronj14.0088
- Linde, D. T., Stowell, L. J., Gelernter, W., & McAuliffe, K. (2011). Monitoring and managing putting green firmness on golf courses. *Applied Turfgrass Science*, 8(1), 1-9. doi:10.1094/ATS-2011-0126-01-RS.
- Lu, S., Su, W., Li, H., & Guo, Z. (2009). Abscisic acid improves drought tolerance of triploid bermudagrass and involves H<sub>2</sub>O<sub>2</sub>- and NO-induced antioxidant enzyme activities. *Plant Physiology and Biochemistry*, 47(2), 132-138. doi:10.1016/j.plaphy.2008.10.006

- Mahdavi, R., Parsa, M., Gazanchian, A., & Khazaie, H. (2017). The Effect of Different levels of Soil Moisture on Visual Quality, Morphological and Physiological Characteristics of Three Native Grass Species. *Journal Of Horticultural Science*, 31(1), 216-225.  
<https://doi.org/10.22067/jhorts4.v0i0.56264>
- Maslova, T., Markovskaya, E., & Slemnev, N. (2021). Functions of carotenoids in leaves of higher plants. *Biology Bulletin Reviews*, 11, 476-487. doi: 10.1134/S2079086421050078
- McCall, D., Zhang, X., Sullivan, D., Askew, S., & Ervin, E. (2017). Enhanced soil moisture assessment using narrowband reflectance vegetation indices in creeping bentgrass. *Crop Science*, 57(S1), 161-168. doi: 10.2135/cropsci2016.06.0471
- McCann, S. E., & Huang, B. (2008). Drought Responses of Kentucky Bluegrass and Creeping Bentgrass as Affected by Abscisic Acid and Trinexapac-ethyl. *Journal of the American Society for Horticultural Science J. Amer. Soc. Hort. Sci.*, 133(1), 20-26.  
<https://doi.org/10.21273/JASHS.133.1.20>
- McLaughlin, S. P. (2021). *Water Conservation on Hybrid Bermudagrass Fairways (Cynodon Dactylon x C. Transvaalensis) in Golf Courses Using Soil Moisture Sensors*. California State Polytechnic University, Pomona].
- Medina, C., Camacho-Tamayo, J. H., & Cortés, C. A. (2012). Soil penetration resistance analysis by multivariate and geostatistical methods. *Engenharia Agrícola*, 32, 91-101.  
<https://doi.org/10.1590/S0100-69162012000100010>
- Meron, M., Tsipris, J., Orlov, V., Alchanatis, V., & Cohen, Y. (2010). Crop water stress mapping for site-specific irrigation by thermal imagery and artificial reference surfaces. *Precision Agriculture*, 11, 148-162. doi: 10.1007/s11119-009-9153-x
- Milesi, C., Running, S. W., Elvidge, C. D., Dietz, J. B., Tuttle, B. T., & Nemani, R. R. (2005). Mapping and modeling the biogeochemical cycling of turf grasses in the United States. *Environmental management*, 36, 426-438. doi: 10.1007/s00267-004-0316-2
- Miller, G., Dukes, M., & Pressler, N. (2014). Golf course irrigation systems' distribution uniformity affects soil moisture variability. *European Journal of Horticultural Science*, 79(3), 135-141.
- Miller, G. L., & Dickens, R. (1996). Potassium fertilization related to cold resistance in bermudagrass. *Crop Science*, 36(5), 1290-1295.  
<https://doi.org/10.2135/cropsci1996.0011183X003600050036x>
- Miller, R., & Wilkinson, J. (1977). Nature of the organic coating on sand grains of nonwetttable golf greens. *Soil Science Society of America Journal*, 41(6), 1203-1204.  
<https://doi.org/10.2136/sssaj1977.03615995004100060039x>
- Moeller, A. (2012). Identify soil moisture status more accurately than ever before. *Michigan State Univ Green Section Rec*, 50(9), 1-5.

- Moreno-Espíndola, I. P., Rivera-Becerril, F., de Jesús Ferrara-Guerrero, M., & De León-González, F. (2007). Role of root-hairs and hyphae in adhesion of sand particles. *Soil Biology and Biochemistry*, 39(10), 2520-2526. <https://doi.org/10.1016/j.soilbio.2007.04.021>
- Noborio, K. (2001). Measurement of soil water content and electrical conductivity by time domain reflectometry: a review. *Computers and electronics in agriculture*, 31(3), 213-237. [https://doi.org/10.1016/S0168-1699\(00\)00184-8](https://doi.org/10.1016/S0168-1699(00)00184-8)
- Norman, G., & Throssell, C. (2009). Golf Course Environmental Profile. II, 1-49.
- O'neil, K., & Carrow, R. (1983). Perennial Ryegrass Growth, Water Use, and Soil Aeration Status under Soil Compaction 1. *Agronomy Journal*, 75(2), 177-180. <https://doi.org/10.2134/agronj1983.00021962007500020005x>
- Oerke, E.-C., Steiner, U., Dehne, H.-W., & Lindenthal, M. (2006). Thermal imaging of cucumber leaves affected by downy mildew and environmental conditions. *Journal of Experimental Botany*, 57(9), 2121-2132. <https://doi.org/10.1093/jxb/erj170>
- Park, D., Cisar, J., Fidanza, M., Nangle, E., Snyder, G., & Williams, K. (2017). Seasonal cultural management practices for aging Ultradwarf bermudagrass greens in the subtropics: I. Nitrogen and potassium fertilization. *International Turfgrass Society Research Journal*, 13(1), 280-290. doi: 10.2134/itsrj2016.05.0328
- Park, D. M., Cisar, J. L., Williams, K. E., McDermitt, D. K., Miller, W. P., & Fidanza, M. A. (2007). Using spectral reflectance to document water stress in bermudagrass grown on water repellent sandy soils. *Hydrological Processes: An International Journal*, 21(17), 2385-2389. doi: 10.1002/hyp.6752
- Parra, L., Ahmad, A., Zaragoza-Esquerdo, M., Ivars-Palomares, A., Sendra, S., & Lloret, J. (2024). A Comprehensive Survey of Drones for Turfgrass Monitoring. *Drones*, 8(10), 563. <https://doi.org/10.3390/drones8100563>
- Peñuelas, J., Filella, I., Biel, C., Serrano, L., & Save, R. (1993). The reflectance at the 950–970 nm region as an indicator of plant water status. *International Journal of Remote Sensing*, 14(10), 1887-1905. doi: 10.1080/01431169308954010
- Peñuelas, J., Gamon, J., Fredeen, A., Merino, J., & Field, C. (1994). Reflectance indices associated with physiological changes in nitrogen-and water-limited sunflower leaves. *Remote Sensing of Environment*, 48(2), 135-146. [https://doi.org/10.1016/0034-4257\(94\)90136-8](https://doi.org/10.1016/0034-4257(94)90136-8)
- Peñuelas, J., Pinol, J., Ogaya, R., & Filella, I. (1997). Estimation of plant water concentration by the reflectance water index WI (R900/R970). *International Journal of Remote Sensing*, 18(13), 2869-2875. <https://doi.org/10.1080/014311697217396>
- Pessaraki, M. (2007). *Handbook of turfgrass management and physiology* (1st ed.). CRC press. <https://doi.org/10.1201/9781420006483>

- Peterson, K., Bremer, D., Shonkwiler, K., & Ham, J. (2017). Measurement of evapotranspiration in turfgrass: A comparison of techniques. *Agronomy Journal*, *109*(5), 2190-2198. doi:10.2134/agronj2017.02.0088
- Peterson, K. W., Bremer, D. J., & Blonquist Jr, J. M. (2017). Estimating transpiration from turfgrass using stomatal conductance values derived from infrared thermometry. *International Turfgrass Society Research Journal*, *13*(1), 113-118. doi: 10.2134/itsrj2016.09.0788
- Roberson, T. L., Badzmierowski, M. J., Stewart, R. D., Ervin, E. H., Askew, S. D., & McCall, D. S. (2021). Improving Soil Moisture Assessment of Turfgrass Systems Utilizing Field Radiometry. *Agronomy*, *11*(10), 1-17. <https://doi.org/10.3390/agronomy11101960>
- Romero, C. C., & Dukes, M. D. (2008). Turfgrass Crop Coefficients in the US. Irrigation Association Conference Proceedings,
- Rosegrant, M. W., & Cai, X. (2002). Global water demand and supply projections: part 2. Results and prospects to 2025. *Water International*, *27*(2), 170-182.
- Rosegrant, M. W., Cai, X., & Cline, S. A. (2002). *Global Water Outlook to 2025: Averting an Imending Crisis*. <https://doi.org/10.1080/02508060208686990>
- Sandor, D., Karcher, D., & Richardson, M. (2022). Return on investment and water savings of add-on irrigation sensors for bermudagrass lawn irrigation in Northwest Arkansas. *Crop, Forage & Turfgrass Management*, *8*(2), 1-10. doi: 10.1002/cft2.20181
- Saxton, K., Rawls, W. J., Romberger, J. S., & Papendick, R. (1986). Estimating generalized soil-water characteristics from texture. *Soil Science Society of America Journal*, *50*(4), 1031-1036. <https://doi.org/10.2136/sssaj1986.03615995005000040039x>
- Schwank, M., Naderpour, R., & Mätzler, C. (2018). “Tau-Omega”-and two-stream emission models used for passive L-band retrievals: Application to close-range measurements over a forest. *Remote Sensing*, *10*(12), 1-24. doi:10.3390/rs10121868
- Selig, E. T., & Mansukhani, S. (1975). Relationship of soil moisture to the dielectric property. *Journal of the Geotechnical Engineering Division*, *101*(8), 755-770. <https://doi.org/10.1061/AJGEB6.0000184>
- Serraj, R., & Sinclair, T. (2002). Osmolyte accumulation: can it really help increase crop yield under drought conditions? *Plant, cell & environment*, *25*(2), 333-341. <https://doi.org/10.1046/j.1365-3040.2002.00754.x>
- Shaddox, T. W., Unruh, J. B., Johnson, M. E., Brown, C. D., & Stacey, G. (2022). Water use and management practices on US golf courses. *Crop, Forage & Turfgrass Management*, *8*(2), e20182. doi: 10.1002/cft2.20182
- Sharma, V. (2018). Methods and techniques for soil moisture monitoring.

- Shearman, R. (1986). Kentucky bluegrass cultivar evapotranspiration rates. *HortScience*, 21(3), 455-457.
- Stowell, L., Gross, P., Gelernter, W., & Burchfield, M. (2009). Measuring greens firmness using the USGA TruFirm and the Clegg Soil Impact Tester at Victoria Country Club: A preliminary study. *PACE Turf*
- Straw, C., Bolton, C., Young, J., Hejl, R., Friell, J., & Watkins, E. (2022). Soil moisture variability on golf course fairways across the United States: An opportunity for water conservation with precision irrigation. *Agrosystems, Geosciences & Environment*, 5(4), 1-12. doi: 10.1002/agg2.20323
- Straw, C. M., Bowling, W. J., & Henry, G. M. (2017). Rainfall versus irrigation influences penetration resistance and surface hardness on a recreational sports field. *International Turfgrass Society Research Journal*, 13(1), 619-623. doi: 10.2134/itsrj2016.10.0842
- Straw, C. M., Carrow, R., Bowling, W., Tucker, K., & Henry, G. (2018). Uniformity and spatial variability of soil moisture and irrigation distribution on natural turfgrass sports fields. *Journal of Soil and Water Conservation*, 73(5), 577-586. doi:10.2489/jswc.73.5.577
- Straw, C. M., Grubbs, R. A., & Henry, G. M. (2020). Short-term spatiotemporal relationship between plant and soil properties on natural turfgrass sports fields. *Agrosystems, Geosciences & Environment*, 3(1), 1-11. doi: 10.1002/agg2.20043
- Straw, C. M., & Henry, G. M. (2018). Spatiotemporal variation of site-specific management units on natural turfgrass sports fields during dry down. *Precision Agriculture*, 19(3), 395-420. <https://doi.org/10.1007/s11119-017-9526-5>
- Straw, C. M., Samson, C. O., Henry, G. M., & Brown, C. N. (2018). Does variability within natural turfgrass sports fields influence ground-derived injuries? *European journal of sport science*, 18(6), 893-902. <https://doi.org/10.1080/17461391.2018.1457083>
- Straw, C. M., Samson, C. O., Henry, G. M., & Brown, C. N. (2020). A review of turfgrass sports field variability and its implications on athlete–surface interactions. *Agronomy Journal*, 112(4), 2401-2417. doi: 10.1002/agj2.20193
- Straw, C. M., Wardrop, W. S., & Horgan, B. P. (2020). Golf course superintendents' knowledge of variability within fairways: a tool for precision turfgrass management. *Precision Agriculture*, 21(3), 637-654. <https://doi.org/10.1007/s11119-019-09687-1>
- Strunk, W., Dickson, K., Sorochan, J., & Thoms, A. (2022). Effects of mowing height and *Cynodon* spp. cultivar on traffic tolerance. *International Turfgrass Society Research Journal*, 14(1), 412-415. doi: 10.1002/its2.74
- Taghvaeian, S., Chávez, J. L., Hattendorf, M. J., & Crookston, M. A. (2013). Optical and thermal remote sensing of turfgrass quality, water stress, and water use under different soil and irrigation treatments. *Remote Sensing*, 5(5), 2327-2347. doi:10.3390/rs5052327

- Thenkabail, P. S., Smith, R. B., & De Pauw, E. (2000). Hyperspectral vegetation indices and their relationships with agricultural crop characteristics. *Remote Sensing of Environment*, 71(2), 158-182. [https://doi.org/10.1016/S0034-4257\(99\)00067-X](https://doi.org/10.1016/S0034-4257(99)00067-X)
- Throssell, C., Carrow, R., & Milliken, G. (1987). Canopy Temperature Based Irrigation Scheduling Indices for Kentucky Bluegrass Turf 1. *Crop Science*, 27(1), 126-131. <https://doi.org/10.2135/cropsci1987.0011183X002700010031x>
- Throssell, C., & Norman, G. (2007). *Golf Course Environmental Profile* (Vol. I). GCSAA.
- Throssell, C., & Norman, G. (2014). Golf Course Environmental Profile. Water Use and Conservation Practices on U.S. Golf Courses. In (Vol. I). Golf Course Superintendent Association of America.
- Throssell, C. S., Lyman, G. T., Johnson, M. E., Stacey, G. A., & Brown, C. D. (2009). Golf course environmental profile measures water use, source, cost, quality, management and conservation strategies. *Applied Turfgrass Science*, 6(1), 1-20. <https://doi.org/10.1094/ATS-2009-0129-01-RS>.
- Topp, G., Davis, J., & Annan, A. (1982). Electromagnetic determination of soil water content using TDR: I. Applications to wetting fronts and steep gradients. *Soil Science Society of America Journal*, 46(4), 672-678. <https://doi.org/10.2136/sssaj1982.03615995004600040002x>
- Trenholm, L., Carrow, R., & Duncan, R. (1999). Relationship of multispectral radiometry data to qualitative data in turfgrass research. *Crop Science*, 39(3), 763-769. <https://doi.org/10.2135/cropsci1999.0011183X003900030025x>
- Trenholm, L. E. (2000). *Low temperature damage to turf*. University of Florida Extension Institute Food and Agriculture Sciences.
- Trenholm, L. E., Schlossberg, M. J., Lee, G., Parks, W., & Geer, S. A. (2000). An evaluation of multi-spectral responses on selected turfgrass species. *International Journal of Remote Sensing*, 21(4), 709-721. doi: 10.1080/014311600210524
- Tuller, M., Or, D., & Hillel, D. (2004). Retention of water in soil and the soil water characteristic curve. *Encyclopedia of Soils in the Environment*, 4, 278-289. <https://www.researchgate.net/publication/268055840>
- White, R., Engelke, M., Morton, S. J., & Ruennele, B. (1992). Competitive turgor maintenance in tall fescue. *Crop Science*, 32(1), 251-256. <https://doi.org/10.2135/cropsci1992.0011183X003200010050x>
- Whitlark, B., Umeda, K., Leinauer, B. R., & Serena, M. (2023). Considerations with water for turfgrass in arid environments. <http://dx.doi.org/10.19103/AS.2022.0110.2>
- Young, M., Wierenga, P., & Mancino, C. (1997). Monitoring near-surface soil water storage in turfgrass using time domain reflectometry and weighing lysimetry. *Soil Science Society*

*of America Journal*, 61(4), 1138-1146.  
<https://doi.org/10.2136/sssaj1997.03615995006100040021x>

Zarco-Tejada, P. J., González-Dugo, V., & Berni, J. A. (2012). Fluorescence, temperature and narrow-band indices acquired from a UAV platform for water stress detection using a micro-hyperspectral imager and a thermal camera. *Remote Sensing of Environment*, 117, 322-337. doi:10.1016/j.rse.2011.10.007

Zarco-Tejada, P. J., González-Dugo, V., Williams, L., Suarez, L., Berni, J. A., Goldhamer, D., & Fereres, E. (2013). A PRI-based water stress index combining structural and chlorophyll effects: Assessment using diurnal narrow-band airborne imagery and the CWSI thermal index. *Remote Sensing of Environment*, 138, 38-50.  
<http://dx.doi.org/10.1016/j.rse.2013.07.024>

Zotarelli, L., Dukes, M. D., & Morgan, K. T. (2010). Interpretation of Soil Moisture Content to Determine Soil Field Capacity and Avoid Over-Irrigating Sandy Soils Using Soil Moisture Sensors: AE460/AE460, 2/2010. *EDIS*, 2010(2).

Zúñiga Espinoza, C., Khot, L. R., Sankaran, S., & Jacoby, P. W. (2017). High resolution multispectral and thermal remote sensing-based water stress assessment in subsurface irrigated grapevines. *Remote Sensing*, 9(9), 961. doi:10.3390/rs9090961

## Chapter 2: Assessing the Influence of Leaf Wetness on Remote Sensing Data for Creeping Bentgrass and Hybrid Bermudagrass

### Abstract

Locating patterns of soil moisture variability may minimize water waste when irrigating across large areas such as golf course fairways. The use of drones has been explored to harness light reflectance data to capture plant response to varying soil water content gradients. However, these data are best collected around solar zenith conditions when peak golf activity occurs and with the absence of leaf wetness from atmospheric dew deposition. This research explored how leaf wetness, from dew accumulation, and light irrigation effects two visual color indices from small unmanned aerial vehicle data collected at different time periods (morning = 9:00 and afternoon = 14:00) on creeping bentgrass (*Agrostis stolonifera*) and hybrid bermudagrass (*Cynodon dactylon* x *C. transvaalensis*) (CBG and HBG) on golf course fairways (12.7 mm height of cut) and putting greens (3.17 mm height of cut). The study was conducted across four locations using a randomized complete block design with four replications of three treatments: natural dew accumulation categorized as surface moisture, simulated lightweight rolling for dew removal, and light irrigation for dew removal. Leaf wetness was estimated after treatment implementation by implementing a custom PVC roller over a 387.35 cm<sup>2</sup> area equipped with a medical absorbent material to gather the weight of water on the leaf surface. Four subsamples per plot of soil water content data were collected using a time-domain reflectometer along with light reflectance data using a hyperspectral radiometer. The green to red ratio index (GRI) and green to blue ratio index (GBI) were utilized due to their known association with soil water content and were calculated from sUAV imagery. Leaf wetness was highest in the morning where leaf wetness was not removed (238.92 g m<sup>-2</sup>) and in the afternoon following light irrigation (36.93 g

m<sup>-2</sup>) ( $P < 0.001$ ). However, despite varying levels of leaf wetness at different times across treatments, there was minimal influence observed by treatment effects compared to aerial-derived GRI data. Furthermore, GRI showed a moderate relationship with soil water content data collected within this study ( $R^2 = 0.48$ ) and a strong relationship with comparison between ground-based GRI spectral and drone-derived GRI pixel data ( $R^2 = 0.72$ ). Moreover, this research suggests that drone data is minimally influenced by leaf wetness derived from either atmospheric dew deposition or light-irrigation applications for both CBG and HBG. This study demonstrates that drone-derived GRI values can reliably be used in the morning for plant-health assessments and estimations of volumetric water content without the requirement of displacing moisture off the leaf surface. These findings support the use of flexible data collection times, considering enhancing drone data collection focused towards practical water management strategies on large-scale golf courses.

## Introduction

Dew deposition plays an important role in plant disease epidemiology by affecting leaf wetness duration, the time that moisture remains on turfgrass or other plant surface. This duration is crucial for the development of various fungal pathogens that aid in germination, sporulation, and colonization of certain spores of diseases (Huber & Gillespie, 1992). Leaf wetness duration has been modeled for managing plant pathogens on onions, cucurbits, and turfgrass (Jespersen & Sutton, 1987; Madeira et al., 2002; Neufeld & Ojiambo, 2012; Rowlandson et al., 2015; Uddin et al., 2003). One example of research on leaf wetness includes using electronic wetness sensors on tomato plants and adjacent turfgrass to account for microclimate differences within tomato canopies for early disease warning alerts along with assessing temperature and leaf wetness duration of gray leaf spot (*Pyricularia grisea*) development on perennial ryegrass (*Lolium perenne*) (Potratz et al., 1994; Uddin et al., 2003)..

Since direct measurements of leaf wetness duration requires intensive sampling, various methods using weather data have been developed to estimate this parameter (Dalla Marta et al., 2005; Sentelhas et al., 2008). However, leaf wetness estimation methods often display variations across different leaf morphology and canopy structure due to numerous crops with varying leaf sizes, shapes, textures, and emissivity (Gillespie & Duan, 1987; Lau et al., 2000). Within turfgrass systems, variation of dew leaf wetness assessments are incorporation through measurement means such as dabbing or vacuuming the area to collect the necessary field data (Williams, 1996), Vegetation indices from optical sensors that detect solar-radiation reflectance in the near-infrared and visible-light ranges can estimate plant parameters such as tissue water content, nutrient levels, plant health, clippings yield, and total leaf biomass (Bell et al., 2004; Bell et al., 2002; Marín et al., 2020; Purevdorj et al., 1998; Sekerli et al., 2021; Trenholm et al.,

1999). For turfgrass, these indices generally align with the plant's canopy structure, but research indicates that the leaf angle distribution should also be considered (Madeira et al., 2001; Moran et al., 1989).

Dew deposition on creeping bentgrass (*Agrostis stolonifera*), Kentucky bluegrass (*Poa pratensis*), collected by means of dabbing with medical absorbent materials and wheat has been shown to cause anomalies in specific light spectrum calculations for normalized green-to-red ratio (NGRI) and the normalized difference vegetation index (NDVI) (Deery et al., 2021; Madeira et al., 2001; Pinter Jr, 1986). Although drone flights used for remote sensing applications typically occur around solar noon for optimal sunlight, this timing can conflict with high golfer density on golf courses. However, data collected in the early morning with less golfer interference may be negatively impacted by dew. One promising use of drones on golf courses is estimating soil water content status to make informed irrigation decisions. Research by Hong et al. (2019) demonstrated a strong relationship between creeping bentgrass canopy temperatures, collected via drone-mounted thermal imagery, and soil water content ( $r = -0.58$  to  $-0.72$ ), resulting in remote drought-stress detection five days before visible symptom expression.

Drones can collect vast amounts of data across large areas, like golf course fairways, which may be useful to assess general soil water content availability for site-specific management. Straw and Henry (2018) used a TORO Precision Sense 6000 mobile multi-sensor device traversing in a 15 m x 15 m spatial grid pattern to measure soil water content, penetration resistance, and NDVI on athletic fields during dry-down periods. These data were used to generate site-specific irrigation management zones, but developing these maps is either labor intensive to develop similar insights through manual sampling or expensive to purchase the necessary technology to expedite the sampling procedures. Incorporating similar spatial-analysis

methods from Straw and Henry's research (2018) into aerial remote-sensing data could offer an efficient, accurate, and data-driven approach to significant water savings. However, understanding how leaf wetness may affect aerial remote-sensing data is essential to determine whether early-morning drone flights are viable. The goal of this study was to investigate the influence of leaf wetness of creeping bentgrass and hybrid bermudagrass (*Cynodon dactylon* × *C. transvaalensis*) on visual-color indices derived from aerial drone data collected with and without dew presence.

## Materials and Methods

### 2.1 Experimental Design

Studies were conducted at two golf course locations that included creeping bentgrass (CBG) (*Agrostis stolonifera*) and hybrid bermudagrass (HBG) (*Cynodon dactylon* × *C. transvaalensis*) fairways mown at 12.70 mm and putting greens mown at 3.20 mm. The creeping-bentgrass fairway experimental area consisted of a stand of 'L-93' on a Wheeling Fine-loamy, mixed, active, mesic Ultic Hapludalfs soil at one golf course location, The Pete Dye River Course of Virginia Tech in Radford, Virginia (37.15°N, -80.52°W). The other three experimental areas, with creeping bentgrass on greens and hybrid bermudagrass on both greens and fairways, were all at a second golf course location, The Country Club of Virginia in Richmond, Virginia (37.67°N, -77.62°W). The 'Northbridge' hybrid bermudagrass fairway was established on Fine, mixed, semiactive, thermic Aquic Paleudults soil, while the 'A1/A4' creeping bentgrass and 'TifEagle' hybrid bermudagrass greens were grown in a USGA-specification greens-mix soil medium. These golf course locations were selected based on species availability, their widespread use in the golf industry, and their planophile growth habits.

Each experimental area used a randomized complete block design with four replications and three treatments. Plots measured  $1.83 \times 1.83$  m, with 0.30 m buffers between them to ensure leaf wetness was retained during experimentation. The three treatments were no dew removal, rolling with a 91.44 cm AccuForm green roller squeegee (Par Aide, St. Paul, MN) to remove leaf wetness, and light irrigation with 3.54 L of water applied by hand in two directions across each experimental replicate using a hand-watering can to simulate 6 mm of water, and based off recommendations for moving pesticides through the thatch/soil interface to remove dew (Hutchens, 2018). Treatments were applied in the morning (9:00) and afternoon (14:00) with all data collected for each time period at each location after treatment implementation (Figure 1).

## *2.2 Wetness Measurements*

Leaf wetness of the turfgrass canopy was quantified immediately after treatments were applied using medical-absorbent material as a moisture collector adhered to 12.7 cm long  $\times$  3.18 cm diameter PVC tubes (Figure 2). Prior to sampling, dry weight of moisture collectors were measured. Following data collection, all moisture collectors were immediately sealed in Ziploc bags to prevent atmospheric absorption or evaporation after collecting water within the plots. Each leaf wetness collector was rolled three times along a linear distance of 30.50 cm within the plot to ensure all moisture in the  $387.35 \text{ cm}^2$  sampled area was fully collected. The weight difference of the moisture collectors before and after collection was assumed to be the grams of water per  $387.35 \text{ cm}^2$ , which was eventually converted into grams of water  $\text{m}^{-2}$  of the plot area. The moisture data collected was used to validate the treatment effect of differing leaf wetness amounts on the tested areas. Soil water content and narrowband canopy reflectance were measured using a Field Scout Time-Domain Reflectometer 350 (TDR, Aurora, IL) and a Spectral

Evolution PSR-1100 hyper-spectral radiometer (HSR, Haverhill, MA), respectively, immediately after canopy moisture collections.

### *2.3 Soil Water Content and Spectral Data*

At each location, four soil water content and canopy reflectance readings were collected by always starting in the lower left corner for each experimental plot and rotating clockwise for each subsequent measurement within the plot. This sampling order was performed throughout the tested area for each replication of each treatment within the study. With each soil water content and canopy reflectance reading, the unit was extended 0.91 meters toward the center of the plot to collect the desired data point. The described format for the collected ground data was used to ensure no edge effect within the plots occurred and to keep all data collection in a standardized, reproducible format. Before collecting data at each location, the TDR and HSR were both calibrated to ensure their accuracy. The TDR was equipped with 3.81cm probes and calibrated according to the manufacturer's specifications using distilled water. The radiometer was fitted with a  $5^\circ \times 5^\circ$  field-of-view lens attached to a fiber-optic cable to transmit the collected spectral solar radiation through the lens and calibrated using a barium sulfate ( $\text{BaSO}_4$ ) white reference panel that represents 100 percent light reflectance. The lens was attached to a custom PVC stand that was 1.23 m in height and extended out 0.92 m from the base of the stand at a  $90^\circ$  position (NADIR-pointing sensor) above the sampling surface. The sun angle was considered to prevent any shadowing within the plot and simulated the angle of a drone camera during flight, providing a spatial resolution sampling area of  $11.07 \text{ cm}^2$  (Figure 3).

Four samples per plot of both soil water content and canopy reflectance data were taken from the corners of the plot and sampled in a clockwise pattern. All soil water content and canopy reflectance data were averaged per plot and used for further analysis, comparing the

ground spectral data to the aerial remotely sensed pixel value data. The averaged spectral reflectance data per plot were then used to construct two vegetation indices, Green-to-Blue Ratio Index ( $GRI = R_{550}/R_{475}$ ) and the Green-to-Red Ratio Index ( $GRI = R_{550}/R_{670}$ ) that are known to be correlated with soil water content through greenhouse and small plot research on CBG and HBG areas (Gitelson et al., 2002; Hong et al., 2019; Jia et al., 2019; Roberson et al., 2021).

#### *2.4 Remote Sensing Data and Pixel Processing*

Remote sensing data were collected using a Mavic 2 Enterprise Advanced (DJI, Shenzhen, China), equipped with a 48 Megapixel camera and flown to acquire all aerial imagery. All images were captured within minutes of finishing the soil water content and canopy reflectance ground data collected for both morning and afternoon treatment events to ensure that pixel color values represent the ground truth data collected in a proximal timeframe. A series of aerial images were collected via a mission plan to simulate data collection across larger areas, such as a golf course fairway. The small unmanned aerial vehicle (sUAV) was flown at an above-ground level of 60 m, providing a ground sampling distance of 0.52 cm with a front and side overlap of both 80% to ensure enough pixel overlap for accurate image georeferencing. Approximately 260 images were captured for testing locations in the Richmond, Virginia area, while 122 images were captured for the Radford, Virginia tested location. Images were georeferenced using spatial data corresponding to field ground control points collected using an Emlid Reach RS+ (Budapest, Hungary) survey equipment and orthomosaicked using Pix4DMapper (version 4.8.2, Prilly, Switzerland). A polygon layer for each plot at each tested location  $1.80 \text{ m} \times 1.80 \text{ m}$  was created over the orthomosaic base layer using QGIS (version 3.28) open-source software. A 0.30 m buffer was applied to each plot to minimize edge effects, creating a plot sampling size of  $1.50 \text{ m} (0.0000135^\circ) \times 1.50 \text{ m} (0.0000135^\circ)$ . This plot buffer was

accomplished by calculating the centroid of each plot and using the processing tool, ‘Rectangles, Ovals, and Diamonds,’ to create polygons within each plot centered by the centroid and rotated appropriately to align with each plot at each location before ‘Raster Extraction’ using the ‘clipped raster by mask layer’ function (Figure 4).

Each location and time of data collection (morning or afternoon), equaling a total of 96 images with approximately 116,000 pixels per single plot image, were processed using Python (version 3.22). Within Python, the NumPy library was used to split each image into three layers of red, green and blue pixel values and calculate the total average red, green and blue color value for each extracted plot image. These average pixel values were used to calculate the Green-to-Blue Ratio Index ( $GRI = \text{Green}/\text{Blue}$ ), and the Green-to-Red Ratio Index ( $GRI = \text{Green}/\text{Red}$ ) previously listed and stored into a Data Frame to export for further analysis. All data was analyzed using SAS JMP Pro (version 16.0.2 Cary, NC). Data were subjected to a mixed model effects test for grass species, grass height, treatment, time of data collection and their associated interactions with the physical golf course location and replication incorporated as a random effects. Further analysis was interpreted based on an analysis of variance with least square means separated using Tukey-Kramer honest significant difference at a  $\alpha = 0.05$ .

## **Results and Discussion**

Two vegetation indices GBI and GRI were calculated through ratios using wavelengths of light centered within the blue, green, and red regions of visible light due to their known relationships with soil water content and the ability for cheaper data collection with a RGB camera compared to multi-spectral data (Badzmierowski et al., 2019; McCall et al., 2017; Roberson et al., 2021). Between the two indices, the green-to-red ratio index was found to be the most related with soil water content ( $R^2 = 0.48$ ) (Figure 5). This finding is similar to the reporting by McCall et al.

(2017) who found that GRI was moderately related to soil water content across two trials ( $r = 0.50 - 0.73$ ). However, one key point is their study was in a controlled greenhouse environment using a spot lens with direct contact on the turfgrass surface, whereas our study sees these same relationships within field conditions and larger sampling distance from the turfgrass plant. Furthermore, since the same green wavelength of light is used for both GBI and GRI, it is presumed that the red wavelength of light is what provides the relationship to soil water content. Similar findings were reported with Nagy et al. (2014) using a laboratory spectrometer between 400 – 1000 nm wavelengths to evaluate the wetting fronts of differing soil textures to identify soil texture classes through the high absorption characteristics of water. They found that within the visible spectrum, blue light was 10 – 20% reflectance, green light was 12 – 35% reflectance, and red wavelengths of light had a 15 – 50% reflectance ranging from sandy to heavy clay soils, respectively. Furthermore, they determined that through principal component analysis that 550 – 710 nm wavelengths were the most sensitive to soil water content and texture ( $r^2 = 0.60$ ), corresponding to the upper green and red regions of light. Our data follow similar trends when looking at Pearson correlation relationships (Table 1).

Our data showed that a significant relationship exists between soil water content and ground based individual spectral bands of blue and green wavelengths ( $P < 0.0003$ ) but not for red wavelengths (Table 1). However, a significance is observed with soil water content and ground based spectral data for GRI and not seen with GBI. Furthermore, GRI also displayed a non-significant relationship when compared to leaf wetness, meaning, it is related to soil water content and not influenced by any moisture present on the turfgrass surface during this study. Additionally, no drone aerial derived index from pixel data showed any significance when compared with leaf wetness, but a stronger relationship was observed with aerial derived GRI ( $P$

< 0.0001) compared to GBI ( $P = 0.0027$ ) when examined with soil water content. These results also align with digital image analysis looking at incremental soil water content additions to six oven dried soils from sandy loam to heavy clay compared with red, green, and blue pixel values extracted from imagery (Dos Santos et al., 2016). They found that red pixel values had the strongest negative correlation ( $r = -0.76$  to  $-0.90$ ) as with varying soil types as they were wetted and the associated Munsell color ratings compared, with green ( $r = -0.63$  to  $-0.94$ ) followed by blue ( $-0.05$  to  $-0.94$ ) pixel values within the visible region of light. This could be due to the shorter wavelengths of blue light that may be more influenced by the leaf wetness from treatment effects on the turfgrass canopy being scattered or refracted before penetrating through the plant canopy. Whereas red light may penetrate and be absorbed by water beyond the surface and leaf water content related to the plant because red light has a higher dependency on plant pigments concentrations and not plant water content (Gausman, 1983; Ollinger, 2011).

The data suggest that the best of the two explored vegetation indices was GRI; however, understanding how these ground-based spectral data related to the drone pixel data was a crucial component. The ground based GRI data compared with color pixel data extracted from imagery showed a strong relationship ( $R^2 = 0.72$ ) for all locations (data not shown). The comparison was separated by time of data collection (morning and afternoon) with all data pooled across grass species and treatments to understand how leaf wetness may influence these relationships. Morning ground and drone-based spectral data showed a moderate relationship when compared ( $R^2 = 0.62$ ) compared to a strong relationship with spectral data sampled in the afternoon time period ( $R^2 = 0.88$ ) (Figure 6). Higher variation is seen with field conditions involving light diffusion and/or scattering that occurs during the spectral data sampled in the morning. This could be due to the incidence solar angle not being at solar zenith which can cause up to 50%

variation in light refraction back to the sUAV camera to capture associated light data (Jafarbiglu & Pourreza, 2023). Furthermore, while our flight plans were scheduled around full sun conditions to avoid any pixel data degradation observed from partly cloudy conditions (Hama et al., 2022; Stow et al., 2019; Wang et al., 2023), early morning periods can have a boundary layer of atmospheric moisture due to higher humidity that amplifies the scattering effect across blue, green, and red wavelengths at flight altitudes of 125 and 200 m (Kedzierski et al., 2019). The humidity boundary layer could allude to the source of variation seen in our data due to a range of 35% and 83% humidity at the time of sampling for morning and afternoon pixel data, respectively.

Grass species, time of data collection (Time), and treatment were all significant for leaf wetness data ( $P < 0.001$ ) and grass species  $\times$  time, grass species  $\times$  treatment and time  $\times$  treatment interactions also significant ( $P < 0.001$ ) (Table 2). Within the model, time has the largest F-score (246.28) signifying that the overall variation between groups is largest compared to within group variation. In fact, time of data collection for morning sampling was significantly different ( $101.43 \text{ g m}^{-2}$ ) of water compared to afternoon data sampling ( $13.09 \text{ g m}^{-2}$ ) (data not shown). Furthermore, for all data pooled by treatment, rolled areas showed the least amount of leaf wetness ( $9.04 \text{ g m}^{-2}$ ) followed by light irrigation ( $42.56 \text{ g m}^{-2}$ ) and untreated ( $120 \text{ g m}^{-2}$ ) suggesting that the untreated check treatment with no displacement of water on the turfgrass canopy had the most water collected. Looking at the time  $\times$  treatment interaction, we notice that the untreated check in the morning had the highest leaf wetness ( $238.92 \text{ g m}^{-2}$ ) and was statistically different ( $P \leq 0.0001$ ) compared to light irrigation ( $48.19 \text{ g m}^{-2}$ ) and rolled ( $17.20 \text{ g m}^{-2}$ ), respectively. These trends shift for the afternoon sampling period with light irrigation showing the highest leaf wetness ( $36.94 \text{ g m}^{-2}$ ), compared to the untreated check ( $1.45 \text{ g m}^{-2}$ ) and

rolled ( $0.889 \text{ g m}^{-2}$ ), respectively. These observations make sense considering atmospheric dew deposition occurs naturally through the condensation of water vapor into a liquid on a substrate, but can continually deposit when removed from the surface, and may explain why minimal amounts of water were collected for rolled treatments during morning periods (Beysens, 1995). Furthermore, the absence of leaf wetness for untreated areas in afternoon time periods would be due to the evaporation of the undisturbed leaf wetness naturally formed on the turfgrass canopy. Another observation is the leaf wetness differences between grass species with creeping bentgrass having more leaf wetness on the canopy ( $74.19 \text{ g m}^{-2}$ ) compared to hybrid bermudagrass ( $40.34 \text{ g m}^{-2}$ ), however, this was not significant ( $P = 0.0715$ ). The difference in leaf wetness relative to grass species is most likely attributed to the soil water content characteristics at the time of the study.

Soil water content for grass species was found to be higher for creeping bentgrass (39.10%) compared to hybrid bermudagrass (27.88%). These soil moisture differences most likely influence the variation in leaf wetness observed due to the findings by Hughes and Brimblecombe (1994) who reported a strong correlation between soil water content and dew formation ( $r^2 = 0.87$ ). Moreover, for soil water content we see for all data pooled and separated by time for data collected, was significant for morning sampling periods having higher soil water content (35.14%) compared to afternoon (31.83%) ( $P = 0.0413$ ). Treatment effects also show a significance for soil water content with light irrigation (35.57%) compared to untreated (33.10%) and rolled (31.79%) treatments, respectively. These findings align with the treatment inputs of light irrigation (6.35 mm) adding additional water into the soil profile evaluating the movement of insecticides (isazofos) and fungicides (metalaxyl, myclobutanil, and tebuconazole) (Hutchens, 2018; Starrett et al., 2000).

Examining pixel data shows that there is a strong significance with a grass species  $\times$  grass height interaction with creeping bentgrass having a higher green-to-red ratio value for both green and fairway heights (1.11 and 1.29) respectively, compared to hybrid bermudagrass (1.00 and 1.04 respectively). In fact, for both grass species fairways had higher green-to-red ratio pixel values compared to greens and attributed a larger surface area of tissue material being sampled by drone imagery. Moreover, treatment was significant with untreated check having a lower significant green to red ratio value (1.10) compared to rolled and light irrigation (1.11 and 1.12) respectively, and likely due to more atmospheric dew deposition that naturally formed on the untreated plots compared to other treatment effects. This layer of surface leaf wetness may lead to a higher absorption band coefficient observed in the red region of light with pure water (Sogandares & Fry, 1997). An significant interaction between grass height  $\times$  time was further observed with fairway height of cut areas in the morning (1.18) higher than afternoon (1.16) readings compared to morning color pixel data being higher for greens in the afternoon (1.07) compared to morning (1.04) sampling periods. The lower leaf wetness previously reported for greens could allude to these data for green to red pixel data seen with water influencing the amount of red light being absorbed.

A -three-way interaction was observed between grass species  $\times$  time of data collection  $\times$  treatment for both leaf wetness and green-to-red ratio index and separated by treatment for further analysis (Table 3). Overall, leaf wetness was highest for both bentgrass and bermudagrass in the morning periods for the untreated treatment (314.15 and 163.7 g m<sup>-2</sup>) and light irrigation (47.38 and 26.49 g m<sup>-2</sup>) for the afternoon. However, examining the color pixel values shows little-to-no influence of pixel data with the same three-way interaction. Green-to-red ratio pixel data showed there was no influence for morning data sampled on both creeping bentgrass and

bermudagrass separated by treatment and only bermudagrass sampled in the morning timeframe. Only bermudagrass showed differences for the untreated and rolling treatments being similar (1.01 and 1.02) compared to light irrigation (1.04) during afternoon data collection periods. These data suggest that while leaf wetness is affected by atmospheric dew deposition and light irrigation and that will pose some influence on spectral and color pixel data, the effects are less than previously hypothesized?. Further research is required to understand under different lighting and weather characteristics what standard green to red ratio values would be representative for these grass species tested and others not included within this study. Standardizing these values would provide relevance towards what is expected compared to anomalies observed.

### **Conclusions**

This research investigated the impact of leaf wetness on remote sensing data derived from drones, specifically focusing on creeping bentgrass and hybrid bermudagrass in golf course environments. The research aims to assess how dew accumulation and light irrigation influence visual color indices, namely the Green to Red Ratio Index (GRI) and Green to Blue Ratio Index (GBI), which are associated with soil water content. Conducted across four locations with a randomized complete block design, the study employed treatments including natural dew accumulation, simulated rolling for dew removal, and light irrigation. Leaf wetness was measured by implementing a customized rolling collection unit alongside soil water content using time-domain reflectometry and light reflectance data via a hyperspectral radiometer. Findings revealed that leaf wetness was highest in the morning and post-irrigation in the afternoon, yet treatment effects showed minimal influence on GRI data. The GRI exhibited a moderate correlation with soil water content data and a strong correlation when comparing ground-based GRI spectral data with drone-derived GRI pixel data. The results suggest that

sUAV derived GRI values remain reliable in assessing turfgrass health or estimating volumetric water content without needing to displace surface moisture on the turfgrass canopy. This flexibility in data collection timing could enhance practical water management strategies for conducting on course drone flights with a wider range of flight times acceptable considering that environmental conditions such as cloud cover remain stable throughout the flight acquisition. The study highlights the importance of considering leaf wetness in remote sensing applications and supports the viability of earlier morning drone flights for future remote sensing data acquisition needs. Overall, the research underscores the potential for utilizing drone technology for visual pixel color data while addressing the complexities introduced by atmospheric dew deposition to evaluate potential aerial imagery data collection outside of solar zenith timeframes.

#### References

- Badzmierowski, M. J., McCall, D. S., & Evanylo, G. (2019). Using hyperspectral and multispectral indices to detect water stress for an urban turfgrass system. *Agronomy*, 9(8), 1-15. <https://doi.org/10.3390/agronomy9080439>
- Bell, G., Howell, B., Johnson, G., Raun, W., Solie, J., & Stone, M. (2004). Optical sensing of turfgrass chlorophyll content and tissue nitrogen. *HortScience*, 39(5), 1130-1132.
- Bell, G., Martin, D., Wiese, S., Dobson, D., Smith, M., Stone, M., & Solie, J. (2002). Vehicle-mounted optical sensing: An objective means for evaluating turf quality. *Crop Science*, 42(1), 197-201. doi: 10.2135/cropsci2002.1970
- Beysens, D. (1995). The formation of dew. *Atmospheric research*, 39(1-3), 215-237. [https://doi.org/10.1016/0169-8095\(95\)00015-J](https://doi.org/10.1016/0169-8095(95)00015-J)
- Dalla Marta, A., Magarey, R., & Orlandini, S. (2005). Modelling leaf wetness duration and downy mildew simulation on grapevine in Italy. *Agricultural and Forest Meteorology*, 132(1-2), 84-95. <https://doi.org/10.1016/j.agrformet.2005.07.003>
- Deery, D. M., Smith, D. J., Davy, R., Jimenez-Berni, J. A., Rebetzke, G. J., & James, R. A. (2021). Impact of varying light and dew on ground cover estimates from active NDVI, RGB, and LiDAR. *Plant Phenomics*, 2021. <https://doi.org/10.34133/2021/9842178>

- Dos Santos, J. F., Silva, H. R., Pinto, F. A., & Assis, I. R. d. (2016). Use of digital images to estimate soil moisture. *Revista Brasileira de Engenharia Agrícola e Ambiental*, 20, 1051-1056. DOI: <http://dx.doi.org/10.1590/1807-1929/agriambi.v20n12p1051-1056>
- Gausman, H. W. (1983). Visible light reflectance, transmittance, and absorptance of differently pigmented cotton leaves. *Remote Sensing of Environment*, 13(3), 233-238. [https://doi.org/10.1016/0034-4257\(83\)90041-X](https://doi.org/10.1016/0034-4257(83)90041-X)
- Gillespie, T., & Duan, R.-X. (1987). A comparison of cylindrical and flat plate sensors for surface wetness duration. *Agricultural and Forest Meteorology*, 40(1), 61-70. [https://doi.org/10.1016/0168-1923\(87\)90055-4](https://doi.org/10.1016/0168-1923(87)90055-4)
- Gitelson, A., Stark, R., Grits, U., Rundquist, D., Kaufman, Y., & Derry, D. (2002). Vegetation and soil lines in visible spectral space: A concept and technique for remote estimation of vegetation fraction. *International Journal of Remote Sensing*, 23(13), 2537-2562. doi: 10.1080/01431160110107806
- Hama, A., Sato, M., Tsukamoto, Y., & Matsuoka, N. (2022). Estimation of sunlight conditions through a drone-mounted solar irradiation sensor. *Journal of Agricultural Meteorology*, 78(3), 113-120. doi: 10.2480/agrmet.D-21-00049
- Hong, M., Bremer, D. J., & van der Merwe, D. (2019). Using small unmanned aircraft systems for early detection of drought stress in turfgrass. *Crop Science*, 59(6), 2829-2844. doi: 10.2135/cropsci2019.04.0212
- Huber, L., & Gillespie, T. (1992). Modeling leaf wetness in relation to plant disease epidemiology. *Annual review of phytopathology*, 30(1), 553-577. <https://doi.org/10.1146/annurev.py.30.090192.003005>
- Hughes, R., & Brimblecombe, P. (1994). Dew and guttation: formation and environmental significance. *Agricultural and Forest Meteorology*, 67(3-4), 173-190. [https://doi.org/10.1016/0168-1923\(94\)90002-7](https://doi.org/10.1016/0168-1923(94)90002-7)
- Hutchens, W. J. (2018). *Effect of Irrigation Amount and Soil Surfactants on Fungicide Movement and Efficacy in Turfgrass Systems*. North Carolina State University.
- Jafarbiglu, H., & Pourreza, A. (2023). Impact of sun-view geometry on canopy spectral reflectance variability. *ISPRS Journal of Photogrammetry and Remote Sensing*, 196, 270-286. <https://doi.org/10.1016/j.isprsjprs.2022.12.002>
- Jespersion, G., & Sutton, J. (1987). Evaluation of a forecaster for downy mildew of onion (*Allium cepa* L.). *Crop protection*, 6(2), 95-103.
- Jia, S., Kim, S. H., Nghiem, S. V., & Kafatos, M. (2019). Estimating live fuel moisture using SMAP L-band radiometer soil moisture for Southern California, USA. *Remote Sensing*, 11(13), 1575. doi:10.3390/rs11131575

- Kedzierski, M., Wierzbiński, D., Sekrecka, A., Fryskowska, A., Walczykowski, P., & Siewert, J. (2019). Influence of lower atmosphere on the radiometric quality of unmanned aerial vehicle imagery. *Remote Sensing*, *11*(10), 1214. doi:10.3390/rs11101214
- Lau, Y. F., Gleason, M. L., Zriba, N., Taylor, S. E., & Hinz, P. N. (2000). Effects of coating, deployment angle, and compass orientation on performance of electronic wetness sensors during dew periods. *Plant disease*, *84*(2), 192-197. <https://doi.org/10.1094/PDIS.2000.84.2.192>
- Madeira, A., Gillespie, T., & Duke, C. (2001). Effect of wetness on turfgrass canopy reflectance. *Agricultural and Forest Meteorology*, *107*(2), 117-130. [https://doi.org/10.1016/S0168-1923\(00\)00230-6](https://doi.org/10.1016/S0168-1923(00)00230-6)
- Madeira, A., Kim, K., Taylor, S., & Gleason, M. (2002). A simple cloud-based energy balance model to estimate dew. *Agricultural and Forest Meteorology*, *111*(1), 55-63. [https://doi.org/10.1016/S0168-1923\(02\)00004-7](https://doi.org/10.1016/S0168-1923(02)00004-7)
- Marín, J., Yousfi, S., Mauri, P. V., Parra, L., Lloret, J., & Masaguer, A. (2020). RGB vegetation indices, NDVI, and biomass as indicators to evaluate C3 and C4 turfgrass under different water conditions. *Sustainability*, *12*(6), 2160. doi:10.3390/su12062160
- McCall, D., Zhang, X., Sullivan, D., Askew, S., & Ervin, E. (2017). Enhanced soil moisture assessment using narrowband reflectance vegetation indices in creeping bentgrass. *Crop Science*, *57*(S1), 161-168. doi: 10.2135/cropsci2016.06.0471
- Moran, M. S., Pinter Jr, P. J., Clothier, B. E., & Allen, S. G. (1989). Effect of water stress on the canopy architecture and spectral indices of irrigated alfalfa. *Remote Sensing of Environment*, *29*(3), 251-261. [https://doi.org/10.1016/0034-4257\(89\)90004-7](https://doi.org/10.1016/0034-4257(89)90004-7)
- Nagy, A., Riczu, P., Gálya, B., & Tamás, J. (2014). Spectral estimation of soil water content in visible and near infra-red range. *Eurasian Journal of Soil Science*, *3*(3), 163-171. <https://doi.org/10.18393/ejss.69645>
- Neufeld, K., & Ojiambo, P. (2012). Interactive effects of temperature and leaf wetness duration on sporangia germination and infection of cucurbit hosts by *Pseudoperonospora cubensis*. *Plant disease*, *96*(3), 345-353. <http://dx.doi.org/10.1094/PDIS-07-11-0560>
- Ollinger, S. V. (2011). Sources of variability in canopy reflectance and the convergent properties of plants. *New phytologist*, *189*(2), 375-394. doi: 10.1111/j.1469-8137.2010.03536.x
- Pinter Jr, P. J. (1986). Effect of dew on canopy reflectance and temperature. *Remote Sensing of Environment*, *19*(2), 187-205. [https://doi.org/10.1016/0034-4257\(86\)90071-4](https://doi.org/10.1016/0034-4257(86)90071-4)
- Potratz, K. J., Gleason, M. L., Hockmuth, M. L., Parker, S. K., & Pearston, G. A. (1994). Testing the accuracy and precision of wetness sensors in a tomato field and on turfgrass. *Journal of the Iowa Academy of Science: JIAS*, *101*(2), 56-60. <https://scholarworks.uni.edu/jias/vol101/iss2/8>

- Purevdorj, T., Tateishi, R., Ishiyama, T., & Honda, Y. (1998). Relationships between percent vegetation cover and vegetation indices. *International Journal of Remote Sensing*, *19*(18), 3519-3535. doi: 10.1080/014311698213795
- Roberson, T. L., Badzmierowski, M. J., Stewart, R. D., Ervin, E. H., Askew, S. D., & McCall, D. S. (2021). Improving Soil Moisture Assessment of Turfgrass Systems Utilizing Field Radiometry. *Agronomy*, *11*(10), 1-17. <https://doi.org/10.3390/agronomy11101960>
- Rowlandson, T., Gleason, M., Sentelhas, P., Gillespie, T., Thomas, C., & Hornbuckle, B. (2015). Reconsidering leaf wetness duration determination for plant disease management. *Plant disease*, *99*(3), 310-319. <https://doi.org/10.1094/PDIS-05-14-0529-FE>
- Sekerli, Y. E., Keskin, M., & Soysal, Y. (2021). A low-cost prototype optical sensor to evaluate water, macro and micro elements of turfgrass clippings. *Sensors and Actuators A: Physical*, *323*, 112615. <https://doi.org/10.1016/j.sna.2021.112615>
- Sentelhas, P. C., Dalla Marta, A., Orlandini, S., Santos, E. A., Gillespie, T. J., & Gleason, M. L. (2008). Suitability of relative humidity as an estimator of leaf wetness duration. *Agricultural and Forest Meteorology*, *148*(3), 392-400. <https://doi.org/10.1016/j.agrformet.2007.09.011>
- Sogandares, F. M., & Fry, E. S. (1997). Absorption spectrum (340–640 nm) of pure water. I. Photothermal measurements. *Applied optics*, *36*(33), 8699-8709. <https://doi.org/10.1364/AO.36.008699>
- Starrett, S., Christians, N., & Al Austin, T. (2000). Movement of herbicides under two irrigation regimes applied to turfgrass. *Advances in environmental Research*, *4*(2), 169-176. [https://doi.org/10.1016/S1093-0191\(00\)00020-4](https://doi.org/10.1016/S1093-0191(00)00020-4)
- Stow, D., Nichol, C. J., Wade, T., Assmann, J. J., Simpson, G., & Helfter, C. (2019). Illumination geometry and flying height influence surface reflectance and NDVI derived from multispectral UAS imagery. *Drones*, *3*(3), 55. doi:10.3390/drones3030055
- Straw, C. M., & Henry, G. M. (2018). Spatiotemporal variation of site-specific management units on natural turfgrass sports fields during dry down. *Precision Agriculture*, *19*(3), 395-420. <https://doi.org/10.1007/s11119-017-9526-5>
- Trenholm, L., Carrow, R., & Duncan, R. (1999). Relationship of multispectral radiometry data to qualitative data in turfgrass research. *Crop Science*, *39*(3), 763-769. <https://doi.org/10.2135/cropsci1999.0011183X003900030025x>
- Uddin, W., Serlemitsos, K., & Viji, G. (2003). A temperature and leaf wetness duration-based model for prediction of gray leaf spot of perennial ryegrass turf. *Phytopathology*, *93*(3), 336-343. <https://doi.org/10.1094/PHTO.2003.93.3.336>
- Wang, Y., Yang, Z., Kootstra, G., & Khan, H. A. (2023). The impact of variable illumination on vegetation indices and evaluation of illumination correction methods on chlorophyll

content estimation using UAV imagery. *Plant Methods*, 19(1), 51.  
<https://doi.org/10.1186/s13007-023-01028-8>

Williams, D. W. (1996). *The role (s) of dew in the epidemiology of dollar spot*. University of Kentucky.

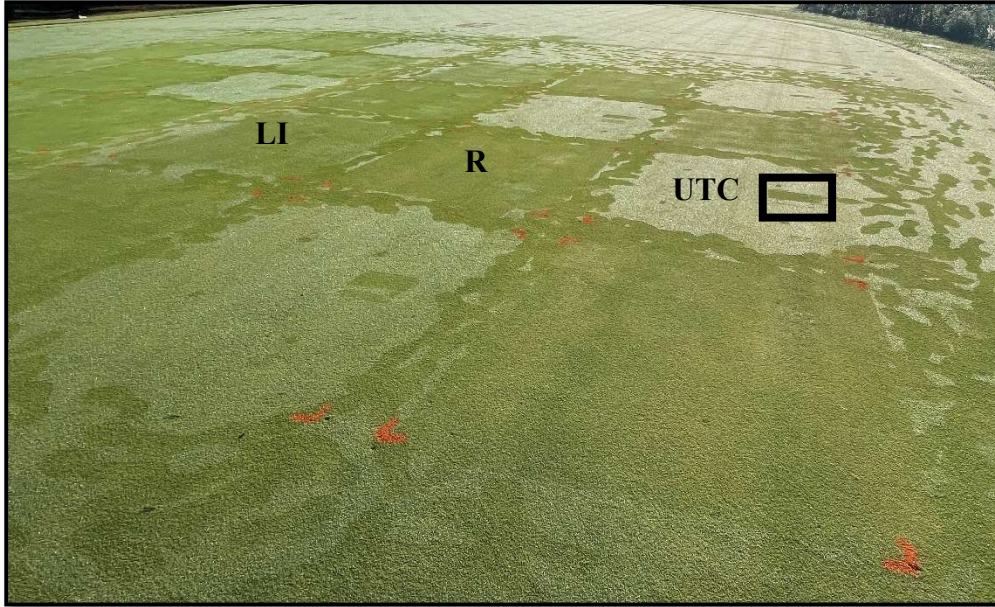


**Figure 1.** Visual example of the experimental treatments of light irrigation (LI), rolling (R), and leaf wetness (UTC) on a ‘TifEagle’ ultradwarf bermudagrass (*Cynodon dactylon* x *C. transvaalensis*). The small square with an absence of surface moisture (black box) within the UTC plot is an example of the reference area where surface moisture data were collected using the custom PVC roller with a spatial sampling size of 387.35 cm<sup>2</sup> post treatment initiation.



**Figure 2.** Visual example of the Custom PVC roller measuring 3.18 cm in diameter x 12.7 cm in length that has a smaller PVC handle inserted through the center and traversed across a length of 30.48 cm sampling a total area of 387.35 cm<sup>2</sup> on ‘Northbridge’ hybrid bermudagrass (*Cynodon dactylon* x *C. transvaalensis*) at the Country Club of Virginia in Richmond, Virginia.



**Figure 3.** Representation of the custom-made PVC stand with a retrofitted arm that extends out 91.44 cm in length and holds the radiometer 5° field of view lens in order at a height of 127 cm to standardize the ground spectral data collection process at a spot sampling size of 10 cm<sup>2</sup>. This sampling standard was done for each location at the Pete Dye River Course in Radford, Virginia and The Country Club of Virginia in Richmond, Virginia.

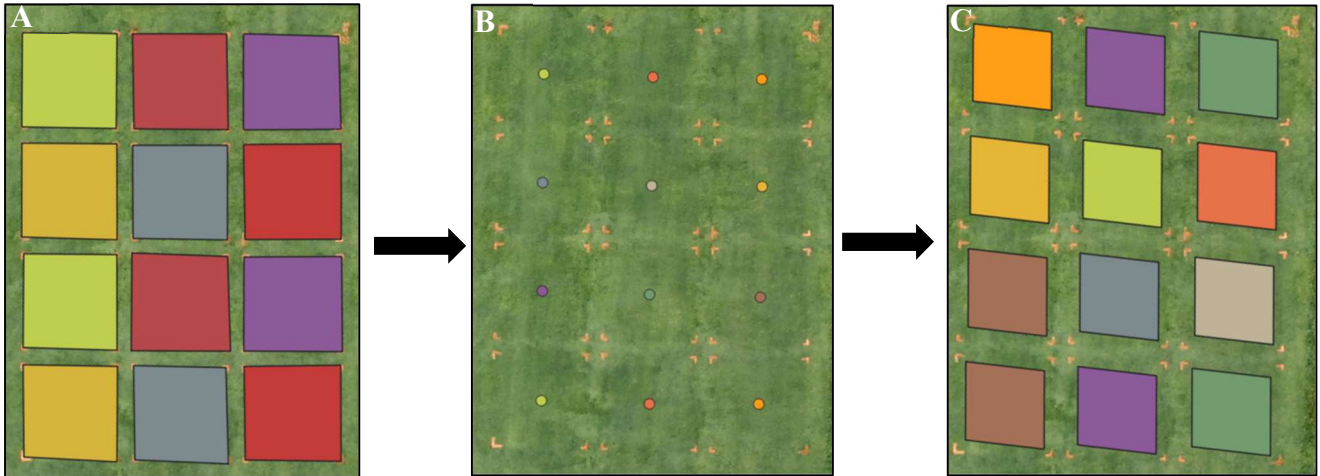


**Figure 4.** Visual for standardized process flow using QGIS (version 3.28) spatial analysis software to A) Generate individual plot polygons from stitched orthomosaic at the time of study B) determining the centroid of the polygons comprised of the entire plot areas and C). using the processing tool ‘Rectangles, Ovals, and Diamonds’, to generate 1.5 m × 1.5 m polygons to eliminate potential edge effects of plots for a ‘L-93’ creeping bentgrass (*Agrostis stolonifera*) fairway at the Pete Dye River Course in Radford, Virginia.

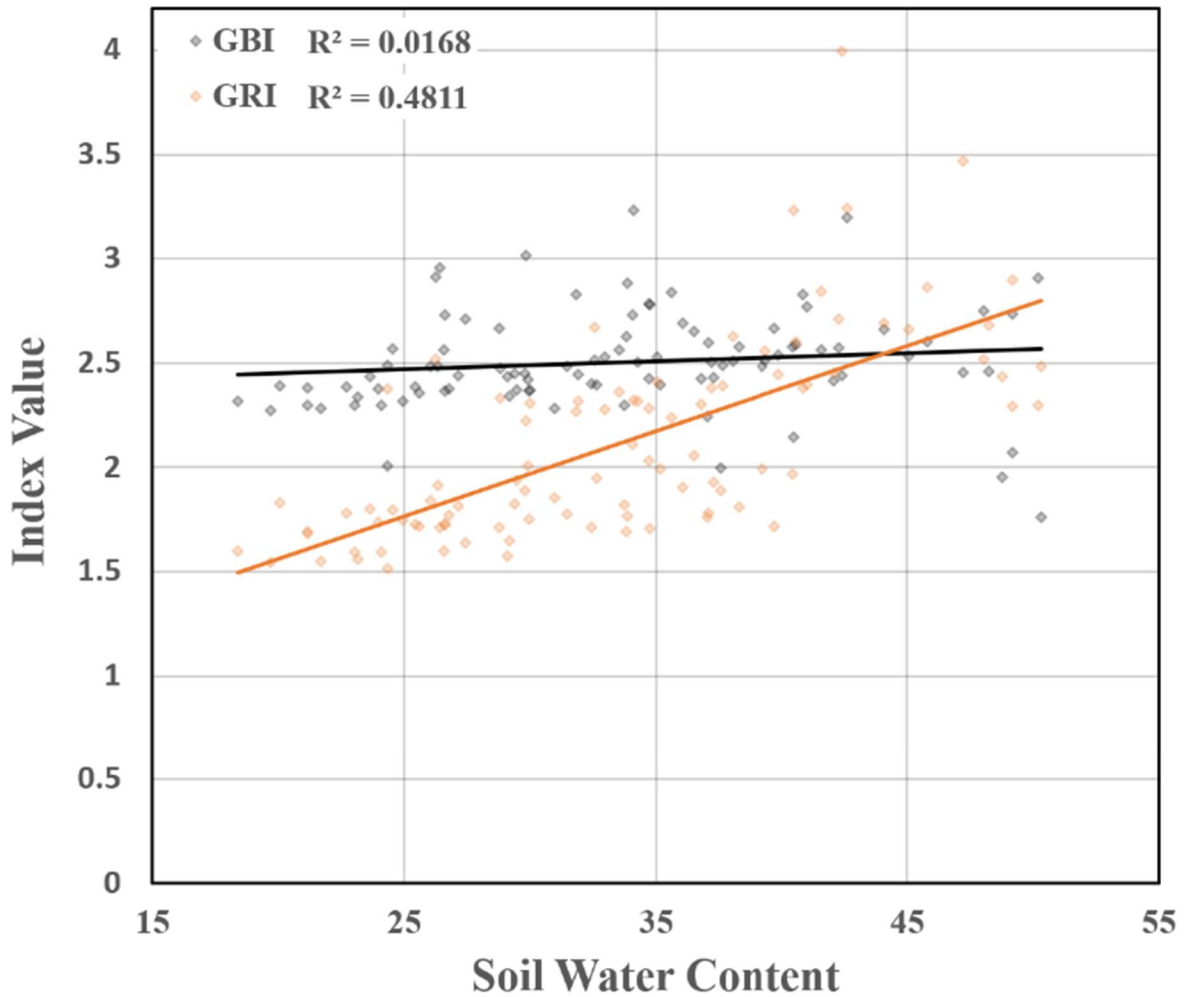


**Figure 5.** Relationship between Green to Blue Ratio Index (GBI) and Green to Red Ratio Index (GRI) pixel data derived from Mavic 2 drone aerial imagery and soil water content estimated as volumetric water content derived from a time-domain reflectometer for all locations between The Pete Dye River Course and Country Club of Virginia in Radford and Richmond, Virginia in 2022.

**Table 1.** Multivariate analysis showing the significant probabilities for leaf wetness, soil water content, ground derived hyper-spectral data (blue = 475 nm, green = 550 nm and red = 670 nm bands along with green to blue (GBI = Green/Blue) and red (GRI = Green/Red) ratios) and aerial drone pixel derived data (blue green and red pixel values along with GBI and GRI ratios for all data sampled at the Pete Dye River Course in Radford, Virginia and The Country Club of Virginia in Richmond, Virginia for 2022.

	<b>Leaf Wetness <math>\Psi</math></b>	<b>Soil Water Content <math>f</math></b>	<b>Ground: Blue</b>	<b>Ground: Green</b>	<b>Ground: Red</b>	<b>Ground: GBI</b>	<b>Ground: GRI</b>	<b>Aerial: Red</b>	<b>Aerial: Green</b>	<b>Aerial: Blue</b>	<b>Aerial: GBI</b>	<b>Aerial: GRI</b>
<b>Leaf Wetness</b>	<.0001	0.0011	<.0001	<.0001	0.0001	0.0028	NS	NS	NS	NS	NS	NS
<b>Soil Water Content</b>	0.0011	<.0001	0.0003	0.0002	NS	NS	<.0001	<.0001	<.0001	<.0001	0.0027	<.0001
<b>Ground: Blue</b>	<.0001	0.0003	<.0001	<.0001	<.0001	NS	NS	NS	NS	NS	NS	NS
<b>Ground: Green</b>	<.0001	0.0002	<.0001	<.0001	<.0001	NS	NS	NS	NS	NS	NS	NS
<b>Ground: Red</b>	0.0001	NS	<.0001	<.0001	<.0001	NS	0.0002	0.0076	0.0193	0.0058	NS	0.022
<b>Ground: GBI</b>	0.0028	NS	NS	NS	NS	<.0001	NS	NS	NS	NS	0.0067	NS
<b>Ground: GRI</b>	NS	<.0001	NS	NS	0.0002	NS	<.0001	<.0001	<.0001	<.0001	<.0001	<.0001
<b>Aerial: Red</b>	NS	<.0001	NS	NS	0.0076	NS	<.0001	<.0001	<.0001	<.0001	<.0001	<.0001
<b>Aerial: Green</b>	NS	<.0001	NS	NS	0.0193	NS	<.0001	<.0001	<.0001	<.0001	<.0001	<.0001
<b>Aerial: Blue</b>	NS	<.0001	NS	NS	0.0058	NS	<.0001	<.0001	<.0001	<.0001	<.0001	<.0001
<b>Aerial: GBI</b>	NS	0.0027	NS	NS	NS	0.0067	<.0001	<.0001	<.0001	<.0001	<.0001	<.0001
<b>Aerial: GRI</b>	NS	<.0001	NS	NS	0.022	NS	<.0001	<.0001	<.0001	<.0001	<.0001	<.0001

Note: Significant probabilities are at the tested 0.05 probability level and NS denotes no significance between the tested response variables.

$\Psi$  Leaf wetness as denoted as the difference between weight of custom PVC roller sampling a 387.35 cm<sup>2</sup> area with collected water and initial PVC roller weight as grams of water per m<sup>2</sup>.

$f$  Soil water content calculated using the time-domain reflectometry (TDR) using 3.8 cm probes as an estimation of water in a given volume of soil sampled.

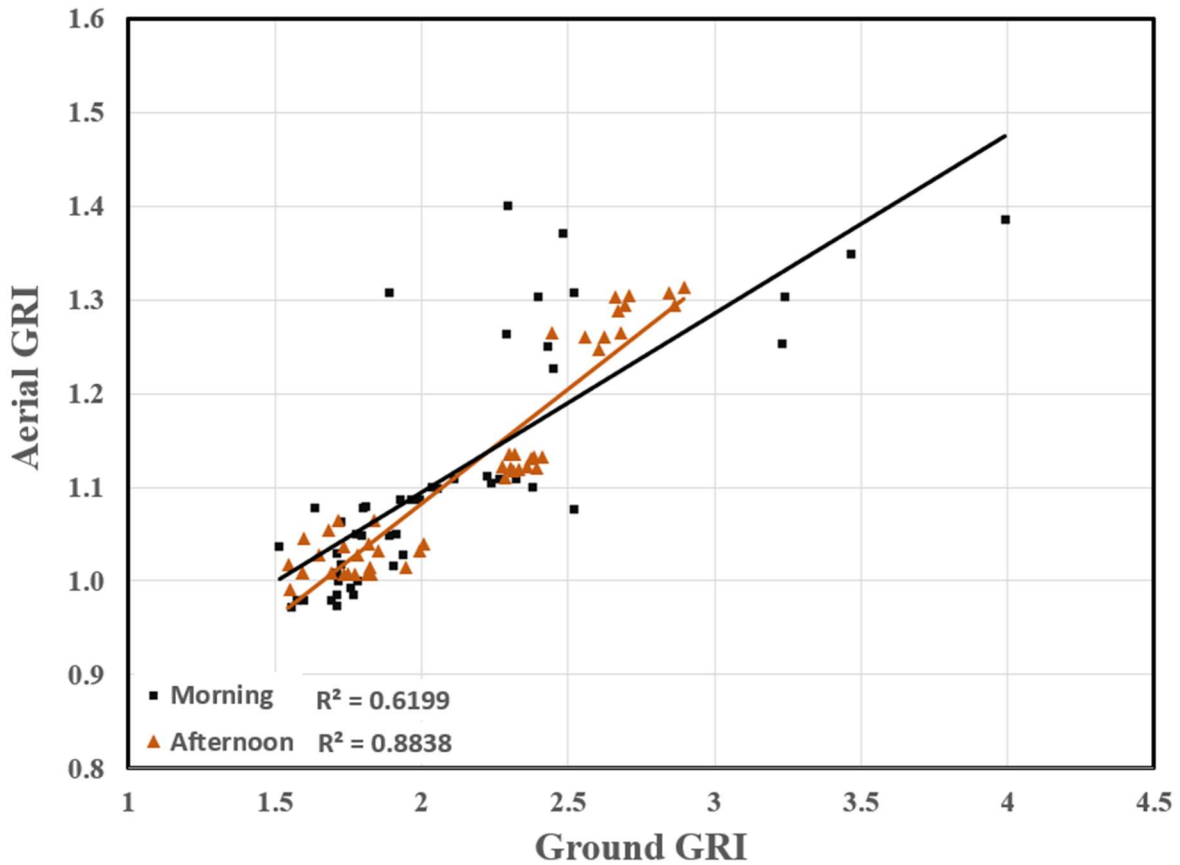


**Figure 6.** Relationship between Green to Red Ratio Index (GRI) pixel data derived from Mavic 2 drone aerial imagery and ground-based GRI data extracted from spectral data samples using a Spectral Evolution hyper-spectral radiometer for all locations separated by the time of data collection (morning or afternoon) at The Pete Dye River Course and Country Club of Virginia in Radford and Richmond, Virginia in 2022.

**Table 2.** Mixed model effects test results for the response variables of leaf wetness collected by way of a custom PVC roller sampling a 387.35 cm<sup>2</sup> area, soil water content derived as percent volumetric water content from a time-domain reflectometer and the green to red ratio (GRI = Green/Red) index derived from drone pixel data from field data collected at the Pete Dye River Course in Radford, Virginia and The Country Club of Virginia in Richmond, Virginia in the Fall of 2022.

Source	Leaf Wetness $\Psi$		Soil Water Content †		Green to Red Ratio +	
	F Ratio	Prob > F	F Ratio	Prob > F	F Ratio	Prob > F
Grass Species	36.15	<.0001	237.81	<.0001	2017.01	<.0001
Grass Height	6.20	0.0152	5.33	0.0239	747.30	<.0001
Grass Species*Grass Height	3.70	NS	101.89	<.0001	336.89	<.0001
Time	246.28	<.0001	20.68	<.0001	0.19	NS
Grass Species*Time	22.31	<.0001	0.37	NS	0.27	NS
Grass Height*Time	3.19	NS	0.05	NS	39.60	<.0001
Grass Species*Grass Height*Time	0.22	NS	0.01	NS	0.03	NS
Treatment	136.75	<.0001	9.26	0.0003	12.29	<.0001
Grass Species*Treatment	14.82	<.0001	2.72	NS	2.68	NS
Grass Height*Treatment	0.51	NS	0.78	NS	3.15	0.049
Grass Species*Grass Height*Treatment	0.58	NS	3.58	0.0331	1.19	NS
Time*Treatment	175.50	<.0001	1.03	NS	6.88	0.0019
Grass Species*Time*Treatment	18.28	<.0001	0.12	NS	5.54	0.0058
Grass Height*Time*Treatment	0.08	NS	0.46	NS	2.84	NS
Grass Species*Grass Height*Time*Treatment	1.70	NS	0.01	NS	2.15	NS

Note: NS denotes that no significance is observed between the single source or the associated interactions.

$\Psi$  Leaf wetness as denoted as the difference between weight of custom PVC roller sampling a 387.35 cm<sup>2</sup> area with collected water and initial PVC roller weight as grams of water per m<sup>2</sup>.

† Soil water content calculated using the time-domain reflectometry (TDR) using 3.8 cm probes as an estimation of water in a given volume of soil sampled.

μ Green to red ratio data is derived from pixel data extracted through geospatial rectified imagery acquired by a DJI Mavic 2 Enterprise drone.

**Table 3.** One way analysis of variance test results for creeping bentgrass (*Agrostis stolonifera*) and bermudagrass (*Cynodon dactylon* x *C. transvaalensis*) response variables of leaf wetness collected by way of a custom PVC roller sampling a 387.35 cm<sup>2</sup> area, soil water content derived as percent volumetric water content from a time-domain reflectometer, and the green to red ratio (GRI = Green/Red) index derived from drone pixel data from field data. Treatment effects are separated by the interactions of time of data collection × grass species with mean separation across rows from field data collected at the Pete Dye River Course in Radford, Virginia and The Country Club of Virginia in Richmond, Virginia in the Fall of 2022.

	Time of Data Collection	Grass Species	Treatment		
			Untreated	Light Irrigation	Rolled
<b>Leaf Wetness Ψ</b>	Morning	Bentgrass	314.15 A	60.24 B	20.58 B
		Bermudagrass	163.7 A	36.14 B	13.82 B
	Afternoon	Bentgrass	1.97 B	47.38 A	0.80 B
		Bermudagrass	0.94 B	26.49 A	0.97 B
<b>Soil Water Content †</b>	Morning	Bentgrass	41.97 A	41.35 A	38.26 A
		Bermudagrass	28.45 A	31.64 A	29.18 A
	Afternoon	Bentgrass	37.76 A	40.38 A	34.86 A
		Bermudagrass	24.22 A	28.92 A	24.88 A
<b>Green to Red Ratio +</b>	Morning	Bentgrass	1.17 A	1.22 A	1.23 A
		Bermudagrass	1.01 A	1.03 A	1.02 A
	Afternoon	Bentgrass	1.21 A	1.21 A	1.20 A
		Bermudagrass	1.01 B	1.04 A	1.02 AB

Note: All connecting letter reports indicate a difference across rows using Tukey-Kramer HSD at a  $\alpha = 0.05$  level.

Ψ Leaf wetness as denoted as the difference between weight of custom PVC roller sampling a 387.35 cm<sup>2</sup> area with collected water and initial PVC roller weight as grams of water per m<sup>-2</sup>.

† Soil water content calculated using the time-domain reflectometry (TDR) using 3.8 cm probes as an estimation of water in a given volume of soil sampled.

+ Green to red ratio data is derived from pixel data extracted through geospatial rectified imagery acquired by a DJI Mavic 2 Enterprise drone.

### **Chapter 3: An Evaluation of Aerial Thermal Imagery for Assessing the Distribution Uniformity of Golf Course Irrigation Systems**

#### **Abstract**

Golf course irrigation systems are designed to deliver water efficiently because water plays such a crucial role in maintaining turfgrass aesthetics through proper distribution across playing surfaces (Bastug & Buyuktas, 2003; Troy et al., 2015). However, challenges such as system wear, design limitations, proper scheduling, and environmental factors can reduce their effectiveness. Catch cans can be evenly distributed across a given surface to identify limitation related to the irrigation infrastructure, however, can be very time consuming to implement. Canopy temperature through thermal imagery has been correlated to limited soil moisture conditions inducing drought stress but not investigated for use in monitoring how an irrigation system delivers water. This study evaluated the efficiency of a golf course irrigation system by comparing traditional distribution uniformity (DU) calculations with thermal imaging data obtained from a small unmanned aerial vehicles (sUAV). Field experiments were conducted on ultradwarf bermudagrass greens and hybrid bermudagrass tees at the Par 3 Short Course at Independence Golf Club in Virginia. Soil analyses, irrigation methods, and weather data were monitored to assess system performance. Thermal imaging data from a DJI Mavic 3T were compared with ground-truth measurements to evaluate the effects of irrigation on surface radiometric temperatures. The highest correlation existed between irrigation applied as measured by catch can volume (CCV) and thermal mean canopy temperature ( $T_c$ ) values ( $r = 0.40$ ). Furthermore, the coefficient of determination between  $T_c$  and CCV, varied between tee ( $r^2 = 0.19-0.41$ ) and green ( $r^2 = 0.54-0.68$ ) locations, influenced by turfgrass

canopy density and soil physical properties due to larger coarse sand percentages for tee locations compared to greens. Moreover, soil moisture distribution uniformity before irrigation was always lower compared to measurements post-irrigation applications for greens locations compared to inconsistencies for tee locations. The study highlighted the importance of considering soil properties and irrigation efficiency in turfgrass management. Further research is needed to explore the interactions between irrigation systems, soil moisture distribution, and turfgrass health, as well as how  $T_c$  data can expedite irrigation system assessments in a noninvasive, labor-efficient-manner. The results highlight the potential of thermal imaging as a valuable tool for evaluating irrigation-system efficiency and identifying areas of improvement. This study supports ongoing efforts to enhance water management practices in golf course maintenance by integrating innovative technologies with traditional assessment methods.

## Introduction

A golf course irrigation system is a crucial component designed to achieve uniform water distribution across an area to help maintain the quality of a turfgrass surface (Lorenzini & De Wrachien, 2005). The crop water needs can be met through rainfall but during prolonged periods without it, proper functioning irrigation systems are required to address the irrigation-water balance which is the total fractions of irrigation water applied compared to what is used by the plant and soil-water movement (Burt et al., 1997). However, this goal is not met consistently due to factors such as irrigation head wear, nozzle selection, head spacing, throw distance, system design, spacing, water pressure, and uncontrollable environmental conditions. For example, Louie and Selker (2000) demonstrated that simple maintenance practices, such as proper nozzle selection, could improve irrigation efficiency in agriculture, with proper nozzle replacement reducing mean water application rates by 13%. Although routine maintenance is often underappreciated, it plays a critical role in irrigation success and can significantly impact plant health (Pereira, 1999). Neglecting regular maintenance can result in financial and environmental consequences (Solomon, 1984).

In turfgrass management, irrigation supports nutrient uptake, pesticide applications, reduced nutrient leaching, reduced compaction, and improved user safety through healthy turfgrass in high-traffic areas (Gómez-Armayones et al., 2018; Straw et al., 2018). Since the irrigation system functionality is so vital, established industry protocols allow for irrigation efficiency estimations through the placement of collection devices to record the irrigation applied across a given area. While variations of catch can minimum quantities exist (12 – 24), the consensus is to determine the average distance between irrigation heads of an area and divide into thirds. The tester then places all catch cans evenly across the area in a grid pattern prior to

activating the irrigation system (Allen et al., 2010; Mecham, 2004). Irrigation system application efficiency is then estimated from these protocols using mathematical ratios such as the coefficient of uniformity (CU) and distribution uniformity (DU) (Christiansen, 1942; Latif & Ahmad, 2008; Zoldoske et al., 1994). Coefficient of Uniformity, helps to treat overirrigation and underirrigation equally compared to the average and calculated as follows:

$$CU = 1 - \frac{\sum |D_a - D_d|}{\sum_n D_a}$$

where  $D_a$  is the volume of application from each catch can,  $D_d$  is the mean volume, and  $n$  is the number of catch cans. Although the CU does not consider areas with the lowest water applied, DU addresses this by focusing on the lowest quartile of catch can measurements, providing a more detailed evaluation (Mecham, 2004). distribution uniformity varies slightly from CU and is calculated as follows:

$$DU = \frac{DU_{avg1q}}{D_{avg}} \times 100$$

where  $DU_{avg1q}$  is the distribution of the lowest quartile average of catch can water volumes and  $D_{avg}$  is the average of all catch can volume across all catch cans (Ascough & Kiker, 2002; Pitts et al., 1996). In pressurized irrigation systems, a DU of at least 60% is considered good or acceptable; values below this threshold warrant action (Li & Rao, 2000; Mecham, 2004). However, DU only considers water distribution on the surface, without addressing how it impacts subsurface soil moisture, which can be influenced by slope and soil properties (Miller et al., 2014; Straw et al., 2018).

Miller et al. (2014) reported that the irrigation DU did not significantly affect soil moisture spatial variability; rather, soil properties and slope were more influential. Straw et al. (2018) found that soil characteristics significantly affect correlation between catch-can  $DU_{1q}$  and volumetric water content, suggesting that variations in soil type impact water retention and distribution. Determining DU is often time-consuming, involving catch-can setup, irrigation operation, and data collection, which may explain why it is not always part of routine irrigation audit practice (Oki, 2016).

An alternative approach, using thermal imaging from small unmanned aircraft vehicles (sUAV) or drones, can identify water stress, locate irrigation leaks, and assess the overall irrigation distribution effectiveness (Agam et al., 2014; Thomson et al., 2010). The crop water stress index (CWSI), which utilizes canopy-to-air temperature differences, links soil water availability with plant physiological responses, allowing identification of water-limited areas through transpiration patterns (Cohen et al., 2005; Colaizzi et al., 2003; Gardner et al., 1992; Stockle & Dugas, 1992). However, issues such as canopy density, low vapor-pressure deficits in humid climates, and periodic cloud cover can limit CWSI effectiveness (Irmak et al., 2000; Thomson & Sullivan, 2006).

In turfgrass systems, the dense, uniform canopy structure facilitates the use of thermal imaging for irrigation assessments. Hong et al. (2019) validated that radiometric canopy temperature ( $T_c$ ) values can detect areas with reduced soil moisture in deficit-irrigated turfgrass, with  $T_c$  values moderately correlating with visual quality and green cover ratings ( $r \geq 0.58$ ). However, these findings were under small-plot research that exhibited controlled conditions and does not account environmental conditions such as shade that could influence these data. On a broader scale, thermal modeling has shown that artificial turf can contribute to water

conservation in urban landscapes by reducing irrigated surface needs (Yaghoobian et al., 2010). Although thermal imaging may help detect irrigation issues in some climates, it does not directly assess DU; instead, it indicates stress responses, making it a reactive rather than preventative tool.

Thermal land surface temperature derived from Landsat 8 optical imagery on a 0.6-10 m resolution have successfully differentiated irrigated from non-irrigated vegetation in urban semi-arid areas such as Los Angeles, California (Coleman et al., 2020). However, limited research has examined the use of any remotely sensed  $T_c$  data to potentially determine DU of irrigation systems. Therefore, the objectives of this study were to 1) evaluate the validity of using radiometric data from sUAV generated orthomosaic and 2) compare these data with traditional catch-can water volume measurements on golf course greens and tee areas.

## **Materials and Methods**

### *Experimental Design and Field Conditions*

All tested locations were performed on the Par 3 Short Course at Independence Golf Club in Richmond, Virginia (37.54°N, -77.68° W), on four ultra-dwarf-bermudagrass greens (UDB) and hybrid-bermudagrass tees (HBT). The varieties for UDB [*Cynodon dactylon* (L.) Pers. × *C. transvaalensis* Burt-Davy] were as follows: green 4 ('TifEagle'), green 5 ('G12'), green 7 ('The University of Georgia Experimental'), and green 9 ('TifEagle'), while all HBT (*Cynodon dactylon* × *Cynodon transvaalensis*) tee 3, 4, 5, and 7 ('Midlawn') were the same variety. Soil particle size and organic matter analyses were conducted in June 2022 on all tested areas with 20 cores harvested using a soil probe with a 2.22 cm diameter opening to a depth of 7.62 cm across each tested location and homogenized. Ultradwarf bermudagrass sites had sand  $\geq 95.6\%$ , while HBT sites had sand  $\geq 93.2\%$  due to being sand-capped tees to a 15.24 cm depth and organic

matter ranged from 9.30 - 15.80% for UDB and 5 – 8% for HBT. All UDBs were maintained at a mowing height of 3.18 mm, and all HBT were maintained at 11.43 mm. The UDB was managed more intensively by supplemental applications of a foliar nutrient program throughout the field season on bi-weekly applications for a cumulative total of 195.30 kg N ha<sup>-1</sup> yr<sup>-2</sup> along with fungicides incorporated into these applications to limit all foliar diseases possible. Furthermore, all UDB locations were vertical mown to a depth of 6 mm bi-weekly with light sand top-dressing application applied to a depth of 3.175 mm to incorporate into the upper thatch profile. During the summer months, all HBT received one fertilizer application on June 8<sup>th</sup>, 2023, using Harrell's (Lakeland, Florida) slow-release fertilizer (25-0-12, containing 85% polymer coated urea) for season-long nutrient supplement throughout the field season. Each UDB and HBT location, were managed the same by mowing height throughout the extent of this experiment in the summer of 2023.

All locations were irrigated for this study using the Toro Lynx computerized irrigation software control system (Bloomington, Minnesota) and either 760 or 780 Toro irrigation heads; however, UDB locations were part circle heads adjusted to only apply water on the green's surfaces (130°-180° radial pattern), while HBT areas were full circle (360° radial pattern) heads because these same heads also irrigate the fairways adjacent to HBT areas. All UDB areas were irrigated with 10 min of irrigation and 20 min for HBT areas. These runtimes were based on management regimes of varying mowing heights, which categorize them between greens and fairway types (Association, 2004) and the radial pattern differences between the irrigation heads of the two area types requiring a double runtime for HBT for both UDB and HBT to apply 12.7 mm of water during experimental testing. All weather data is listed in Table 1, displaying the wind speed, direction, humidity (%) and cloud conditions one hour prior, current, and one hour

post drone flights and irrigation applications involved with all locations. A Protomex PT625B handheld anemometer was used to determine thresholds of when to start irrigation applications.

Since irrigation applications came immediately after initial sUAV thermal imagery, at any point wind speeds exceeded  $12 \text{ km hr}^{-1}$ , pre-irrigation sUAV imagery acquisition was delayed until wind speeds were more suitable based on previous research and field recommendations to account for any potential irrigation delivery deviations (Kumar et al., 2023). Furthermore, we also monitored cloud cover to ensure drone flights were during periods when no cloud cover occurred during the drone flight events because cloud cover variations that occur simultaneously with sUAV land surface temperature pixel data collection have been shown to produce temperature variations (Elfarkh et al., 2023). The timing was crucial, so detailed scouting occurred for these field studies to monitor proper conditions. Early morning or late evening is generally recommended for irrigation efficiency testing, but these data collection timings were not an option since drone data were incorporated within the study parameters.

#### *Field Data Collection*

No data collection ever occurred during a window when rainfall occurred within 48 hours of field experimentation, and no irrigation applications were made 48 hours prior to the study events to minimize any water percolation during testing. Orbit B-Hyve (Salt Lake City, Utah) sprinkler catch cans with an opening diameter of 12.7 cm and a depth of 20.32 cm were used to catch water from irrigation applications for DU calculations and comparison to sUAV thermal and soil volumetric water content data. All catch cans for UDB and HBT areas were placed on a 3-m spacing on center, and for UDB, a quantity of 47-80 catch cans were used, whereas 50-94 catch cans were used for HBT locations. These quantities varied based on the total surface area, which was  $272\text{-}525 \text{ m}^2$  for UDB and  $321\text{-}656 \text{ m}^2$  for HBT locations. Once all catch cans were

strategically placed for each location, soil volumetric water content was collected using a Field Scout TDR 350 (Spectrum Technologies, Aurora, IL) equipped with 3.81 cm probes before irrigation delivery and directly after the irrigation application was finalized. Miller et al. (2014) observed a low consistency of spatial variance between soil moisture and irrigation delivery when using the 20 cm probes. For this reason, the shortest probes offered on the market were utilized because we were more concerned with a comparison of direct, immediate changes to soil moisture between before- and after-irrigation applications within the thatch-rootzone interface compared to deeper within the soil profile. At each catch can location, one soil volumetric water content sampling point was taken in a strategic sampling order that corresponds with the catch can identifier. Each sampled soil volumetric water content data point was taken at a 6:00 position based on a tee-to-green orientation for all UDB and HBT areas before and after irrigation events. During irrigation events, each irrigation head that was actively operating was pressure tested using an Underhill pressure gauge and pitot tube (Irvine, California) held 0.6 cm away from the main nozzle to ensure the pressure at the irrigation heads met the operating standards specified by the manufacturer. For all UDB and HBT locations, only four irrigation heads were running at one time. After irrigation runtime ended and sUAV flights concluded, soil volumetric water content measurements were immediately collected after the sUAV took the final image at each location and subsequently, all catch can water volumes were documented by individually pouring the water into a 250 mL graduated cylinder for accurate assessments. All collected irrigation water was utilized to determine the lower quartile distribution uniformity ( $DU_{LQ}$ ) and was determined from the following equation:

$$DU_{LQ} = \frac{AVG_{LQ}}{AVERAGE} \times 100$$

Where  $DU_{LQ}$  = the lower quarter distribution uniformity as a percentage of all catch can volumes,  $AVG_{LQ}$  = average volume of the lower 25% of the catch can volume samples and  $AVERAGE$  = average volume of total catch can sample points in a given area being tested.

### *Drone Flight Details*

All aerial radiometric data were collected using a DJI Mavic 3T sUAV (Nanshan, Shenzhen, China) at an above-ground level of 60 m equipped with a  $650 \times 512$  DJI thermal lens with a  $-20^{\circ}$  to  $150^{\circ}\text{C}$  temperature measurement range derived from 8-14  $\mu\text{m}$  infrared wavelengths. The total number of images acquired varied based on the locations being tested due to surface area size deviations, and all flights had a front and side overlap of 90%. Thermal imagery was gathered pre- and post-irrigation applications with no more than 15 minutes occurring between the flight events per tested location to document the changes in surface radiometric data due to irrigation applications. A total of 58-114 thermal images were taken for UDBs and 70-129 thermal images for HBT locations. Moreover, the average flight times for these images to be collected were 43-87 seconds and 49-98 seconds, respectively. The considerably short flight times for these images taken help to provide confidence that all thermal data were collected within the same climatic conditions during each experimental run, with time gaps between sUAV flights only occurring due to the wait time equal to the runtime of irrigation heads (Table 1). All images were ground-truthed using ground control points where geospatial coordinates were collected using Emlid Reach RS+ (Budapest, Hungary) survey equipment to ensure all images were spatially accurate to identify the catch can locations within the images for data extraction. After image procurement, images were uploaded and converted from JPEG images to radiometric JPEG (RJPEG) format with temperature values embedded within each pixel in the image. Image conversions were carried out using Thermoconverter version 1.7

(Chichester, West Sussex, England), and following format conversion, RJPEG images were stitched together using Pix4D version 4.8.2 (Lausanne, Switzerland). Ground control point spatial information from survey equipment was uploaded during the processing phase to ensure all orthomosaic imagery had a spatial accuracy of 8 cm or less. Once all radiometric images were processed into a before and after irrigation orthomosaic for each location, then pixel data were extracted using geospatial software.

#### *Radiometric Data Extraction*

Extracting radiometric data from thermal orthomosaic required several post-processing steps within the QGIS version 3.32 (London, England) geospatial software. First, with all orthomosaic imagery, manual identification of catch cans within the images was required to be performed for each separate file by using the shapefile's multipoint feature to minimize any erroneous pixel sampling in case any image shifting occurred (Figure 1). After catch cans were identified in the imagery, a buffer was placed around the catch can's locations to extract the radiometric data embedded within pixels of the image. A processing function within the vector geometry toolbox called 'Buffer' was used to generate buffers around these designated points (Figure 2). The buffer size, crucial for accurate data extraction, was set at 1.5 m. This radius was carefully determined due to the distance from one catch can to another to sample the pixels within the buffer area without resampling other pixels from other adjacent catch-can. The polygon buffer areas yielded a range of pixels sampled, from approximately 378-410 pixels for UDB areas and 293-386 pixels for HBT areas. These pixel ranges represent the total number of pixels used to derive the average surface radiometric temperature extracted from the thermal orthomosaic pre- and post-irrigation, which is used for further comparison with other collected data.

### *Data Processing*

The data analysis was conducted using the robust JMP version 17 (SAS Institute, Cary, NC). Mean separation was performed using Tukey-Kramer honest significance difference test for location types (green or tee). Further analyses were determined using linear regression to numerically investigate the relationship between thermal radiometric mean data compared to the DU values of each location tested.

### **Results and Discussion**

In total, for all locations, the lowest operating pressure was 447.85 kPa on green 7 and 496.08kPa for tee 7, and the maximum was 592.54 kPa for Green 4 and 9 and 626.99 kPa observed at tee 3 (Table 2). For both Toro 760 and 780 series irrigation heads, the operating pressure is 342-684 kPa for adequate irrigation water distribution, given other parameters such as current climate conditions and in-field head spacing. During testing, no head was outside of this pressure range, indicating that anything seen in the data results would not be due to any erroneous water pressure being supplied to any of the irrigation heads during application events. Furthermore, the overall average range for all greens locations was 485.75-570.15 kPa compared to 530.53-585.65 kPa for all tee locations, respectively (Table 2). There seemed to be less pressure fluctuation between tee locations compared to greens areas, which could be attributed to different pipe sizes, volumes of water, and velocity of water transported from pump → mainline → zonetines → irrigation heads.

A multivariate analysis was conducted to determine the parameter most associated with a catch can volume measured in millimeters (Table 3). Catch can volume had the lowest correlation with soil moisture compared to all other measured data points. This is agreeable with the weak correlations of other literature published (Li & Rao, 2000; Warrick & Gardner, 1983).

Interestingly, Red and Blue mean pixel values had weak to moderate correlations (0.32 and 0.38) to catch can volume, respectively. However,  $T_c$  is the continuous variable chosen because of the slightly stronger correlation between  $T_c$  estimated by means of sUAV technology compared to the locations where irrigation volume was collected as a representation of catch can volume ( $r = 0.40$ ) and also aligns with the original objectives of the research study. Understanding these correlations led to investigating the relationship between turfgrass mowing heights (green or tee) and comparing all locations (Figure 3A and 3B).

All tee locations (Figure 3B) ranged from a weak to moderate correlation between  $T_c$  pixel values and catch can volume ( $r^2 = 0.19-0.41$ ); however, all greens locations (Figure 3A) were all moderate correlations ( $r^2 = 0.54-0.68$ ), respectively. Furthermore, by location-management regime, green 4 had the lowest relationship between the  $T_c$  of the turfgrass compared to the locations of water applied ( $r^2 = 0.54$ ). Moreover, green 9 observed the highest relationship between thermal values and irrigation applied ( $r^2 = 0.68$ ). As far as tee locations were concerned, tee 3 observed the strongest correlation ( $r^2 = 0.41$ ) compared to tee 7, with the lowest correlation ( $r^2 = 0.19$ ). One potential reason for the stronger correlations observed with all green locations is the uniformity of UDB canopies due to a more compact, lateral phenotypic growth with a denser canopy structure.

All tee locations had low canopy density compared to all green locations, which were a mixture of several UDB varieties *with* significantly higher turfgrass canopy density. It is plausible that canopy openness exposes the soil surface beneath, leading to background noise in thermal imagery since thermal conductivity microclimates inherently are found to exist based on varying soil densities, organic matter and total dissolved salts (Abu-Hamdeh & Reeder, 2000). Canopy structure was reported as an influential factor within the Steinke et al. (2009) study that

showed for warm-season grasses subjected to soil moisture stress, a degradation of canopy density and an increase in canopy temperature was observed at  $-5.60-6.10^{\circ}\text{C}$  and  $-9.40-3.30^{\circ}\text{C}$  higher than air temperatures for 2006 and 2007, respectively. Furthermore, we know with other warm and cool season grasses for turf quality, canopy temperature, and multispectral data *can vary when using* NDVI depending on the turfgrasses *phenotypic* canopy structure with a high canopy resistance and shoot density (Haghverdi et al., 2021; Jiang et al., 2009; Kim & Beard, 1988). While our study did not delineate between stress and non-stressed turfgrass, it shows the variability of densities of turfgrass related to one another under normal irrigation conditions. Another reason could be the climate conditions between each experimental run. While either complete shade or sun coverage occurred during any data collection event, there were times with minor variable wind flow that could not be mitigated due to the time of day when the irrigation application and sUAV flights materialized. It is essential to note the range of canopy temperatures observed within location types,  $26.40-36.40^{\circ}\text{C}$  for green compared to  $30.90-36.50^{\circ}\text{C}$  for tee, respectively. These temperature ranges occurred due to the varying ambient temperature between the times each location was tested throughout the field season 2023 (Table 1).

The two locations with the lowest ambient temperature during testing were  $23.33^{\circ}\text{C}$  for green 9 and  $28.33^{\circ}\text{C}$  for tee 3, respectively. These two locations were also the locations with the strongest observed correlations between  $T_c$  and catch can volume, as previously stated. This suggests that there may be a limitation or threshold when using data derived from aerial thermal imagery to estimate the efficiency of irrigation delivery under elevated ambient temperatures. We hypothesize this limitation exists due to measuring the response of applied water on the turfgrass surface and under the right climatic conditions, the velocity of water evaporation may

exceed sUAV total flight times for a given area. Furthermore, our hypothesis aligns within each management area, the locations with the highest correlations, green 9 ( $r^2 = 0.68$ ) and tee 3 ( $r^2 = 0.40$ ), were also the locations with the lowest ambient temperature during these data collections stated previously. Additionally, the locations with the highest ambient temperature at the time of testing were green 4 and tee 5, at 27.22 and 33.33°C but this is not congruent with  $T_c$  pixel data, which showed that tee 5 did have the highest max  $T_c$  value (49.60°C) but green 7 actually had the max  $T_c$  value at 39°C. This further alludes to the complexities of these studies, where optimal conditions are always difficult to achieve in relation to climatic data since these influences cannot be controlled. Moreover, green 9 also had the highest humidity at the time of testing as well (87%), while tee 3 was comparable to other tee locations (53%). The weather data suggest that lower air temperatures and higher humidity could lead to a slower vaporization rate of water on the turfgrass surface after irrigation delivery and be more desirable conditions to evaluate irrigation efficiency using sUAV  $T_c$  data.

Furthermore, when considering the climate conditions for these locations, the  $T_c$  values ranged from 25.20-27.70°C and 30.90-37.60°C for green 9 and tee 3, respectively, when considering both before and after sampling events (Table 4). When considering the aforementioned ambient temperature ranges, these same locations had the lowest mean thermal values at 26.40 and 34.10°C. Moreover, their delta ( $\Delta$ ) change in  $T_c$  values before and after irrigation events were the lowest at -0.50 and -2.70°C between green 9 and tee 3, meaning the mean change between  $T_c$  before and after irrigation applications was only  $\leq -2.70^\circ\text{C}$ . Furthermore, soil moisture green 9 had the lowest soil moisture mean value (30.70%) and  $\Delta$  soil moisture values (3.07%) between before and after irrigation; however, this same trend was not observed with tee 3, where tee 4 actually had the lowest standard deviation in total soil moisture

values documented (6.14%). Additionally, tee 5 had the lowest soil moisture mean value for all tee locations (32.19%), but tee 4 had the lowest  $\Delta$  soil moisture mean (3.33%) and a weak correlation with catch can volume (mL) ( $r^2 = 0.27$ ). All of this suggests that soil moisture and  $\Delta$  soil moisture are not the driving factors for where  $T_c$  values are observed but rather where the physical water applications land and cool the  $T_c$  based on trends observed with  $T_c$  data derived from sUAV image acquisition. Furthermore, when we consider all locations in terms of the  $\Delta$  soil moisture and  $\Delta$  canopy temperature, we see that all green locations had a standard deviation of 2.70-4.03 and tee 4.92-9.64 related to the  $\Delta$  soil moisture, but for  $T_c$ , greens were 0.40-0.90 and tees were 0.90-1.50. These ranges suggest that all thermal data had much less variation post-irrigation applications when compared to soil moisture related data and congruent with literature that soil moisture is not as reliable for estimating the efficiency of irrigation distribution (Miller et al., 2014). One note, though, is all locations had a positive change, or increase, in total soil moisture values before and after irrigation events, meaning we have in-ground data to corroborate a positive change but with less confidence compared to thermal data. These trends and observations help to delineate that soil moisture is useful; however, the  $T_c$  may be more reliable because it avoids the complexities of soil physical properties when evaluating the post irrigation events in relation to the efficiency of an irrigation system.

Additionally, another point is the different soil sand fractions observed between green and tee locations (Table 5). All green locations had a higher percentage of fine sand of 14.69-39.86% compared to tee locations of 9.04-12.34%. These different particle sizes of fine sand could lead to elevated infiltration rates for tee locations compared to green locations. Moreover, all tee locations had coarse sand range of 32.09-40.56% compared to green locations of 22.61-33.30%. There was a higher percentage of coarse sand for tee locations, because they were all

sand-capped to a depth of 15.24 cm with more angular sand particles, to promote water infiltration into the soil and, we believe, helped to mask the  $T_c$  differences for tee compared to green locations. This masking effect would help to explain why all tee locations observed a lower correlation between  $T_c$  and catch can volume (mL) compared to green locations. The rapid infiltration of water post-irrigation delivery potentially never allowed the thermal lens of the sUAV during image acquisition to document proportionally where water droplets landed in reference to the sampled pixels for tee compared to green areas. In contrast, the green locations limited infiltration rates into the thatch interface allowing the water to remain on the canopy surface longer for sUAV thermal data to document  $T_c$  discrepancies directly proportional to where irrigation water were physically delivered based on the irrigation system efficiency.

Lastly, the distribution uniformity for both soil moisture before and after irrigation ( $SMDU_{BI}$  and  $SMDU_{AI}$ ) and the DU of the irrigation system (DU) were investigated (Figure 4). For all locations,  $SMDU_{BI}$  was always lower than  $SMDU_{AI}$  except for tee 3 and tee 4. Moreover, for all green locations, DU was lower than  $SMDU_{BI \text{ and } AI}$ , but this was only noncongruent for tee 5 and 7, in which DU was higher than  $SMDU_{BI}$  for tee 5 and  $SMDU_{BI \text{ and } AI}$  for tee 7. The DU for green locations was 77-84%, whereas tee locations were 78-91%. While the tee locations had higher DU for irrigation, this is not necessarily the case for SMDU. The  $SMDU_{BI}$  for greens were 77-93%, and tees were 77-91%. For most cases, the observed  $SMDU_{AI}$  compared to DU being higher is also congruent with Chen et al. (2023) that showed the same effects investigating through soil water movement in soils compared to sprinkler irrigation systems. Furthermore, knowing the sand fractions per locations, we presumed infiltration rates for the tee locations would inherently have higher  $SMDU_{BI \text{ and } AI}$  due to historical irrigation and rainfall and irrigation during testing leading to a higher overall SMDU, but this was not the case. This could be due to

the sampling method using the 3.81 cm probes because the shorter probes are potentially sampling an area where water has infiltrated past the sampling depth, which is another reason why soil moisture is not the most dependable method for documenting the efficiency of an irrigation system. Furthermore,  $SMDU_{AI}$  was 84-93% for greens and 87-91% for tee locations, lending to the feasibility of  $SMDU_{AI}$  as a method to assess irrigation efficiency immediately post-application with shorter TDR probes but not for historical irrigation efficiency assessments since soil physical properties factor in the subsurface water movement after infiltration occurs (Yetbarek et al., 2020). Considering the response of both  $SMDU_{BI}$  and  $AI$  becoming more relative for green and tee locations from the immediate effects of irrigation, the DU was also compared from physical water collection and found that the DU for greens were 76-84% and 78-91% for tees. The more uniform distribution of water could also help to mask differences in  $T_c$  for tee locations, lending to the lower correlations observed comparing catch can volume (mL) contrasted to green locations. In essence, you would see a stronger correlation between  $T_c$  pixel values when collated with catch can volume because the less uniform the delivery of irrigation volumes over the designated surface area, the more variability observed to extrapolate trends. Couple these greater DU values for the tee locations with the theorized elevated infiltration rates and this is why we hypothesize from our dataset to have observed a degradation of correlation between  $T_c$  to irrigation applied.

### **Conclusions**

This study underscores the pivotal role of irrigation maintenance and emphasizes the critical metrics of DU in gauging irrigation distribution efficiency. The comprehensive evaluation of aerial thermal imagery for assessing the DU of golf course irrigation systems yields insightful findings. By leveraging detailed field data, including irrigation

pressure, soil volumetric water content, weather data at the time of sampling, catch can volume, and soil particle analysis, the study delves deep into the intricacies of water distribution dynamics. The multivariate analysis emphasized the significance of  $T_c$  data in estimating irrigation efficiency, showing stronger correlations with catch can volume compared to other parameters. The differences observed between green and tee locations in terms of correlations, canopy densities, and particle sizes underscored the complexity of factors influencing water distribution and canopy temperatures. Climate conditions, such as ambient temperatures, cloud coverage, and humidity, play a crucial role in affecting post-irrigation  $T_c$ . Furthermore, the study revealed that thermal data post-irrigation showed less variation compared to soil moisture data, indicating the reliability of thermal data in assessing irrigation efficiency. The DU analysis highlighted the importance of considering soil moisture distribution before and after irrigation events as another indicator when evaluating a shallower sampling depth post-irrigation event. Overall, the findings suggest that factors like canopy density, particle sizes, infiltration rates, and climate conditions significantly impact the distribution of water and  $T_c$  in turfgrass management. These insights can inform better management practices to enhance irrigation efficiency and optimize turfgrass health. We aim to strengthen the understanding of the practical applications of thermal imaging in assessing irrigation systems and underscore the paramount importance of maintaining uniform water distribution for sustainable crop growth and resource conservation in agriculture. Furthermore, the study alludes to the complexities involved in manually deriving the results through field sampling, orthomosaic image generation, and computer-driven workflows to validate the locations of critical portions of the radiometric orthomosaic.

These steps require an individual who has knowledge of how the tools relate to one another and the ability to perform basic computer image processing. Future research should look more thoroughly into automating this process where information about the irrigation efficiency can be derived with confidence in minutes compared to days that were required. However, additional research should evaluate isolating key climate parameters, along with isolating the effects of crucial soil conditions, soil type, organic matter, and infiltration rates, when estimating irrigation efficiency of golf courses solely using thermal imagery derived data.

### References

- Abu-Hamdeh, N. H., & Reeder, R. C. (2000). Soil thermal conductivity effects of density, moisture, salt concentration, and organic matter. *Soil Science Society of America Journal*, 64(4), 1285-1290. <https://doi.org/10.2136/sssaj2000.6441285x>
- Agam, N., Segal, E., Peeters, A., Levi, A., Dag, A., Yermiyahu, U., & Ben-Gal, A. (2014). Spatial distribution of water status in irrigated olive orchards by thermal imaging. *Precision Agriculture*, 15, 346-359. doi: 10.1007/s11119-013-9331-8
- Allen, R., Baine Carruthers, C., Claude Corcos, C., Howell, T. A., Marlow, R., McCabe, J., Brent Meham, C., & Spofford, T. L. (2010). Turf and Landscape Irrigation Best Management Practices.
- Ascough, G., & Kiker, G. (2002). The effect of irrigation uniformity on irrigation water requirements. *Water Sa*, 28(2), 235-242. doi: 10.4314/wsa.v28i2.4890
- Association, I. (2004). Certified landscape irrigation auditor training manual. *Irrigation Association, Falls Church, VA*.
- Bastug, R., & Buyuktas, D. (2003). The effects of different irrigation levels applied in golf courses on some quality characteristics of turfgrass. *Irrigation Science*, 22, 87-93. Doi: 10.1007/s00271-003-0073-7
- Burt, C. M., Clemmens, A. J., Strelkoff, T. S., Solomon, K. H., Bliesner, R. D., Hardy, L. A., Howell, T. A., & Eisenhauer, D. E. (1997). Irrigation performance measures: efficiency and uniformity. *Journal of irrigation and drainage engineering*, 123(6), 423-442. [https://doi.org/10.1061/\(ASCE\)0733-9437\(1997\)123:6\(423\)](https://doi.org/10.1061/(ASCE)0733-9437(1997)123:6(423))

- Chen, R., Li, H., Wang, J., Guo, X., & Xiang, Y. (2023). Evaluating soil water movement and soil water content uniformity under sprinkler irrigation with different soil texture and irrigation uniformity using numerical simulation. *Journal of Hydrology*, 626, 1-14. <https://doi.org/10.1016/j.jhydrol.2023.130356>
- Christiansen, J. E. (1942). *Irrigation by sprinkling* (Vol. 4). University of California Berkeley.
- Cohen, Y., Alchanatis, V., Meron, M., Saranga, Y., & Tsipris, J. (2005). Estimation of leaf water potential by thermal imagery and spatial analysis. *Journal of Experimental Botany*, 56(417), 1843-1852. <https://doi.org/10.1093/jxb/eri174>
- Colaizzi, P. D., Barnes, E. M., Clarke, T. R., Choi, C. Y., & Waller, P. M. (2003). Estimating soil moisture under low frequency surface irrigation using crop water stress index. *Journal of irrigation and drainage engineering*, 129(1), 27-35. [https://doi.org/10.1061/\(ASCE\)0733-9437\(2003\)129:1\(27\)](https://doi.org/10.1061/(ASCE)0733-9437(2003)129:1(27))
- Coleman, R. W., Stavros, N., Hulley, G., & Parazoo, N. (2020). Comparison of thermal infrared-derived maps of irrigated and non-irrigated vegetation in urban and non-urban areas of Southern California. *Remote Sensing*, 12(24), 4102. doi: 10.3390/rs12244102
- Elfarkh, J., Johansen, K., Angulo, V., Camargo, O. L., & McCabe, M. F. (2023). Quantifying Within-Flight Variation in Land Surface Temperature from a UAV-Based Thermal Infrared Camera. *Drones*, 7(10), 1-18. <https://doi.org/10.3390/drones7100617>
- Gardner, B., Nielsen, D., & Shock, C. (1992). Infrared thermometry and the crop water stress index. I. History, theory, and baselines. *Journal of production agriculture*, 5(4), 462-466. <https://doi.org/10.2134/jpa1992.0462>
- Gómez-Armayones, C., Kvalbein, A., Aamlid, T. S., & Knox, J. W. (2018). Assessing evidence on the agronomic and environmental impacts of turfgrass irrigation management. *Journal of Agronomy and Crop Science*, 204(4), 333-346. doi: 10.1111/jac.12265
- Haghverdi, A., Reiter, M., Singh, A., & Sapkota, A. (2021). Hybrid bermudagrass and tall fescue turfgrass irrigation in central California: II. Assessment of NDVI, CWSI, and canopy temperature dynamics. *Agronomy*, 11(9), 1-16. <https://doi.org/10.3390/agronomy11091733>
- Hong, M., Bremer, D. J., & van der Merwe, D. (2019). Thermal imaging detects early drought stress in turfgrass utilizing small unmanned aircraft systems. *Agrosystems, Geosciences & Environment*, 2(1), 1-9. doi:10.2134/age2019.04.0028
- Irmak, S., Haman, D. Z., & Bastug, R. (2000). Determination of crop water stress index for irrigation timing and yield estimation of corn. *Agronomy Journal*, 92(6), 1221-1227.
- Jiang, Y., Liu, H., & Cline, V. (2009). Correlations of leaf relative water content, canopy temperature, and spectral reflectance in perennial ryegrass under water deficit conditions. *HortScience*, 44(2), 459-462. doi: <https://doi.org/10.21273/HORTSCI.44.2.459>

- Kim, K., & Beard, J. (1988). Comparative turfgrass evapotranspiration rates and associated plant morphological characteristics. *Crop Science*, 28(2), 328-331. <https://doi.org/10.2135/cropsci1988.0011183X002800020031x>
- Kumar, R., Naresh, R., Rani, S., Kumar, A., & Gaat, B. (2023). Effect of wind speed on distribution uniformity and uniformity coefficient of sprinkler irrigation system in Western Haryana. *Environment and Ecology*, 41(4B), 2742-2747. doi: <https://doi.org/10.60151/envec/PWRK6047>
- Latif, M., & Ahmad, F. (2008). Operational analysis of water application of a sprinkler irrigation system installed in a golf course: Case study. *Journal of irrigation and drainage engineering*, 134(4), 446-453. [https://doi.org/10.1061/\(ASCE\)0733-9437\(2008\)134:4\(446\)](https://doi.org/10.1061/(ASCE)0733-9437(2008)134:4(446))
- Li, J., & Rao, M. (2000). Sprinkler water distributions as affected by winter wheat canopy. *Irrigation Science*, 20, 29-35. doi: <https://doi.org/10.1007/PL00006715>
- Lorenzini, G., & De Wrachien, D. (2005). Performance assessment of sprinkler irrigation systems: A new indicator for spray evaporation losses. *Irrigation and Drainage: The journal of the International Commission on Irrigation and Drainage*, 54(3), 295-305. Doi: 10.1002/ird.171
- Louie, M. J., & Selker, J. S. (2000). Sprinkler head maintenance effects on water application uniformity. *Journal of irrigation and drainage engineering*, 126(3), 142-148. [https://doi.org/10.1061/\(ASCE\)0733-9437\(2000\)126:3\(142\)](https://doi.org/10.1061/(ASCE)0733-9437(2000)126:3(142))
- Mecham, B. (2004). Using distribution uniformity to evaluate the quality of a sprinkler system. *Irrigation Association's*, 379-386. <https://www.researchgate.net/publication/268427001>
- Miller, G., Dukes, M., & Pressler, N. (2014). Golf course irrigation systems' distribution uniformity affects soil moisture variability. *European Journal of Horticultural Science*, 79(3), 135-141.
- Oki, L. (2016). Measuring distribution uniformity and calculating run time. *University of California Davis California Center for Urban Horticulture*. Available online: <https://ccuh.ucdavis.edu/measuring-DU-run-time> (accessed on 20 March 2021).
- Pereira, L. S. (1999). Higher performance through combined improvements in irrigation methods and scheduling: a discussion. *Agricultural water management*, 40(2-3), 153-169. [https://doi.org/10.1016/S0378-3774\(98\)00118-8](https://doi.org/10.1016/S0378-3774(98)00118-8)
- Pitts, D., Peterson, K., Gilbert, G., & Fastenau, R. (1996). Field assessment of irrigation system performance. *Applied Engineering in Agriculture*, 12(3), 307-313. doi: 10.13031/2013.25653
- Solomon, K. H. (1984). *Irrigation uniformity and yield theory*. Utah State University.

- Steinke, K., Chalmers, D. R., Thomas, J. C., & White, R. H. (2009). Summer drought effects on warm-season turfgrass canopy temperatures. *Applied Turfgrass Science*, 6(1), 1-11. doi:10.1094/ATS-2009-0303-01-RS.
- Stockle, C. O., & Dugas, W. A. (1992). Evaluating canopy temperature-based indices for irrigation scheduling. *Irrigation Science*, 13, 31-37. doi: <https://doi.org/10.1007/BF00190242>
- Straw, C. M., Carrow, R., Bowling, W., Tucker, K., & Henry, G. (2018). Uniformity and spatial variability of soil moisture and irrigation distribution on natural turfgrass sports fields. *Journal of Soil and Water Conservation*, 73(5), 577-586. doi:10.2489/jswc.73.5.577
- Thomson, S. J., Ouellet-Plamondon, C. M., DeFauw, S. L., Huang, Y., Fisher, D. K., Hanks, J. E., & English, P. J. (2010). Irrigation system management assisted by thermal imagery and spatial statistics. Proceedings of XVIIth World Congress of the International Commission of Agricultural Engineering (CIGR),
- Thomson, S. J., & Sullivan, D. G. (2006). Crop status monitoring using multispectral and thermal imaging systems for accessible aerial platforms. 2006 ASAE Annual Meeting,
- Troy, T. J., Kipgen, C., & Pal, I. (2015). The impact of climate extremes and irrigation on US crop yields. *Environmental Research Letters*, 10(5), 1-11. doi: 10.1088/1748-9326/10/5/054013
- Warrick, A. W., & Gardner, W. R. (1983). Crop yield as affected by spatial variations of soil and irrigation. *Water resources research*, 19(1), 181-186.
- Yaghoobian, N., Kleissl, J., & Krayenhoff, E. S. (2010). Modeling the thermal effects of artificial turf on the urban environment. *Journal of Applied Meteorology and Climatology*, 49(3), 332-345. doi: 10.1175/2009JAMC2198.1
- Yetbarek, E., Kumar, S., & Ojha, R. (2020). Effects of soil heterogeneity on subsurface water movement in agricultural fields: A numerical study. *Journal of Hydrology*, 590, 1-15. <https://doi.org/10.1016/j.jhydrol.2020.125420>
- Zoldoske, D., Solomon, K., & Norum, E. (1994). Uniformity measurements for turfgrass: What's best. *Center for Irrigation Technology November Irrigation Notes*.

**Table 1.** Historical weather data for all ultradwarf bermudagrass (*Cynodon dactylon x C. transvaalensis*) greens and hybrid bermudagrass tees locations at Independence Golf Club in Richmond, Virginia in 2023. Weather data is logged based on DJI Mavic 3T small unmanned aerial vehicles (sUAV) flights before and after irrigation, date and time of one hour prior, current, and one hour after all testing periods, ambient temperature, wind speed and direction, humidity, and cloud conditions.

Location	Flight Times		Date	Ambient Temp. (°C)	Wind Speed (km/hr.)	Wind Direction	Humidity (%)	Cloud Condition
	Before	After						
Green 4	13:02	13:35	6/16/25 12:00	27.78	33.80	NNE	56	Cloudy
			6/16/25 13:00	27.22	0.00	Calm	58	Mostly Cloudy/Windy
			6/16/25 14:00	28.33	0.00	Calm	54	Mostly Cloudy
Green 5	11:59	12:20	7/22/25 11:00	26.11	14.48	NNE	62	Mostly Cloudy
			7/22/25 12:00	26.67	9.66	N	62	Mostly Cloudy
			7/22/25 13:00	28.33	14.48	NNE	62	Mostly Cloudy
Green 7	12:11	12:34	6/24/25 11:00	24.44	0.00	Calm	79	Cloudy
			6/24/25 12:00	26.67	8.05	SSW	76	Mostly Cloudy
			6/24/25 13:00	28.33	9.66	SSW	67	Mostly Cloudy
Green 9	10:05	10:30	6/24/25 9:00	22.78	4.83	Variable	91	Cloudy
			6/24/25 10:00	23.33	8.05	Calm	87	Cloudy
			6/24/25 11:00	24.44	9.66	SSW	76	Cloudy
Tee 3	15:22	16:05	7/22/25 14:00	28.33	12.87	N	56	Mostly Cloudy
			7/22/25 15:00	28.33	16.09	N	53	Mostly Cloudy
			7/22/25 16:00	29.44	14.48	NNE	46	Mostly Cloudy
Tee 4	11:29	12:05	7/29/25 11:00	31.67	20.92	WSW	59	Partly Cloudy
			7/29/25 12:00	32.22	19.31	SW	57	Fair
			7/29/25 13:00	33.33	22.53	SSW	54	Fair
Tee 5	13:17	13:59	7/29/25 12:00	32.22	19.31	SW	57	Fair
			7/29/25 13:00	33.33	22.53	SSW	54	Fair
			7/29/25 14:00	35.00	27.36	SSW	50	Fair
Tee 7	10:46	11:11	7/23/25 10:00	27.78	0.00	Calm	54	Fair
			7/23/25 11:00	28.89	8.05	SSE	51	Fair
			7/23/25 12:00	29.44	9.66	SSE	48	Fair

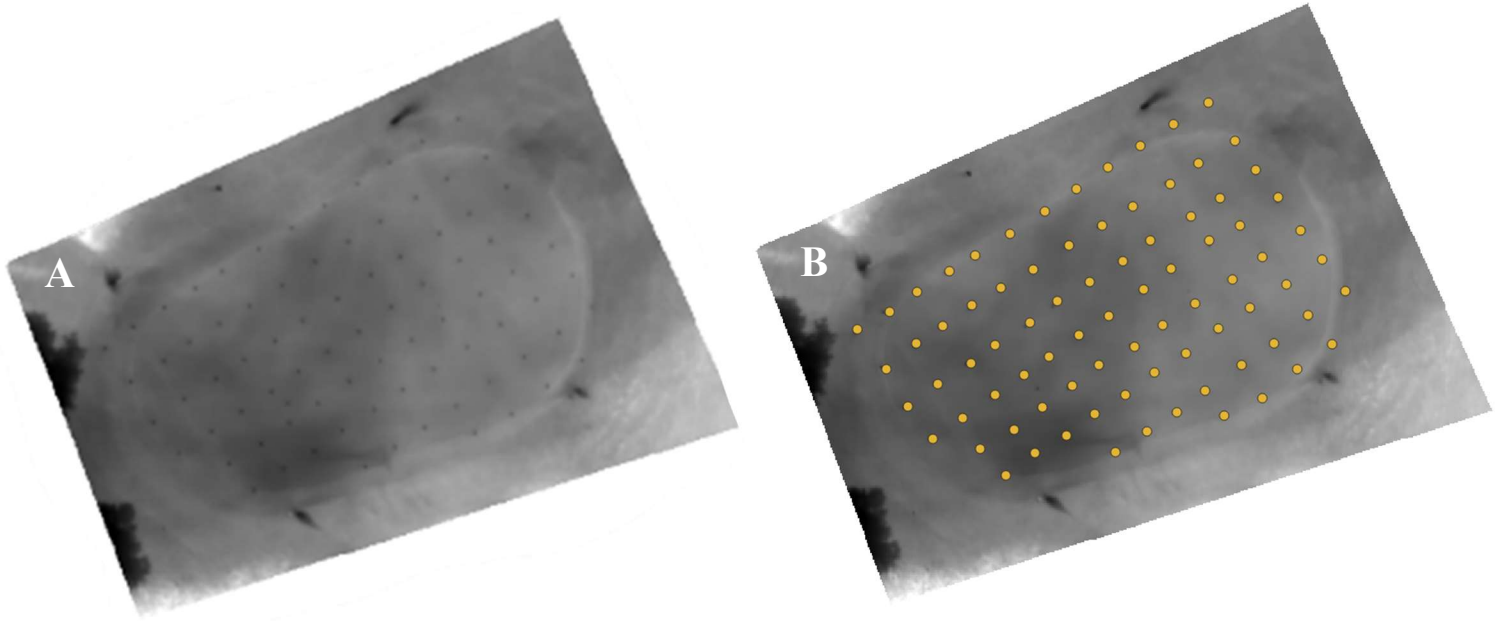


**Figure 1** A). Thermal orthomosaic derived from a DJI Mavic 3T small unmanned aerial vehicle (sUAV) image acquisition displaying the catch can locations on a 'TifEagle' ultradwarf bermudagrass (*Cynodon dactylon* x *C. transvaalensis*) green 4 (G4) at Independence Golf Club in Richmond, Virginia in 2023 after irrigation application occurred and B). thermal orthomosaic showing the multipoint that are used to identify the catch cans within the thermal orthomosaic to be used for further pixel processing and data extraction.

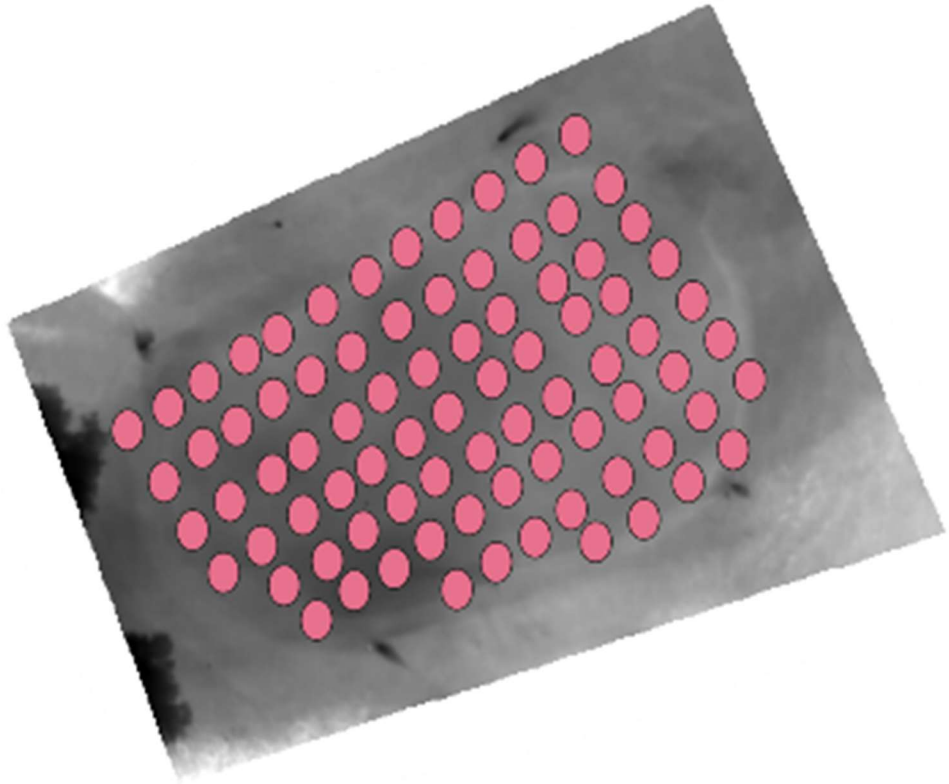


**Figure 2.** Thermal orthomosaic derived from a DJI Mavic 3T small unmanned aerial vehicle (sUAV) image acquisition of a ‘Tif-eagle’ ultradwarf bermudagrass (*Cynodon dactylon x C. transvaalensis*) green 4 at Independence Golf Club in Richmond, Virginia in 2023 displaying polygon buffers centered around points corresponding to catch can locations within the image on a 1.5 m radius with approximately 360 pixels per polygon and designated based on the spacing of the catch cans to compensate for any pixel resampling.

**Table 2.** Irrigation head and model for each ultradwarf bermudagrass (*Cynodon dactylon* × *Cynodon transvaalensis*) green and hybrid bermudagrass tee locations at Independence Golf Club in Richmond, Virginia in 2023 along with minimum, maximum, and average operating pressures in kilopascals for an average of four irrigation heads at each location.

<b>Irrigation Head Information</b>				
<b>Location</b>	<b>Toro Model</b>	<b>Operating Pressure Minimum (kPa)</b>	<b>Operating Pressure Maximum (kPa)</b>	<b>Average Pressure (kPa)</b>
Green 4	760	537.42	592.54	570.15
Green 5	760	482.3	537.42	508.14
Green 7	760	447.85	509.86	485.75
Green 9	760	496.08	592.54	546.03
Tee 3	780	551.2	626.99	585.65
Tee 4	780	509.86	578.76	544.31
Tee 5	780	509.86	606.32	564.98
Tee 7	780	496.08	564.98	530.53

**Table 3.** Multivariate analysis of all continuous data pooled across ultradwarf bermudagrass (*Cynodon dactylon* × *Cynodon transvaalensis*) green and hybrid bermudagrass tee locations at Independence Golf Club in Richmond, Virginia in 2023 were Catch Can Volume in milliliters of irrigation, Soil Moisture, Red Mean, Green Mean, Blue Mean, and Thermal Mean pixel values derived from a DJI Mavic 3T small unmanned aerial vehicle (sUAV) image acquisition.

<b>Multivariate Analysis</b>						
	<b>Catch Can Volume Ψ</b>	<b>Soil Moisture †</b>	<b>Red Mean</b>	<b>Green Mean</b>	<b>Blue Mean</b>	<b>Thermal Mean</b>
<b>Catch Can Volume</b>	-	-0.0147	0.3801	0.1576	0.3224	0.4005
<b>Soil Moisture</b>	-0.0147	-	-0.1787	-0.1497	-0.2733	-0.1849
<b>Red Mean</b>	0.3801	-0.1787	-	0.7667	0.8443	0.4227
<b>Green Mean</b>	0.1576	-0.1497	0.7667	-	0.8602	-0.1264
<b>Blue Mean</b>	0.3224	-0.2733	0.8443	0.8602	-	0.117
<b>Thermal Mean</b>	0.4005	-0.1849	0.4227	-0.1264	0.117	-

**Note:** All data involves an aggregate for after-irrigation applications only because there is no Catch Can Volume data to be measured for before-irrigation applications.

Ψ Catch Can Volume derived by collecting water post irrigation applications in catch cans with an opening of 12.7 cm and depth of 20.32 cm on 3 m x 3 m spacing across the tested locations.

† Soil water content calculated using the time-domain reflectometry (TDR) using 3.8 cm probes as an estimation of water in a given volume of soil sampled.

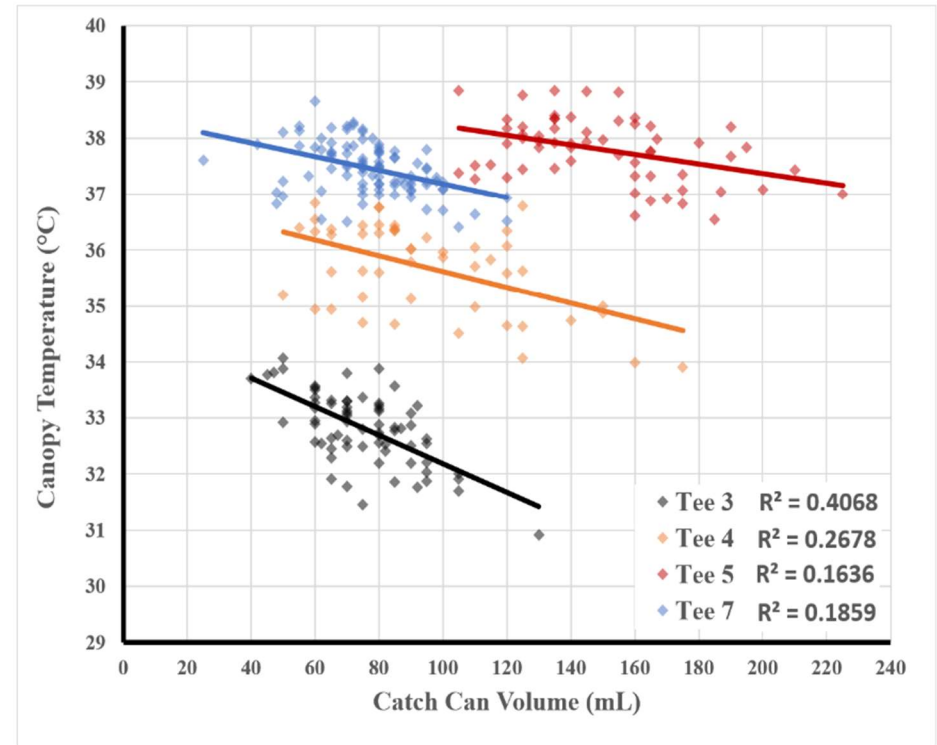
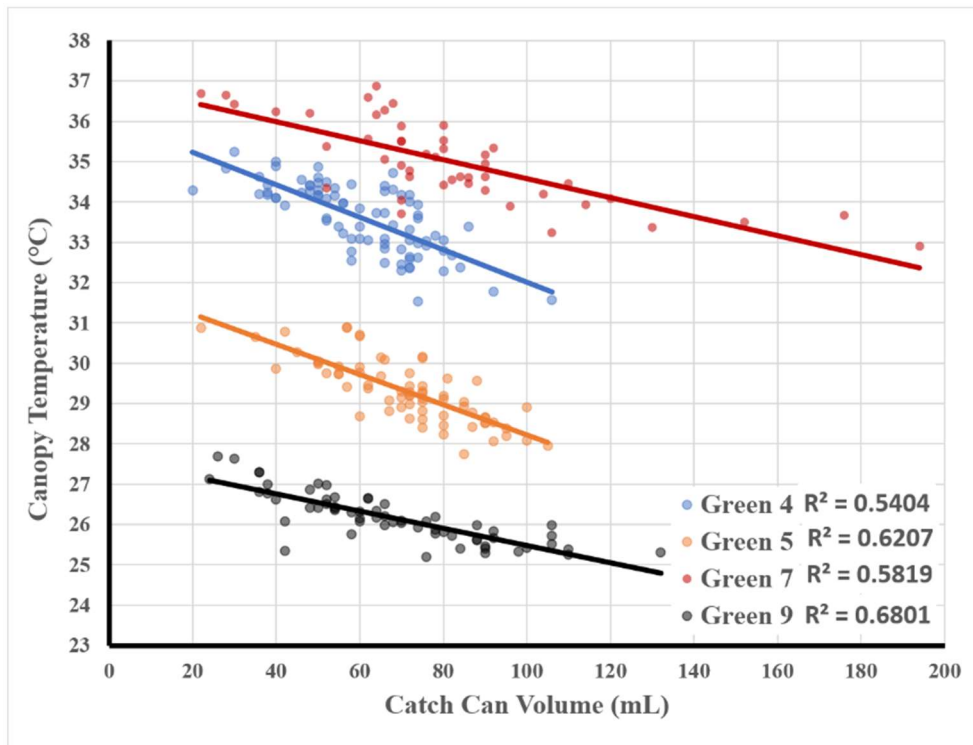


**Figure 3.** Bivariate analysis of canopy temperature pixel values in degrees Celsius derived from a Mavic 3T small unmanned aerial vehicle (sUAV) equipped with a DJI 640 x 512 thermal lens measuring canopy temperature compared to total catch can volume of water post-irrigations applications for all A). ultradwarf bermudagrass (*Cynodon dactylon* × *Cynodon transvaalensis*) greens and B). all hybrid bermudagrass tee locations at Independence Golf Club in Richmond, Virginia in 2023.

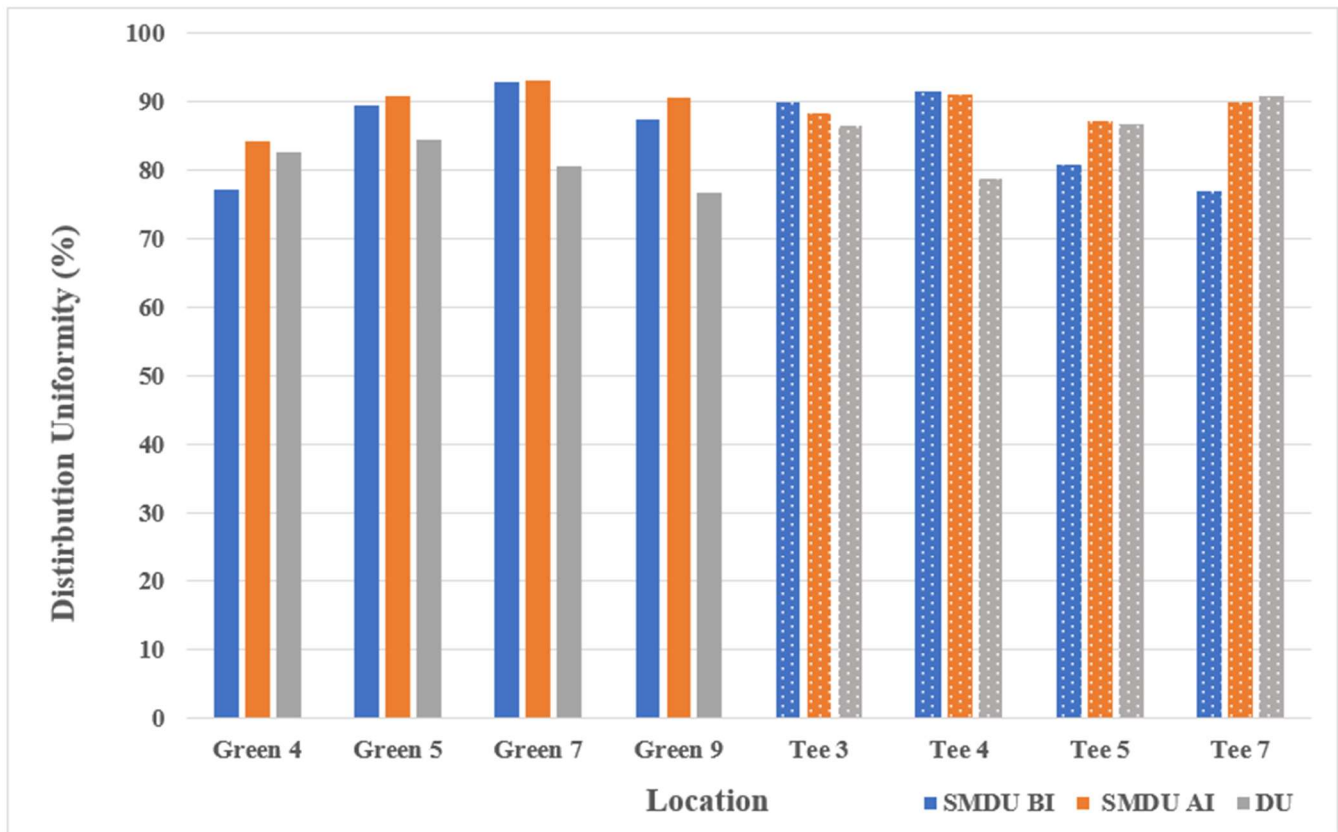
**Table 4.** Displaying summarized statistical data (sample #, minimum and maximum (Min and Max) values, Mean, standard deviation (Std Dev), standard error mean (Std Err Mean), and lower and upper 95%) related to canopy temperature (°C) and soil moisture (%) values along with the delta ( $\Delta$ ) change of before and after sampling events separated by each ultradwarf bermudagrass (*Cynodon dactylon*  $\times$  *Cynodon transvaalensis*) greens and B). all hybrid bermudagrass tee locations at Independence Golf Club in Richmond, Virginia in 2023.

Canopy Temperature						$\Delta$ Canopy Temperature				
Location	Sample #	Min	Max	Mean	Std Dev	Sample #	Min	Max	Mean	Std Dev
Green 4	164	31.5	38.1	34.9	1.5	82	-5.1	0.0	-2.5	0.9
Green 5	140	27.7	32.5	30.5	1.4	70	-3.5	-0.9	-2.5	0.6
Green 7	94	32.9	39.0	36.4	1.6	47	-4.3	-1.5	-2.9	0.8
Green 9	124	25.2	27.7	26.4	0.5	62	-1.3	0.6	-0.5	0.4
Tee 3	140	30.9	37.6	34.1	1.5	70	-4.7	-1.2	-2.7	0.9
Tee 4	100	33.9	43.3	38.0	2.5	50	-8.5	-2.4	-4.6	1.4
Tee 5	120	36.5	49.6	41.8	4.2	60	-11.9	-5.6	-8.1	1.5
Tee 7	188	36.4	47.1	40.1	2.8	94	-10.7	-3.4	-5.3	1.3
Soil Moisture						$\Delta$ Soil Moisture				
Location	Sample #	Min	Max	Mean	Std Dev	Sample #	Min	Max	Mean	Std Dev
Green 4	164	14.80	53.90	32.46	8.30	82	-2.50	21.30	7.37	4.03
Green 5	140	17.60	55.40	35.36	7.76	70	-1.6	18.9	8.32	3.19
Green 7	94	25.60	49.30	37.54	5.39	47	-3.00	10.20	4.91	2.71
Green 9	124	21.60	46.40	30.70	4.84	62	-9.2	10.5	3.07	3.36
Tee 3	140	15.80	55.20	35.93	7.96	70	-1.8	27.5	8.01	4.92
Tee 4	100	19.5	62.8	36.55	6.14	50	-7.6	21.3	3.33	6.25
Tee 5	120	15.2	58.6	32.19	8.08	60	-24.7	31.7	7.41	9.64
Tee 7	188	11.1	56.6	35.51	9.00	94	-2.9	28.9	10.20	7.57

**Table 5.** United States Department of Agriculture particle size percentages displayed by each ultradwarf bermudagrass (*Cynodon dactylon* × *Cynodon transvaalensis*) greens and hybrid bermudagrass tee locations at Independence Golf Club in Richmond, Virginia in 2023 showing very coarse sand (VCS), coarse sand (CS), medium sand (MS), fine sand (FS), very fine sand (VFS), coarse silt (CSI), medium silt (MSI), fine silt (FSI), and clay (C).

<b>Particle size class</b>	<b>VCS</b>	<b>CS</b>	<b>MS</b>	<b>FS</b>	<b>VFS</b>	<b>CSI</b>	<b>MSI</b>	<b>FSI</b>	<b>C</b>
<b>Particle size (mm)</b>	2.00 - 1.00	1.00 - 0.50	0.50 - 0.25	0.25 - 0.10	0.10 - 0.05	0.05 - 0.02	0.02 - 0.005	0.005 - 0.002	< 0.0002
<b>Green 4</b>	7.16	26.94	22.60	39.86	2.62	0.00	0.24	0.00	0.60
<b>Green 5</b>	8.85	25.76	21.43	39.14	1.71	0.97	0.36	0.00	1.80
<b>Green 7</b>	7.54	22.61	43.22	18.29	3.92	1.27	0.36	0.20	2.60
<b>Green 9</b>	4.23	33.30	43.96	14.69	1.71	0.00	0.40	0.08	1.80
<b>Tee 3</b>	12.05	40.56	32.83	9.04	0.90	1.07	0.76	0.32	2.47
<b>Tee 4</b>	7.02	30.59	44.84	12.34	1.00	0.74	0.80	0.20	2.47
<b>Tee 5</b>	8.32	34.67	39.68	11.92	0.90	1.49	0.32	0.48	2.22
<b>Tee 7</b>	8.15	32.09	39.34	11.57	2.72	0.00	1.65	2.58	5.49

**Figure 4.** Distribution uniformity for the soil moisture before irrigation (SMDU<sub>BI</sub>), after irrigation (SMDU<sub>AI</sub>), and for irrigation water physically applied by measuring water volumes caught in evenly distributed catch cans (DU) separated by all ultradwarf bermudagrass (*Cynodon dactylon* × *Cynodon transvaalensis*) greens and hybrid bermudagrass tee locations at Independence Golf Club in Richmond, Virginia in 2023.



## **Chapter 4: Enhancing Winter Cover Decisions for Ultradwarf Bermudagrass Putting Greens Using Capacitive Soil Sensors in the Transition Zone**

### **Abstract**

Cold-related injury presents a significant challenge for managing ultradwarf bermudagrass (UDB) putting greens in the transition zone, necessitating the need for mitigation strategies. This study evaluates the viability of using capacitive soil sensors to monitor soil temperature under different winter covering treatments. Field studies were conducted from November to May during 2022-2023 (Green 9) and 2023-2024 (Green 1) at Independence Golf Club in Richmond, Virginia, on UDB putting greens subjected to no, single, and double polypropylene covering treatments. Soil temperature and moisture were continuously monitored with capacitive soil sensors to assess the effectiveness of the cover treatments in mitigating winter stress. The results indicated soil temperature was highly dependent on covering applications. Double cover and single cover treatments consistently maintained higher daily average soil temperature at 45.70°F and 45.20°F, respectively, compared to the no cover treatment for all covering events at 42°F. No significant differences were found between single and double cover average soil temperature, suggesting that double cover may only be necessary at temperatures below those experienced in this study or when confounding factors necessitate. Moreover, with the lowest recorded soil temperatures at 33°F for Green 9 and 31°F for Green 1 under the no cover treatment—and no winter injury observed, we suggest that UDB may be able to tolerate these temperatures for brief periods under fully dormant conditions. Additionally, soil moisture for Green 9 was highest for the single covering treatment (20.70%) and lowest for the double covering treatment (17.30%). In contrast, Green 1 had the highest soil moisture for the double covering treatment (42.50%) and the lowest for the single covering treatment (35.60%). Lastly, for the coldest covering event

on Green 1, soil moisture fluctuated the most within no covering treatments compared to single and double covering due to freeze-and-thaw cycles of the soil water during cold extremes. These findings provide insights into optimizing winter management practices for UDB, with potential applications in enhancing winter survival and reducing maintenance costs for golf courses by continuously monitoring soil temperature and moisture to determine when to apply or withhold covering applications.

## Introduction

Ultradwarf bermudagrass (UDB) [*Cynodon dactylon* (L.) Pers. × *C. transvaalensis* Burt-Davy] has been a widely used warm-season amenity turfgrass for putting greens throughout the transition zone due to its adaptability and ability to maintain aesthetics under significant stress (Beard & Sifers, 1996). Ultradwarf bermudagrass is particularly valued for its tolerance to summer temperature and drought stress compared to creeping bentgrass (*Agrostis stolonifera*), and reduced susceptibility to fungal pathogens that can diminish turfgrass quality (Beard, 1997; Dunne et al., 2019; Lowe, 2013). These are crucial attributes for quality golf putting surfaces during peak play periods of summer, but present inherent challenges with survival during winter months when grass tolerance to low-temperature extremes is of greater concern.

Winter survivability of UDB involves the survival of nodes within rhizomes and stolons through extreme winter temperatures, followed by normal growth in the subsequent spring (Yu et al., 2022). Winterkill is a generic term for injury to UDB that becomes apparent only as the turfgrass transitions from winter dormancy to a spring green-up period of active growth. Monitoring soil conditions is essential to ensure the survival of UDB from cold-related injury, particularly to avoid winterkill. Golf courses and other intensively managed bermudagrass areas are at an increased risk of winterkill due to late-season fertilization, low mowing heights, and traffic from equipment or people (Hutchens et al., 2024). These conditions, combined with low temperature, lack of crown hydration (leading to winter desiccation), or diseases like pink snow mold, exacerbate winterkill (Gopinath et al., 2021).

Despite these risks, the benefits of UDB during the prime months for golf justify its continued use and the utilization of turfgrass covers to regulate soil and canopy temperatures during winter extreme weather events has become a widely accepted practice by turfgrass

managers (Richardson & Booth, 2023). Custom polypropylene covers have been shown to increase the mean surface temperature when used as a protection against winter conditions driven by ambient temperatures below 25°F for UDB. Furthermore, Goatley et al. (2005) reported an accelerated spring green-up of hybrid bermudagrass athletic fields by four to six weeks and an increase in total nonstructural carbohydrates when covering was implemented at 40°F and remained into the spring. While prolonged covering may be feasible on athletic fields that are closed during dormant winter months, the need for golf courses to remain open during the winter as a revenue source limits this practice on putting greens. Rapid ambient temperature fluctuations during the winter make planning for the application of turfgrass covers a challenge.

The importance of predicting when to cover is crucial for golf courses with UDB putting greens. Covering not only affects revenue from golf rounds but also advanced planning to allocate resources effectively for covering and uncovering greens. The cost of covering can range from \$20,000 to \$30,000 to cover all greens for an 18-hole facility, with approximately \$2,000 in labor for each covering event (application and removal) (Hartwiger & O'Brien, 2008). The industry standard threshold for implementing covers is when forecasted ambient temperatures are  $\leq 25^{\circ}\text{F}$  which is used to enhance the survival of UDB during extended cold periods (Trenholm, 2000).

More recently, research suggests UDB can survive at ambient temperatures of 20°F and that a lower covering threshold of 20°F may be acceptable (DeBoer et al., 2019). DeBoer et al. (2019) also reported that UDB greened up more quickly in the spring when covers were installed at all temperatures of  $\geq 18^{\circ}\text{F}$ . In the United States' transition zone where UDB putting greens are used, but winter extremes are a concern, such temperature thresholds can be met quickly, unexpectedly, and even multiple times during the winter season. Drastic fluctuations of winter

conditions can stimulate UDB growth when cold acclimation is more beneficial for bermudagrass survival. Covering UDB putting greens becomes increasingly more difficult when managers must plan for double covering, which involves using two layers of covers, and is considered necessary by many golf superintendents in certain extreme conditions.

Booth (2022) and DeBoer et al. (2019) investigated the effectiveness of different covering strategies in regulating soil temperatures to prevent winterkill in UDB cultivars. HOB0 (Bourne, MA) and Spectrum (Aurora, IL) Watchdog 1000 series soil sensors were embedded at a 1 in depth below the surface and required direct access to examine the data, making this strategy impractical for routine monitoring by turfgrass professionals. Their findings demonstrated that the use of double covers with and without airgaps regulated soil temperatures more effectively than single covers and covering at temperatures  $\geq 18^{\circ}\text{F}$  resulted in faster spring green-up of three UDB cultivars compared to uncovered treatments. However, both studies focused on average changes in soil temperature and minimum observed values, without examining cumulative daily fluctuations throughout day and night cycles. Moreover, these covering studies were not able to evaluate how covering applications impact soil moisture due to limitations of the soil sensor. The rationale for using soil temperature as an indicator of potential winterkill risk lies in the relationship between soil temperature and solar-radiation energy retained in the soil versus what is lost to the atmosphere (Geiger et al., 2009). Additionally, understanding how soil moisture relates to soil temperature during these winter covering conditions will help expand upon factors that relate to winter desiccation.

During extreme winter conditions, a lack of soil moisture has a direct correlation to tissue desiccation of warm-season grasses (Dunne et al., 2019; Patton & Reicher, 2007). Winter desiccation becomes the most problematic with areas exposed to elevated wind speeds seen

during temporal weather conditions (Kreuser, 2014). However, irrigation has shown direct success in minimizing the onset of tissue desiccation (Doherty et al., 2024; Hutchens et al., 2024). Limiting desiccation through irrigation aids in minimizing the degradation of organelle functions that leads to eventual turfgrass death (Stier & Fei, 2008). Another method is to make wetting agent applications to preserve soil moisture within the soil and plant system which has shown varied results but positive effects during the driest years (DeBoer et al., 2020). Evidence displays a relationship between soil moisture, but limited research shows how soil temperature and moisture relate together in these circumstances. One phenomenon that occurs during cold temperature extremes is the freezing and thawing of soils leading to soil water redistribution (Kahimba et al., 2009). This relationship highlights the importance of understanding soil temperature and moisture dynamics to optimize covering practices.

Continuous soil temperature and moisture monitoring when covering UDB putting greens in real-time over multiple day/night cycles allow researchers and turfgrass practitioners to observe not only soil data extremes but also relative changes throughout a covering event. Capacitive soil sensors are a common tool for continuously measuring soil data, particularly soil moisture with smart irrigation scheduling (Sass & Horgan, 2006; Serena et al., 2020). While capacitive soil sensors have gained popularity in agricultural sectors for smart watering practices (Faqir et al., 2024; Mauri et al., 2021), there is limited research for UDB putting greens sensors to collect soil data and trigger agronomic decisions based on the on-demand, transmitted data they provide.

Our study builds upon existing research by incorporating covering treatments (double cover, single cover, and no cover) and using capacitive soil sensors under transition zone winter conditions for UDB. We hypothesize that by using capacitive soil sensor technology to

continuously monitor UDB soil temperature and moisture during covering events, actionable thresholds for covering decisions can be developed. This approach uses real-time soil temperature and moisture data to establish a correlation between soil temperature and moisture data for covering decisions. We aim to refine strategies for the application of covers for protecting UDB putting greens during winter, thus improving grass survival rates, reducing maintenance costs and loss of golfing revenue.

## **Materials and Methods**

### *Research Site and Management*

A two-year field study was conducted at Independence Golf Club's Par 3 Short Course in Richmond, Virginia (37.54°N, -77.68° W) over two consecutive winter seasons: 2022-2023 (Green 9) and 2023-2024 (Green 1). Green 9 covering events were conducted on a 'Tif-Eagle' UDB putting green, while Green 1 covering events took place on an experimental UDB putting green ('FAES 1302' from University of Florida) (Table 1). Both sites were established in the summer of 2017, so each putting green was mature at the time of the study.

Both UDB putting greens were managed similarly, with 34.5 lb./A of N applied monthly from May to September using an 18-9-18 fertilizer (Contec DG; The Anderson's, Maumee, OH). In July, both greens were aerified using a Pro-Core 648 (The Toro Company, Bloomington, MN) with 0.50-in hollow tines on 2.50-in spacing to a depth of 3 in, and all channels were filled with topdressing sand. From June to September, the greens were verticut to a depth of 0.10 in using a John Deere 2700 E-Cut Hybrid triplex mower equipped with verticut reel attachments (John Deere, Moline, IL). Mowing was done with a John Deere triplex mower at 0.13 in during the growing season and increased to 0.14 in as the cold acclimation period approached in preparation for winter dormancy. During the growing season from May - October, irrigation was applied as

needed to maintain turfgrass quality, with no additional irrigation during the winter months from November – April with soil moisture relied solely on natural rainfall.

### *Experimental Design*

The experiment was a repeated measures study where the same plots were covered multiple times throughout the study at each location. For Green 9 which is indicated as Winter 1 2022-2023, the experiment was organized as a randomized complete block design with four replications of three treatments: no cover, single cover, and double cover. For Green 1 which is indicated as Winter 2 in 2023-2024, a completely randomized design was used because the shading effect was not present, and space limitations prevented symmetrical blocking (Figure 2). Plot sizes for both locations were 3.66 m × 3.66 m. In Winter 1, plot edges overlapped due to the absence of plot buffers. To address this limitation, Winter 2 plots had 0.61 m buffers around all plots to accommodate cover stretching for staking purposes and to increase the tensile force on the covers.

### *Treatment Description and Implementation*

All covering treatments used S&S Turf Covers (Covington, GA) customized to 3.66 × 3.66 m in size and made from 93% pure polypropylene material with 15% porosity to allow moisture, temperature, and gas exchange. Each cover had 12 double-stitched handles around its perimeter to simulate the stretching and staking of a golf course putting green cover for small-plot research. In the double-cover treatments, covers were laid on top of one another without an air gap, and the same stakes were used for both cover handle loops. Each winter had two covering events when forecasted ambient temperatures were expected to fall below 25°F (O'brien & Hartwiger, 2014). The course superintendent used an on-site weather station equipped with Vantage Pro 2 monitoring equipment (Perry Weather, Dallas, TX) to track

forecasts and guide covering decisions for Independence Golf Club's main revenue-generating course. All covering events followed the same protocols used for the putting greens on the 'Champion' UDB greens for the 18-hole golf course at Independence Golf Club where testing occurred.

#### *Capacitive Soil Sensor Description and Installation*

To measure soil conditions, a plug was removed from the center of each plot using a Miltona square plugger (St. Paul, MN), creating a  $7 \times 7 \times 3$  in hole (Figure 3A). A Spiio (SP-110) capacitive soil sensor (CSS; Palo Alto, CA), measuring  $7.08 \times 1.85 \times 1.85$  in, was installed horizontally at a depth of 3 in from the surface where the moisture plate was parallel with the soil wall (Figure 3B). The installation depth was chosen within this study based on the desire of the on-site superintendent to build a relevance of the data generated towards their desired installation within the active root-zone layer. Careful consideration was given to position the sensor properly to only measure soil moisture as it relates to field capacity of the soil and securing the sensor within undisturbed soil, ensuring close contact with the soil and minimizing potential air gaps (Figure 3C). Each capacitive soil sensor was installed in mid-November to provide sufficient time for the sensor to acclimate to soil environment conditions and removed at the beginning of May for both Green 9 and Green 1 to allow for continuous soil data collection. This timing avoided potential cold injury onset and ensured data collection during each cold event. Each capacitive soil sensor was rotated to position the moisture plate vertically along the sensor's width (Figure 3C), allowing it to measure only the soil's inherent moisture without interference from water on the plate or blockage by the sensor body. The capacitive soil sensors are equipped with an integrated chip temperature sensor located adjacent to the moisture plate, providing temperature data within a 0.50% accuracy. Soil moisture is measured by a capacitive plate that

operates with an accuracy of 2% volumetric water content. With the sensor centered in the hole, the moisture plate samples a 2×1 in soil cross-section at an approximate depth of 2.50 in this configuration provides accurate soil moisture and temperature data for evaluating each covering event's effects throughout the two winters.

### *Data Collection and Analysis*

During periods that triggered covering event initiation, soil temperature and soil moisture were continuously monitored at an estimated depth of 2.5 in for all plots using the capacitive soil sensors that logged and transmitted data wirelessly to a cloud server. Data were transmitted hourly and downloaded from the app.spiio.com platform for postprocessing. Due to weather variability from one winter season to the next, repeated covering events from each location were not examined as a comparison across years. All data were converted to daily averages for soil temperature and moisture. A repeated measures analysis of variance was performed using a residual repeated structure mixed-effects model to evaluate the effects of location, treatment, and their interactions on soil temperature and moisture response variables. The analysis was conducted using JMP Pro V16.0.0 (Cary, NC). Treatment means were separated using Tukey-Kramer HSD at a  $\alpha = 0.05$ . To complement the mixed model results, average daily soil temperature and moisture values by treatment during covering events were used to calculate the standard deviation, providing additional insight into variability.

## **Results and Discussion**

The effects of treatment, location, and their interaction on soil temperature and moisture were subjected to ANOVA (Table 1). Results from the mixed model are presented by treatment, pooled across location for soil temperature, and by the treatment-by-location interaction for soil moisture. Soil temperature was presented by treatment rather than the significant treatment-by-

location interaction due to the *F*-ratio's weight in the model and its biological relevance to the original research question. Soil moisture data were pooled across covering events within the Green 9 and Green 1 locations, as the focus was on the effects of no covering, single covering, and double covering, rather than the repeated nature of covering events by location.

Soil temperatures were similar between single- and double-cover treatments but were significantly warmer than the uncovered control by more than 3°F (Table 2). Soil moisture across the combined covering events was lower in Green 9, averaging 19.30%, compared to 39.10% in Green 1 (data not shown). For Green 1, soil moisture was lowest under the single-cover treatment (35.60%) and highest in the double-cover treatment (42.80%). The uncovered control differed significantly from both treatments, with an average soil moisture of 38.90%, falling between the two covering events. Conversely, on Green 9, soil moisture was highest in the single cover treatment (20.70%) and lowest in with a double cover treatment (17.30%). Soil moisture in the non-covered treatment was similar to those with a single cover (19.84%) and higher than the double cover treatment.

During the winter of 2022-2023, the highest daily minimum ambient temperature occurred on 6 Nov 2022, and the lowest minimum ambient temperature on 24 Dec 2022 (Figure 4). During the winter of 2023-2024, the highest daily minimum ambient temperature was recorded on 25 Jan 2024, and the lowest minimum temperature on 17 Jan 2024 (Figure 5).

Cover treatments were not imposed on 23 Dec 2022 due to the uncontrolled reasons during this period; however, the entire test site was covered as a precaution to prevent winterkill. The putting greens were covered for a total of 21 days in Winter 1 and 15 days in Winter 2, with two covering events in each season. Additionally, actual ambient low temperatures reached or crossed the critical level of 25°F threshold on five nights in the winter of 2022-2023 and six

nights during the winter of 2023-2024. However, in each instance, the predicted low temperatures did not meet the threshold requirement for a single night, so covering events were not initiated. The shortest covering event occurred in Nov 2023, while the second covering event in March 2023 was the longest (Table 3). All covering events exhibited similar trends in soil temperature deviations between treatments (Figure 6). Notably, covering event 2 was the longest and warmest covering period, which explains the anomaly observed during this event.

Total precipitation was greater in the winter of 2023-2024 than in 2022-2023, with 23 in and 14 in, respectively. Data collection within test sites showed that Green 1 had more soil water content at cover initiation, while Green 9 received more precipitation during active covering events (Table 3). Only the third covering event had no precipitation during cover application, and the fourth covering event received only 0.15 in of precipitation. In contrast, each of the two covering events for Green 9 received 0.53 in during active covering.

Prior to covering, soil moisture was higher at initiation for Green 1, which can be attributed to precipitation. These rainfall events help explain the variability in soil moisture deviations between treatments, as seen in the box-and-whisker representing each covering event (Figure 6). Despite variable rainfall during these covering events, soil temperature in non-covered treatments consistently deviated from those in single- and double-cover treatments, except during the second covering event for Green 9. This suggests that, at the depth where the capacitive soil sensors were installed, soil moisture may have minimal influence on soil temperature deviations and plays a more significant role closer to the surface (Shashikumar & Nus, 1993).

Establishing critical thresholds based on soil temperature would be more practical due the steady thermal energy transfer via conduction compared to the transient nature of water vapor

flow (Shiozawa & Campbell, 1990). While this approach is theoretically sound, no winter injury or delayed green-up was observed in any of the non-covered treatments during these covering events (data not shown). Capacitive soil sensor data could enable enhanced monitoring and prediction of when to apply or avoid covering. However, further research is needed to build confidence in actionable thresholds and to incorporate weather parameters into the decision-making process.

Covering event 4 had the largest range in soil temperature for the no-cover treatment of 31.23-45.24°F , while covering event 3 had the smallest range for the no-cover treatment of 36.53-47.30°F (Figure 6). For double covers, covering event 2 exhibited the largest soil temperature range of 46.62-58.93°F , while covering event 3 had the lowest range of 48.59-48.23°F . Interestingly enough, single covering observed the same trends as the double covering for covering events 2 and 3. These can be explained due to the microclimates of each location with more shading occurring on Green 9 than Green 1 throughout the day. In three of the four covering events (1, 3, and 4), double covering consistently had the lowest soil temperature range, whereas no covering had the largest spread in data. The exception was covering event 2, where the no-cover treatment showed the lower ranges when compared to single and double covering, and likely due to the extended duration of covering and warmer weather during this period.

For soil moisture, Green 9 (CE1 and 2) had the lowest soil moisture fluctuations compared to Green 1 (CE3 and 4) and was consistent regardless of treatment. These observations are most likely due to the construction method at establishment with all organic matter removed at establishment for Green 9 compared to no-till establishment for Green 1. Across all covering events, the no-cover treatment had the largest range, while double covering consistently had the smallest regardless of location. This suggests that double covering treatments help to retain soil

moisture and that less soil temperature changes lead to less soil moisture movement in the soil profile.

The fourth covering event is highlighted to expand upon soil data during this period, as it exhibited the largest range in soil moisture (Figure 6) and provides a representative treatment influence on soil temperature compared to other covering events (Figure 7). During this event, an observable relationship was noted between the timing of covering and deviations in soil temperature. A delayed response of approximately one to two days was observed between installation of covering treatments and when soil temperature changes became apparent. Similarly, the no-cover soil temperature data showed a one-day delay after the covers were removed before soil temperatures normalized across all treatments. These findings illustrate the buffering of soil temperature compared to ambient temperature (Figure 7). These trends align with other UDB covering research documenting the effects of covers on soil temperature (DeBoer et al., 2019; Goatley et al., 2005; Goatley et al., 2009). However, anecdotal evidence highlights the potential need for double covers during extreme weather events. Another observation is the distinct difference in day and nighttime soil temperature fluctuations. Single and double-cover treatments maintained a colder state and did not exhibit the daytime warming effect seen in the no-cover treatment. Sampling soil temperature at a shallower depth and collecting microclimate data for the experimental area could further refine these observations. For Green 9, the lowest soil temperature recorded was 32.5°F during the first covering event, while the lowest temperature observed during the fourth covering event was 28.5°F (data not shown). These were brief periods recorded during single replications, and no injury was observed. This suggests that UDB can tolerate brief periods of low soil temperatures above these thresholds. The duration of exposure to sustained low soil temperatures may be more relevant for

understanding winterkill events and developing actionable thresholds as leading indicators of such events.

During the fourth covering event, clear evidence of soil moisture variation is observed in relation to a critical low point in soil temperature (Figure 8). The no-cover treatment exhibited a range of approximately 23-44% soil moisture, whereas the single and double-cover treatments maintained steady levels around 35% and 43%, respectively. These observations are consistent with findings that covering applications increase crown hydration retention (Shashikumar & Nus, 1993) and minimize soil moisture variation due to the lack of water penetration through covers (Goatley et al., 2017). Since covers limit water penetration, it is plausible that they also reduce evaporative moisture loss. This results in less latent heat transfer through vaporization and condensation, contributing to reduced soil temperature fluctuations. Soil moisture is directly related to the soil's thermal capacity and conductivity, supporting the reduced variation under covered conditions (Negm et al., 2017).

Under covering events, energy transfer between the solar energy and the covers appears to be retained within the soil, minimizing soil water condensation during colder periods. This limits soil water movement compared to the no-cover treatment. Between 21 Jan 2024 and 23 Jan 2024, significant changes in soil moisture were observed specifically for the no-cover treatment (Figure 8). These dates are noteworthy due to the drastic soil moisture reductions, which can be explained by capacitive soil sensor responses to soil temperatures reaching critical levels where soil water transitions from liquid to solid. As soils freeze, water becomes frozen and less detectable by sensors, resulting in a sharp decline in measured soil moisture when temperatures drop below 32°F. Conversely, as the soil temperature rise above freezing, water

transitions back to a liquid state and redistributes within the soil, causing abrupt increases detected by the sensors.

The reduced availability of soil water for sensor detection during freezing periods also implies limited plant-available water, which is critical for plant and crown hydration. Covers enhance winter survival by retaining moisture around the crown and preventing excessive dehydration (Michael & Kreuser, 2020). Predictive frozen soil thresholds could serve as important leading indicator of determining covering events. Capacitive soil sensor data may provide valuable monitoring capabilities to identify and respond to such conditions effectively.

### **Conclusions**

This study evaluated the use of capacitive soil sensors as a viable tool to continuously monitor soil temperature and moisture of ultradwarf bermudagrass (UDB) putting greens during turfgrass covering events to prevent winterkill from cold temperature extremes. Our data suggests that capacitive soil sensors effectively quantified soil temperature and moisture only during periods when soil moisture was not frozen while differentiating the effects of no covers compared to single and double cover treatments during four covering events across two winter seasons. No winterkill was observed in this study when using previously defined action thresholds for covering UDB putting greens. Our data suggest that the lethal temperature of UDB at a 2 inch soil depth is lower than the temperatures achieved in this study (33.0°F for Green 9 and 31.0°F for Green 1). As the buffering capacity of soils limits temperature fluctuations relative to ambient temperatures, further research is needed to refine a predictive temperature threshold that translates to capacitive soil sensor data. The deployment of capacitive soil sensors provided valuable, real-time data on soil temperature and moisture, offering insights into the micro-environmental conditions under various winter covering regimes. The findings indicate

that soil sensors have the capability to enhance monitoring UDB greens during winter periods and respond to critical changes in soil conditions. These results contribute to the optimization of winter management practices for ultradwarf bermudagrass, offering practical implications for turfgrass managers seeking to improve turfgrass survival and performance under winter stress conditions. Further research is warranted to refine the use of sensor technology, explore additional covering materials influence on soil temperature and moisture data and methods that may enhance winter survival rates for bermudagrass in challenging climates. Additionally, exploring the use of data collection means for justifying why soil radiation is not captured more under double covering compared to single covering treatments such as the use of light sensors underneath these covering events. Moreover, future research should expand upon the benefits of continuous soil monitoring data at these preconceived installation depths compared to soil temperature data collected closer to the turfgrass surface to better understand soil temperature depth relationships under these winter conditions. These data could help elucidate the relationship for a better understanding of temperature closer to the crown of the turfgrass plant. Lastly, if winterkill can be simulated for field conditions, these data could be integrated with local weather station data to investigate the most influential factors that drive the highest probability of observed winterkill damage through correspondence of accurate and local above and below ground data.

### References

- Beard, J., & Sifers, S. (1996). New cultivars for southern putting greens. *Golf Course Manage*, 64(12), 58-62.
- Beard, J. B. (1997). Dealing with heat stress on golf course turf. *Golf Course Management*, 65(7), 54-59.
- DeBoer, E. J., Karcher, D. E., McCalla, J. H., & Richardson, M. D. (2020). Effect of late-fall wetting agent application on winter survival of ultradwarf bermudagrass putting greens. *Crop, Forage & Turfgrass Management*, 6(1), 1-7. <https://doi.org/10.1002/cft2.20035>

- DeBoer, E. J., Richardson, M. D., McCalla, J. H., & Karcher, D. E. (2019). Reducing ultradwarf bermudagrass putting green winter injury with covers and wetting agents. *Crop, Forage & Turfgrass Management*, 5(1), 1-9. doi:10.2134/cftm2019.03.0019
- Doherty, J. R., Hutchens, W. J., Booth, J. C., McCall, D. S., Battaglia, M. V., DeBoer, E. J., & Roberts, J. A. (2024). Improving winter survival of interspecific hybrid bermudagrass in the Mid-Atlantic region through cultural practices. *Crop, Forage & Turfgrass Management*, 10(2), 1-11. <https://doi.org/https://doi.org/10.1002/cft2.20303>
- Dunne, J. C., Tuong, T. D., Livingston, D. P., Reynolds, W. C., & Milla-Lewis, S. R. (2019). Field and laboratory evaluation of bermudagrass germplasm for cold hardiness and freezing tolerance. *Crop Science*, 59(1), 392-399. doi: 10.2135/cropsci2017.11.0667
- Faqir, Y., Qayoom, A., Erasmus, E., Schutte-Smith, M., & Visser, H. G. (2024). A review on the application of advanced soil and plant sensors in the agriculture sector. *Computers and electronics in agriculture*, 226, 1-14. <https://doi.org/10.1016/j.compag.2024.109385>
- Geiger, R., Aron, R. H., & Todhunter, P. (2009). *The climate near the ground*. Rowman & Littlefield.
- Goatley, J., Maddox, V., Lang, D., Elmore, R., & Stewart, B. (2005). Temporary covers maintain fall bermudagrass quality, enhance spring greenup, and increase stem carbohydrate levels. *HortScience*, 40(1), 227-231.
- Goatley, J., Zhang, X., & Hensler, K. (2009). 'Riviera' bermudagrass responses to turf blanket covers during winter. *Applied Turfgrass Science*, 6(1), 1-9. doi: 10.1094/ATS-2009-0824-02-RS
- Goatley, M., Askew, W., Askew, S., Dickerson, J., & McCall, D. (2017). Turfgrass Cover Sources Vary in Temperature, Light and Moisture Penetration, and Weight. *International Turfgrass Society Research Journal*, 13(1), 297-304. doi: 10.2134/itsrj2016.06.0484
- Gopinath, L., Moss, J. Q., & Wu, Y. (2021). Evaluating the freeze tolerance of bermudagrass genotypes. *Agrosystems, Geosciences & Environment*, 4(2), 1-4. doi: 10.1002/agg2.20170
- Hartwiger, C., & O'Brien, P. (2008). The Ultradwarf Investment. *Course Care*. <https://www.usga.org/course-care/the-ultradwarf-investment-26337.html>
- Hutchens, W., Carr, T., Patton, A., Bigelow, C., DeBoer, E., Goatley, J., Martin, D., McCall, D., Miller, G., & Powlen, J. (2024). Management strategies for preventing and recovering from bermudagrass winterkill. *Crop, Forage & Turfgrass Management*, 10(2), 1-23. doi: 10.1002/cft2.20302
- Kahimba, F. C., Ranjan, R. S., & Mann, D. D. (2009). Modeling soil temperature, frost depth, and soil moisture redistribution in seasonally frozen agricultural soils. *Applied Engineering in Agriculture*, 25(6), 871-882. doi: 10.13031/2013.29237

- Kreuser, W. C. (2014). Turfgrass winterkill observations from the upper great plains: desiccation and cold temperature. *Applied Turfgrass Science*, 1-3. doi:10.2134/ATS-2014-0053-BR
- Lowe, T. (2013). Lessons learned with ultradwarf bermudagrasses in Florida. *USGA Green Section Record*, 51(1), 1-4.
- Mauri, P. V., Parra, L., Mostaza-Colado, D., Garcia, L., Lloret, J., & Marin, J. F. (2021). The combined use of remote sensing and wireless sensor network to estimate soil moisture in golf course. *Applied Sciences*, 11(24), 1-17. <https://doi.org/10.3390/app112411769>
- Michael, D. J., & Kreuser, W. C. (2020). Sand topdressing and protective covers impact creeping bentgrass crown moisture during winter. *Agronomy Journal*, 112(2), 1452-1461. doi: 10.1002/agj2.20058
- O'brien, P., & Hartwiger, C. (2014). Covering Guidelines For Ultradwarf Bermudagrass Putting Greens. <https://www.usga.org/course-care/2013/01/covering-guidelines-for-ultradwarf-bermudagrass-putting-greens-21474853349.html>
- Patton, A. J., & Reicher, Z. J. (2007). Zoysiagrass species and genotypes differ in their winter injury and freeze tolerance. *Crop Science*, 47(4), 1619-1627. doi: 10.2135/cropsci2006.11.0737
- Richardson, M., & Booth, J. (2023). Best Management Practices for Preventing Winter Injury on Ultradwarf Bermudagrass Putting Greens. <https://www.usga.org/content/usga/home-page/course-care/green-section-record/59/issue-20/best-management-practices-for-preventing-winter-injury-on-ultrad.html>
- Sass, J. F., & Horgan, B. P. (2006). Irrigation scheduling on sand-based creeping bentgrass: Evaluating evapotranspiration estimation, capacitance sensors, and deficit irrigation in the Upper Midwest. *Applied Turfgrass Science*, 3(1), 1-14. doi:10.2134/cftm2018.03.0012
- Serena, M., Velasco-Cruz, C., Friell, J., Schiavon, M., Sevostianova, E., Beck, L., Sallenave, R., & Leinauer, B. (2020). Irrigation scheduling technologies reduce water use and maintain turfgrass quality. *Agronomy Journal*, 112(5), 3456-3469. doi: 10.1002/agj2.20246
- Shashikumar, K., & Nus, J. (1993). Cultivar and winter cover effects on bermudagrass cold acclimation and crown moisture content. *Crop Science*, 33(4), 813-817. <https://doi.org/10.2135/cropsci1993.0011183X003300040037x>
- Shiozawa, S., & Campbell, G. S. (1990). Soil thermal conductivity. *Remote Sensing Reviews*, 5(1), 301-310. <https://doi.org/10.1080/02757259009532137>
- Stier, J., & Fei, S. (2008). Cold stress physiology and management of turfgrasses. *Handbook of turfgrass management and physiology*. CRC Press, Boca Raton, FL, 473-505.
- Trenholm, L. E. (2000). *Low temperature damage to turf*. University of Florida Extension Institute Food and Agriculture Sciences.

Yu, S., Schoonmaker, A. N., Yan, L., Hulse-Kemp, A. M., Fontanier, C. H., Martin, D. L., Moss, J. Q., & Wu, Y. Q. (2022). Genetic variability and QTL mapping of winter survivability and leaf firing in African bermudagrass. *Crop Science*, 62(6), 2506-2522. doi: 10.1002/csc2.20849

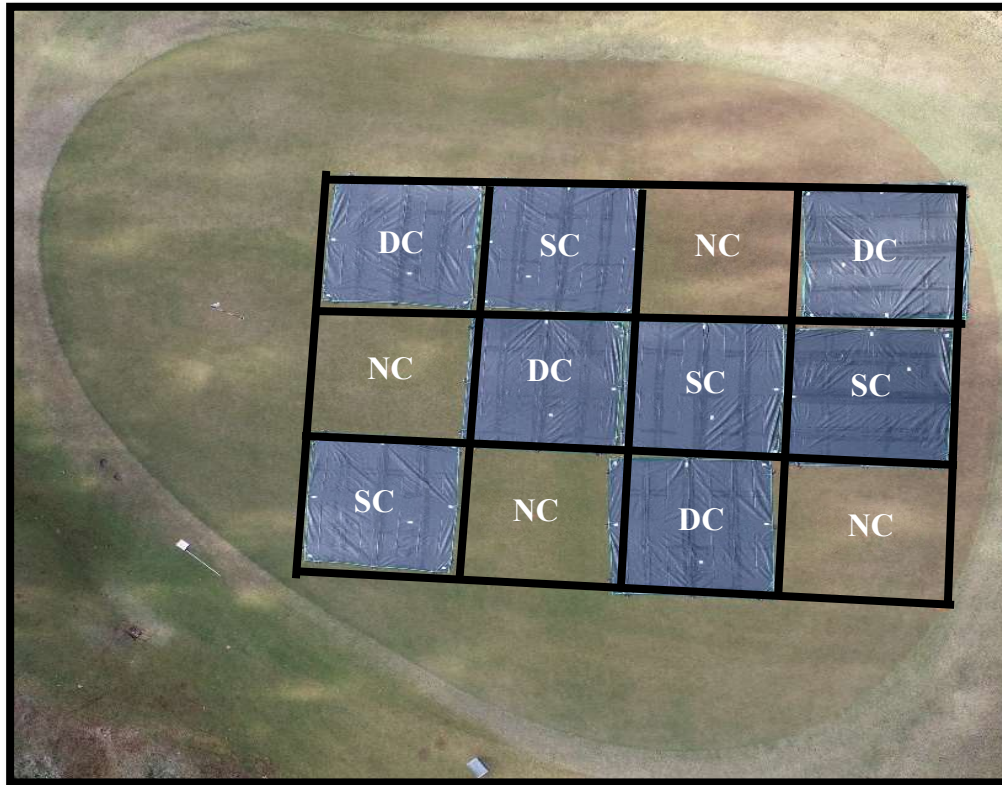


**Figure 1.** Visual representation of the experimental design for two winter covering events on Green 9 in January and March 2023 on a ‘Tif-Eagle’ ultradwarf bermudagrass (*Cynodon dactylon* x *C. transvaalensis*) green at Independence Golf Club showing no cover (NC), single cover (SC), and double cover (DC) treatments.

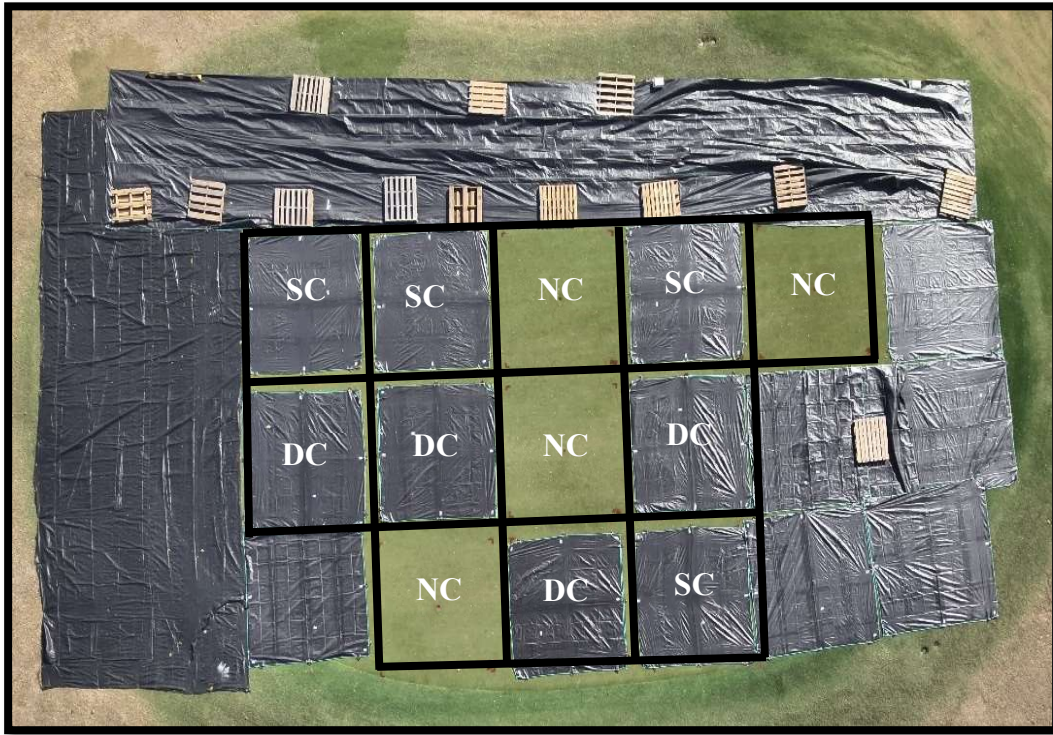


**Figure 2.** Visual representation of the experimental design for two winter covering events on Green 1 in November 2023 and January 2024 on an experimental ultradwarf bermudagrass (*Cynodon dactylon* x *C. transvaalensis*) green variety (FAES 1302 from University of Florida) at Independence Golf Club in Richmond, Virginia showing no cover (NC), single cover (SC), and double cover (DC) treatments.

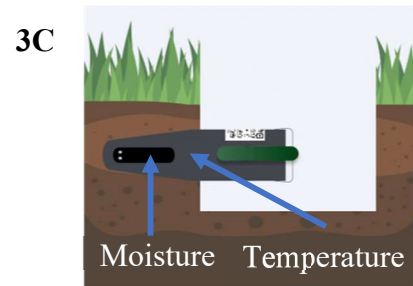


**Figure 3.** Illustrations showing the installation of the capacitive soil sensor using the Miltons square plugger on Green 9 in December 2022 at Independence Golf Club in Richmond, Virginia for (Figure 3A), a close-up of the capacitive soil sensor positioned horizontally before replacing the plug (Figure 3B), and the sensor in the hole rotated to ensure the moisture plate was perpendicular to the soil walls (Figure 3C).

**Table 1.** Mix model effect effects test for sources location, treatment, and their interaction analyzing both daily average soil temperature (°F) and moisture (%) response variables for covering events of Green 9 in 2022-2023 and Green 1 in 2023-2024 at Independence Golf Club in Richmond, Virginia.

<b>Soil Temperature(°C)</b>		
<b>Source</b>	<b>F Ratio</b>	<b>P &gt; F</b>
<b>Location</b>	0.95	0.4324
<b>Treatment</b>	133.5	<0.0001
<b>Location x Treatment</b>	3.02	0.05
<b>Soil Moisture(%)</b>		
<b>Source</b>	<b>F Ratio</b>	<b>P &gt; F</b>
<b>Location</b>	145.44	0.0064
<b>Treatment</b>	7.04	0.001
<b>Location x Treatment</b>	40.95	<0.0001

*Note:* A mixed model with a residual repeated structure was used to test and separate source effects ( $p < 0.05$ ).

**Table 2.** Least square means for covering treatments with location data pooled for soil temperature (°F) and soil moisture (%) separated by locations for covering events on a ‘TifEagle’ ultradwarf bermudagrass (*Cynodon dactylon* x *C. transvaalensis*) Green 9 in 2022–2023 and experimental variety from the University of Florida (FAES 1302 from University of Florida) Green 1 in 2023-2024 at Independence Golf Club in Richmond, Virginia.

<b>Covering Treatment</b>	<b>Soil Temperature (°F)</b>		<b>Soil Moisture (%)</b>	
	<b>Locations Pooled</b>	<b>Green 1</b>	<b>Green 9</b>	<b>Green 9</b>
<b>No Cover</b>	42.00 b+	38.91 B	19.84 A	
<b>Single Cover</b>	45.23 a	35.60 C	20.70 A	
<b>Double Cover</b>	45.72 a	42.79 A	17.31 B	

+ Multiple comparisons analysis with means separated using Tukey-Kramer HSD at  $\alpha = 0.05$  with common letters indicating no treatment separation within columns.

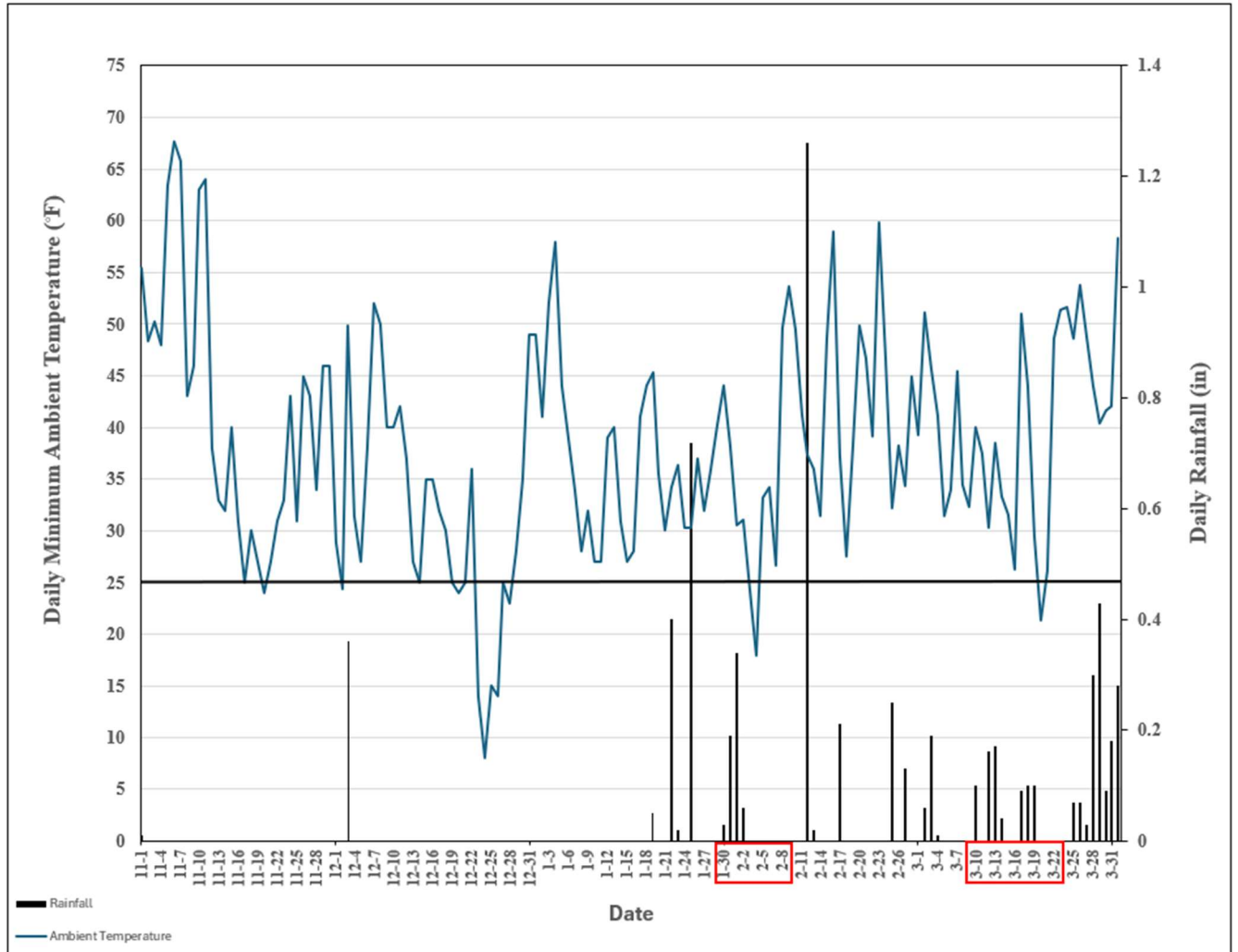


**Figure 4.** The minimum observed daily ambient temperature during the winter season of 2022-2023 in Richmond, Virginia. Red boxes indicate the two covering events that occurred on Green 9. The black horizontal line represents the ambient temperature threshold used to trigger a covering event.

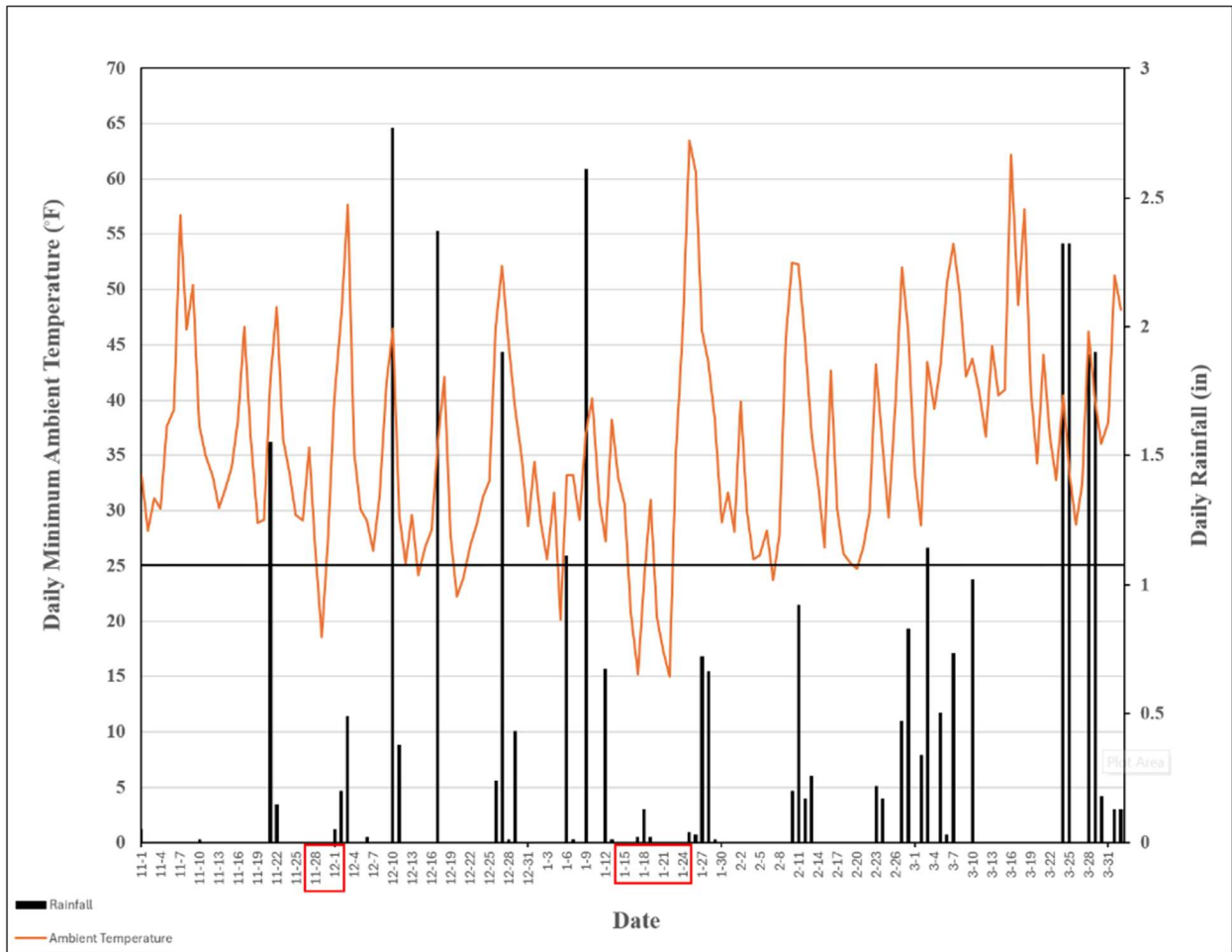


**Figure 5.** The minimum observed daily ambient temperature during the winter of 2023-2024 in Richmond, Virginia. Red boxes indicate the two covering events that occurred on Green 1. The black horizontal line represents the ambient temperature threshold used to trigger a covering event.

**Table 3.** Covering event dates for a ‘TifEagle’ ultradwarf bermudagrass (*Cynodon dactylon* x *C. transvaalensis*) Green 9 in 2022-2023 and an experimental variety from the University of Florida (FAES 1302 from University of Florida) Green 1 in 2023-2024, total covering dates, dates of precipitation before covering (B) and during covering (D) at Independence Golf Club in Richmond, Virginia.

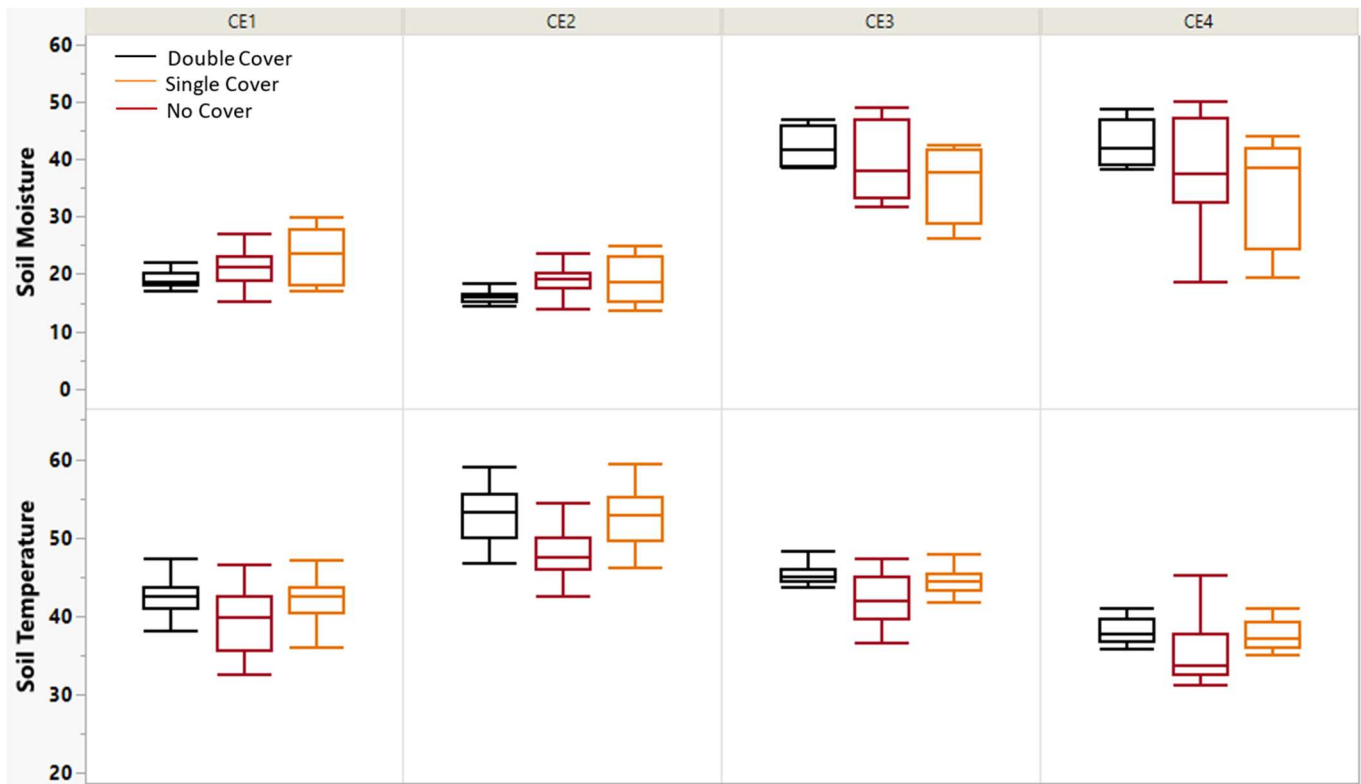
<b>Green 9</b>						
<b>Covering Events</b>	<b>Dates Covered</b>	<b>Total Covered Days</b>	<b>Rainfall</b>			
			<b>Date B+</b>	<b>Amount B (in)</b>	<b>Date(s) D†</b>	<b>Amount D (in)</b>
<b>1</b>	30Jan23-06Feb23	8	01Jan23	0.65	01Feb23	0.53
<b>2</b>	09Mar23-22Mar23	13	03Mar23	0.2	13Mar23, 19Mar23	0.33, 0.2

<b>Green 1</b>						
<b>Covering Events</b>	<b>Dates Covered</b>	<b>Total Covered Days</b>	<b>Rainfall</b>			
			<b>Dates B</b>	<b>Amount B (in)</b>	<b>Date D</b>	<b>Amount D (in)</b>
<b>1</b>	26Nov23-01Dec23	6	21Nov23	1.65	-	-

+ Before covering (B) data is assessed within a five day window prior to covering events occurring.

† During covering (D) data is assessed as days of rainfall that occur during the active days of covering treatments being implemented.



**Figure 6.** Box and whisker plots of soil temperature (°F) and moisture (%) for each covering treatment No Cover, Single Cover, and Double Cover by covering events (CE 1– 4) at each location with CE1 and CE2 in Winter 2022-2023 on a ‘TifEagle’ ultradwarf bermudagrass (*Cynodon dactylon* x *C. transvaalensis*) Green 9 and CE3 and CE4 in Winter 2023-2024 on an experimental variety from the University of Florida (FAES 1302 from University of Florida) Green 1 at Independence Golf Club in Richmond, Virginia.

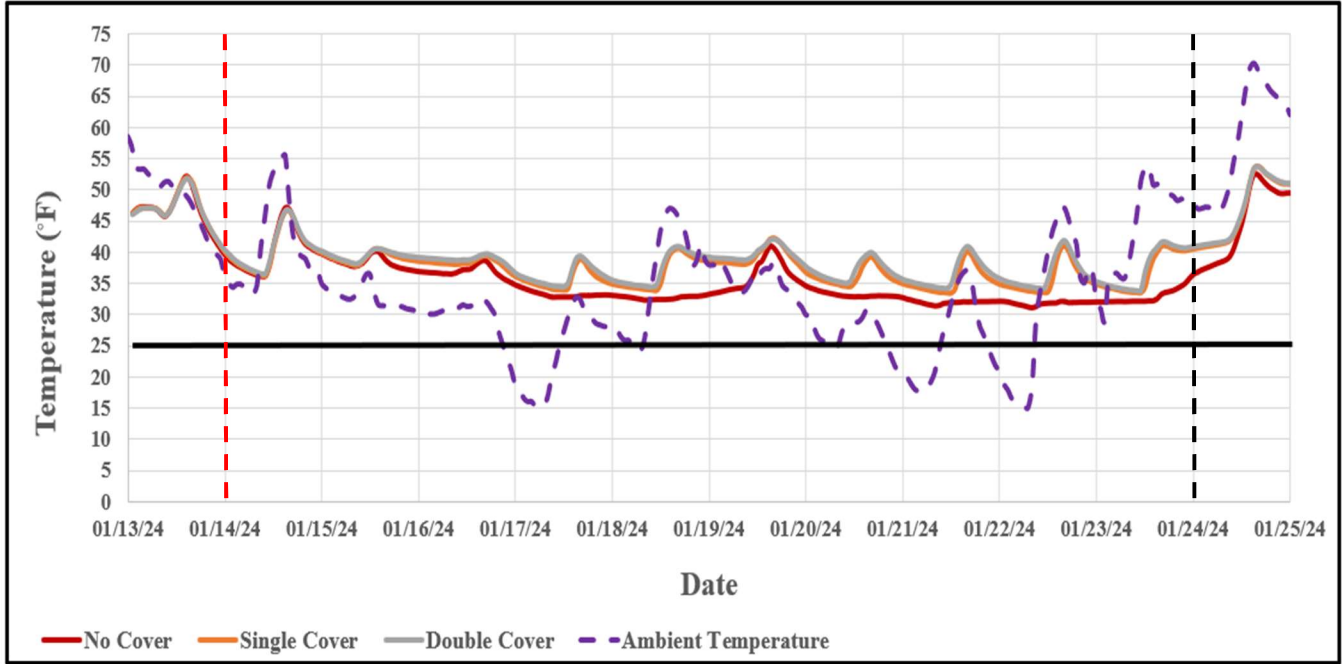


**Figure 7.** Soil temperature data pooled by treatments of no cover, single cover, and double cover during covering event 4 in the winter 2023-2024 season on an ultradwarf bermudagrass (*Cynodon dactylon* x *C. transvaalensis*) Green 1 on an experimental variety from the University of Florida (FAES 1302 from University of Florida). The red dashed line indicates when the covering treatments were applied, and the black dashed line indicates when they were removed. The black horizontal line represents the 25°F ambient temperature threshold used to justify covering events.

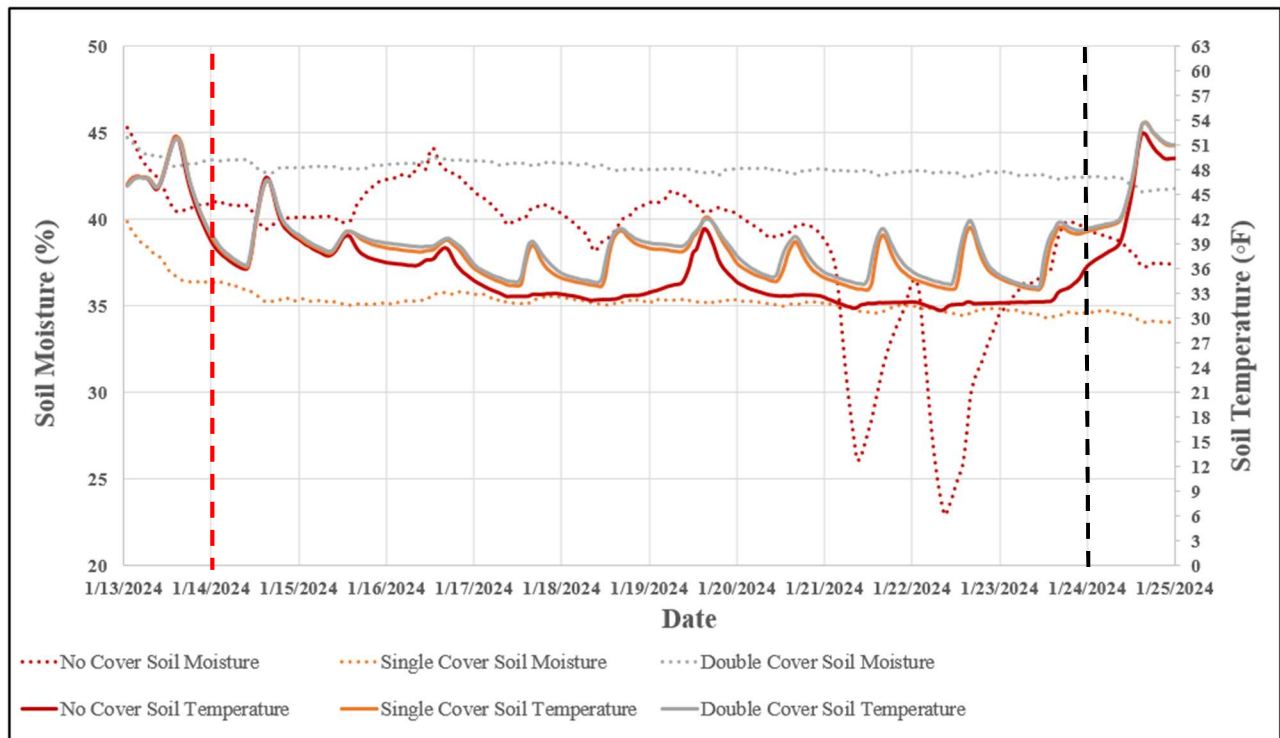


**Figure 8.** Soil temperature and moisture pooled by covering treatments of no cover, single cover and double covering during covering event 4 in winter 2023-2024 season on an experimental ultradwarf bermudagrass (*Cynodon dactylon* x *C. transvaalensis*) green variety (FAES 1302 from University of Florida). Red dashed line indicates when the covering treatments were applied, and the black dashed line indicates when the covers were removed.